A STUDY OF HIGH RESOLUTION SEISMOLOGY AND SEDIMENTOLOGY ON THE OFFSHORE LATE QUATERNARY SEDIMENTS NORTHEAST OF NEWFOUNDLAND

by

Christopher Thomas Dale

Submitted in partial fulfillment of the

requirements for the degree of

Master of Science

at

Dalhousie University

Halifax, Nova Scotia

August, 1979

Examiners:

TABLE OF CONTENTS

ABSTRACT

The Late Quaternary sediments of the northeast Newfoundland continental shelf have been examined and mapped as five surficial seismic facies. Airgun seismic data show constructional glacial features generally occur below the 200 m isobath. Variations in sedimentological and geotechnical parameters in six cores within the area of seismic coverage have provided the basis for correlations between Huntec Deep Tow System (D.T.S.) seismic data and sedimentary facies. Sedimentological analyses indicate both glacial and post-glacial sediments have been recovered. The last major glacial advance in this area has been tentatively dated as approximately 25,000 yBP.

A seismically stratified facies on the D.T.S. data has been attributed to spatially coherent layers of ice-rafted material. This ice rafting is suggested as having occurred during the cold period on the eastern Canadian seaboard, corresponding to the Late Wisconsinan period of continental ice advance.

Comparisons between D.T.S. seismic data and synthetic seismograms have made possible the conclusions that shot to shot incoherencies on D.T.S. data are probably due to local variations in geology, geotechnical results from singular piston core samples are unrepresentative of the "average" geology observed with the D.T.S., and geological studies require a knowledge of the subsurface seabed acoustic impedance structure if an undisputable interpretation is to be made of the high resolution seismic data.

LIST OF FIGURES

LIST OF TABLES

LIST OF PLATES

ACKNOWLEDGEMENTS

I would like to thank my committee, Drs. Richard Haworth, Chris Beaumont, Peter Simpkin and David Piper who provided support and advice during my work. I am particularly indebted to Dr. Richard Haworth for his patience and interest throughout the project and his generosity in allowing ship time during the Hudson 78023 cruise. Further, Dr. H.B.S. Cooke provided valuable criticism of geological interpretation during Dr. Piper's sabbatical absence.

I owe a great deal of thanks to Russell Parrott and Jack Dodds of Huntec for their advice in many aspects of the deep towed seismic system hardware and minicomputer seismic data replay work.

The captain, crew and scientific staff on C.S.S. Hudson cruise 78023 made my time at sea a very valuable and rewarding experience.

I would also like to mention the staff of the Atlantic Geoscience centre for their assistance and encouragement, especially Brian MacIntyre, who readily went out of his way to help.

My friends and fellow students at Dalhousie are also thanked. Many offered constructive criticism and companionship. I specifically thank Ali Aksu for identifying and counting the microfossils and minerals reported herein. Phil Hill, Alan Nelson and Randell Stephenson critically read parts of the manuscript.

Clo Leone cannot be complimented enough on the excellent and speedy job she made of the typing.

Financial support for the project came from an NSERC operating grant to Dr. Piper and support from Dr. Haworth. A. Killam Memorial Scholarship provided support to the author in 1978-9.

Finally, I would like to thank Gail for her moral support at all times.

CHAPTER 1

INTRODUCTION

The northeast Newfoundland continental shelf is a glacially over-deepened area with large fjord-like bathymetric features characterized by White Bay and Notre Dame Bay. These features were probably formed during pre-late Wisconsin glacial ice advances and mirror the areas of more easily eroded offshore bedrock. Glacial till deposits have been identified using reflection seismology records and generally occur at depths greater than the present-day 200 m isobath. This is probably due to grounded glacial ice advancing as far offshore as the equivalent of this depth (which was a lesser depth) during the last major ice advance.

The Late Quaternary sediments on the shelf are critical to an understanding of the local maximum extent of the Laurentide ice sheet during the last (Wisconsin) glaciation. This is relevant to the findings of other workers in the Atlantic Canada region in delimiting the maximum overall extent of the last major ice sheet (Andrews, 1973; Grant, 1977; Andrews and Barry, 1978; Ives, 1978). The relatively deep waters (~ 250 m) in this region (Fig. 1.1) compared with the adjacent shelf areas appear to have prevented reworking of the sediments after the last glaciation, thus preserving to a great extent the geological record.

Onshore studies of Late Quaternary sedimentation in Newfoundland are limited especially in the north of the island (see Tucker, 1976, for a review). Offshore, Grant (1972) made a broad study of the geology and morphology of the northeast Newfoundland and Labrador margins;

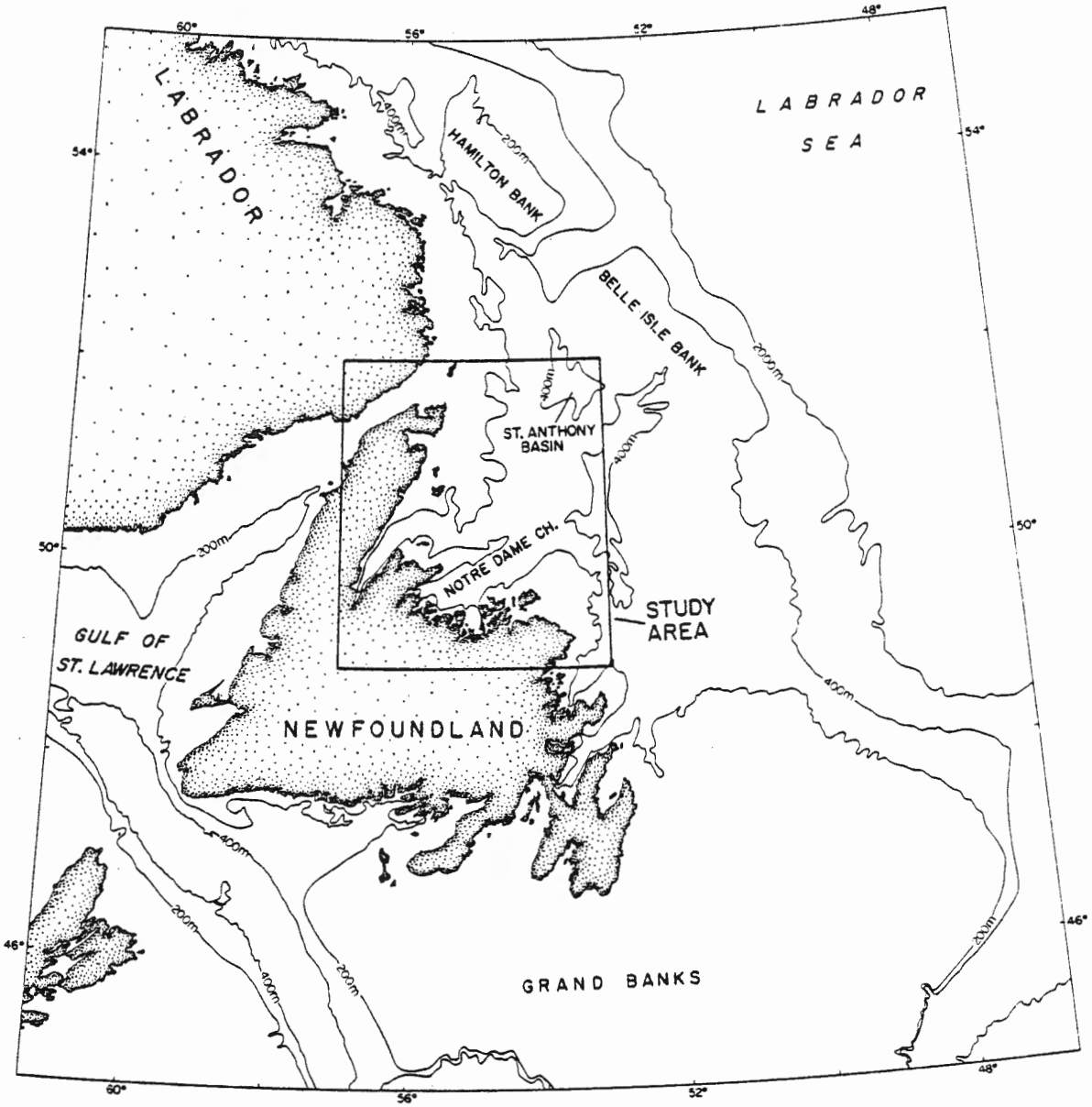

Fig. 1.1: Geographic location of the study area.

Slatt, 1974; Piper and Slatt, 1977 and Piper et al., 1978 have made reconnaissance studies of the Late Quaternary sedimentology.

The continental shelf areas to the north and south have received more attention primarily from workers at Bedford Institute of Oceanography (King, 1969, 1970; MacLean and King, 1971; Drapeau and King, 1972; Loring, 1973; King and Fader, 1976; van der Linden et al., 1976). Earlier studies of surficial geology used echo sounder records of seabed morphology which were also used interpretatively to give sediment texture (King, 1967). Recent geological studies on the Canadian continental margin and elsewhere (e.g. Boulton, 1979; Kögler and Larsen, 1979) have made extensive use of subbottom profiling and employ a qualitative analysis of seismic records (van Overeem, 1978). In this study the sedimentology of the area is examined and measurements of the subbottom variations in some of the physical (or geotechnical) properties of the sediments have been made in order to determine in detail the sedimentary expression of the coherent seismic reflectors observed on high resolution seismic records, before a geological conclusion is drawn.

In 1975, a cruise from the Atlantic Geoscience Centre, Bedford Institute of Oceanography conducted a multiparameter geophysical investigation into the offshore bedrock geology of the northeast Newfoundland continental shelf. Both potential field and reflection seismic data, backed up by bedrock drilling, were collected and used to delineate the geological structure of the offshore bedrock units (Haworth et al., 1976a, b). The reflection seismic systems included both conventional airgun and Huntec high resolution deep towed seismic system (D.T.S.) data. A preliminary

analysis of the 1975 seismic data for information on the surficial sediments provided impetus for a further cruise to the study area in July and August of 1978 to examine in more detail the seismostratigraphic units previously identified. Seismic data, especially D.T.S., were collected in key areas and piston cores were collected at 11 locations identified from D.T.S. records. These locations were chosen where a maximum number of seismostratigraphic horizons could be penetrated beneath the seabed in approximately 10 m, the usual maximum recover length of the Benthos piston corer.

The D.T.S. is a continuous subbottom profiling system towed behind the survey vessel on a faired cable at greater than half the water depth (McKeown, 1975; Hutchins et al., 1976). This eliminates the problems of the sea surface - air interface multiple reflection commonly encountered with other profiling systems and, being closer to the seabed, records higher signal levels and lower ship and sea state ambient noise. The data are output as the usual graphic record and are simultaneously recorded for replay at a later date. The system has a highly repetitive, short (~ 120 μs), impulse-like source which makes it possible to use signal processing to extract and visually enhance the information content of the data (Simpkin et al., 1976). Also, this consistent outgoing pulse makes possible the calculation of the theoretical response of the seabed (Assuming a model for the seismic propagation discussed later) to the incident seismic pulse. Pressure - wave (p-wave) velocities were measured at regular intervals along the length of the cores as soon as they were brought on ship and six of these cores, with maximum sedimentary and p-wave velo-

city variability and adequate D.T.S. coverage, were then chosen for detailed geotechnical and sedimentological analysis.

The results of these analyses are presented and the geotechnical data have been used to compute normal incidence synthetic seismograms which are compared to the field D.T.S. data. Although these comparisons were only partly successful, they do provide a basic understanding of the types of seismic horizons that are observed. The geological implications of these results are discussed and used in extending the sedimentological findings into a more comprehensive understanding of the Late Quaternary sedimentation in this study area.

Thesis Organization

In Chapter 2, the methods used to collect and interpret the bathymetric and seismic data are presented and the collection of the sediment cores is outlined.

Chapter 3 deals with the techniques and results of the geotechnical measurements made on the cores; this includes down core variations observed in the measured parameters and scatter-diagram analysis of the data.

In Chapter 4 the sedimentology is described and interpreted; facies are identified and correlated across the shelf; mineralogy and microfossil data are used in an environmental interpretation.

Chapter 5 describes how the geotechnical results were used to derive synthetic seismograms and how the D.T.S. data were replayed as variations

of acoustic pressure with time or in a comparable "wiggly trace" format. Finally the correlation between these data is discussed.

The conclusions and a synthesis of the results of the study are presented in Chapter 6.

CHAPTER 2

BATHYMETRIC AND SEISMIC DATA COLLECTION AND ANALYSIS, CORE COLLECTION

Navigation

It is difficult to obtain accurate real time navigation in the study area due to the close proximity of the Loran-C baseline and the necessary correction for the overland Loran-C signal phase lag received from the Cape Race transmitter (S.E. Newfoundland) (Haworth et al., 1976a). Using the Austron Loran-C navigation system in range-range mode in this area, expected positioning accuracy is between 150 m and 300 m (D. Wells, Bedford Institute, pers. comm., 1979). The lower accuracy is to be expected close to the Angissoq (southern tip of Greenland) - Cape Race baseline. However, experience gained in 1975 resulted in good real time navigation when returning to proposed sampling sites so that the 150 m accuracy is probably most appropriate. Post-cruise processing of the navigation data has also indicated that only minor errors (~ 150 m) in location exist (J.B. MacIntyre, Bedford Institute, pers. comm., 1979).

Bathymetry

The bathymetric data were collected using a conventional 12 kHz widebeam echo sounder and digitized onboard ship every 5 minutes and at peaks and troughs in the record.

The bathymetric map (Fig. 2.1) is an updated version of Haworth et al., (1976a). Additional data from the northeasterly corner of the

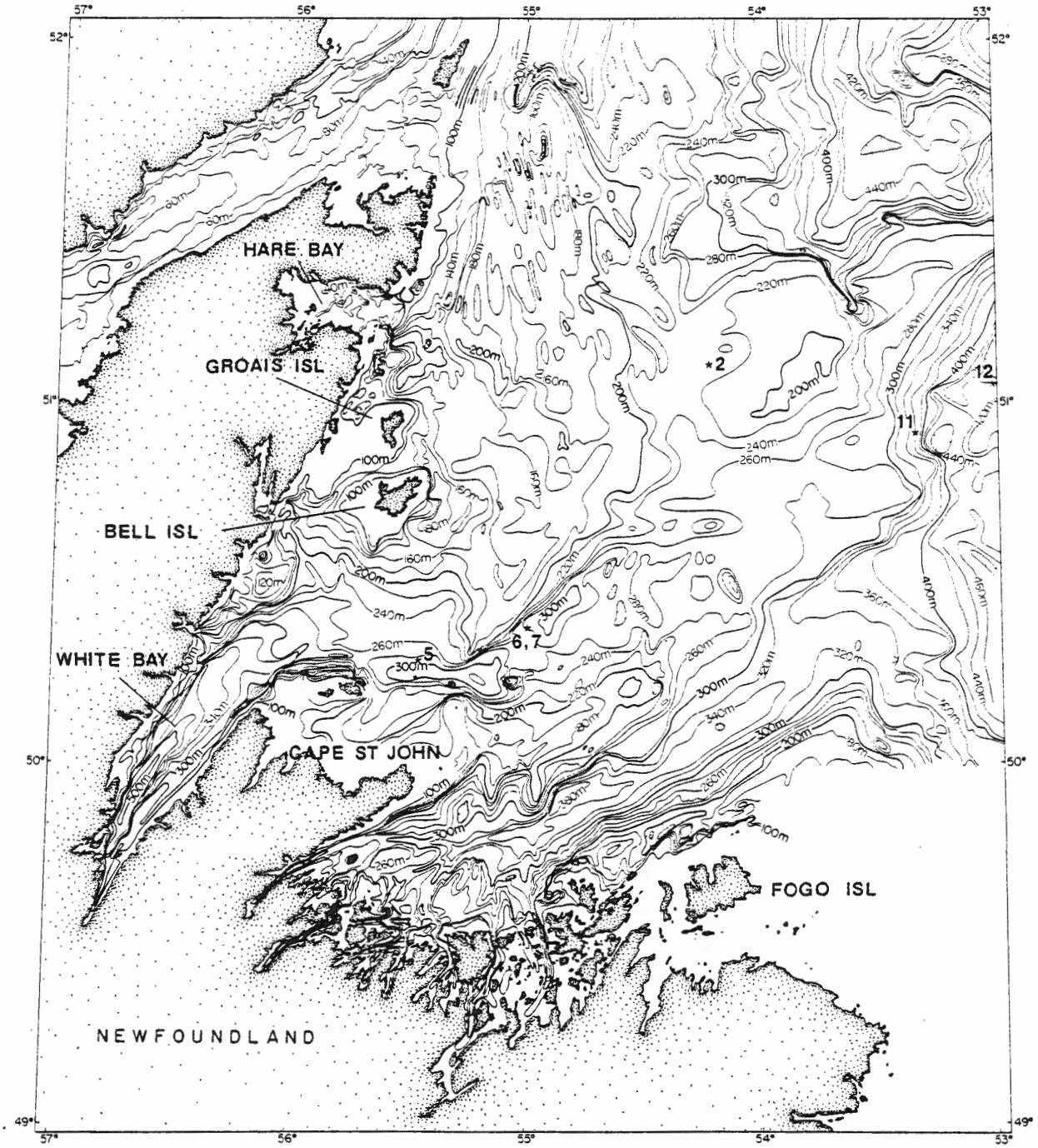

Fig. 2.1: Bathymetric map of the study area, scale 1:2,000,000 (modified after Haworth, 1976a). Core locations are shown by an *.

study area (Karlsen 75-018 cruise, see Haworth et al., 1976b) and manually interpreted bathymetry records from the HN78-023 cruise (Haworth, 1978) were used in the preparation of Figure 2.1 at a scale of 1:250,000 prior to reduction to 1:2,000,000.

Seismic Data

During the Bedford Institute of Oceanography cruises HN75-009 ph. 3 and HN78-023 (Fig. 2.2), simultaneous seismic reflection profiles were collected with both the Huntec D.T.S. (a broadband deep-towed boomer source and receiver, Hutchins et al., 1976) and a single channel airgun system. The Huntec D.T.S. boomer is usually operated at an excitation voltage of 5 kV with a repetition rate of 0.75 sec. and towed at a depth of greater than one half the water depth to exclude interference from the seawater-air interface multiple reflection. A 625 x $10^{-5}m^3$ (40 in^3) airgun operating at 10 MPa (1500 psi) was normally used at a 2 sec. repetition rate in conjunction with the Huntec D.T.S. Both types of seismic data were recorded in analogue form on Hewlett-Packard F.M. tape recorder and filtered and displayed at sea in real time on E.P.C. graphic recorders. Onshore, selected Huntec D.T.S. data were digitized for the more detailed analysis discussed in Chapter 5.

Sidescan sonar data were also collected on some of the 1978 seismic lines using the Bedford Institute of Oceanography system (Jollimore, 1975). However, the deeper troughs and basin regions were out of range of the system even at towing speeds as low as 3 to 4 knots. These data have been used as an aid in identifying the surficial seismic facies described

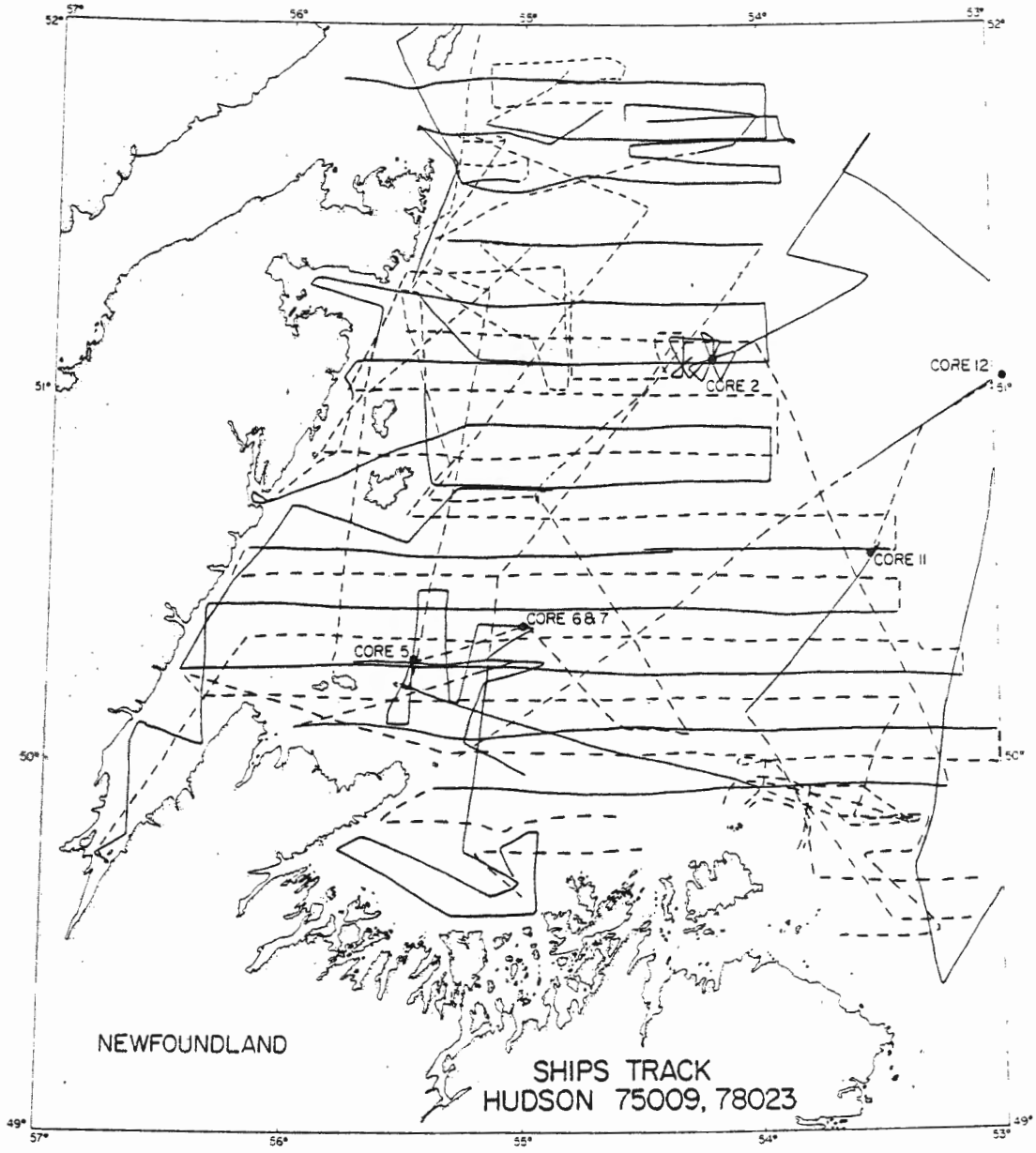

Fig. 2.2: Ship's track for cruises HN75009-ph3 and HN78023. On all the lines bathymetry and potential field data were collected. Solid lines indicate Huntec D.T.S. and airgun data as well.

below, but have not been interpreted separately.

Analysis of Seismic Data

Airgun Reflection Seismic Data

Haworth et al., (1976a, b) used the airgun data in conjunction with magnetic and gravity field measurements to delineate the offshore bedrock geology. Herein, the airgun data have been used to identify bedrock areas thickly covered by unconsolidated glacial drift where the Huntec D.T.S. lacked adequate subsurface penetration.

The seismic cross-sections from the study area are presented as a fence diagram (in foldout pocket at the end of the thesis). This diagram was produced by drawing 4:1 reductions of the original interpretations of the airgun seismic records in the closest fitting positions to the actual seismic lines on the navigation charts. This method assumes that the seismic lines were run at a constant speed and on an east-west grid. This is not precisely the case, but to a first approximation the results are reasonable with an estimated maximum error of 5 minutes of latitude or longitude. The seismic units were classified according to the scheme of Grant (1971) given below.

UNIT COLOR	SURFACE CHARACTER	SEISMIC PENETRATION	REFLECTION CHARACTER	INFERRED LITHOLOGY	INFERRED AGE
Yellow	Smooth to irregular	Good	Highly variable in strength, continuity and attitude	Drift	Quaternary
Blue	Smooth	Good	Weak, poor to fair continuity, depositional attitudes	Mud	Quaternary
Green	Smooth to irregular	Good	Weak to strong, generally good continuity, local and regional warping	Coastal plain sedimentary strata	Mesozoic-Cenozoic
-	Smooth	Fair to Good	Weak to strong, good continuity, gentle folding	Sedimentary strata	Mississippian and Pennsylvanian

Glacial drift is more abundant in the northern and southern regions of the study area where the nearshore water depths are greater than those found in the intermediate region east of Groais and Bell Islands. The bathymetry of the area is largely controlled by the local bedrock (compare Fig. 2.1 with Fig. 2.3). The more resistant Devonian, Ordovician, Silurian and Cambrian volcanic rocks form the bedrock highs of the area, whereas the Mississippian, Pennsylvanian and Tertiary consolidated sedimentary bedrock generally mark areas of troughs and basins. This is presumably due to glacial quarrying during glacial episodes probably prior to the last (Wisconsinan) glaciation; however, which glacial episode is primarily responsible remains an unanswered and pertinent ques-

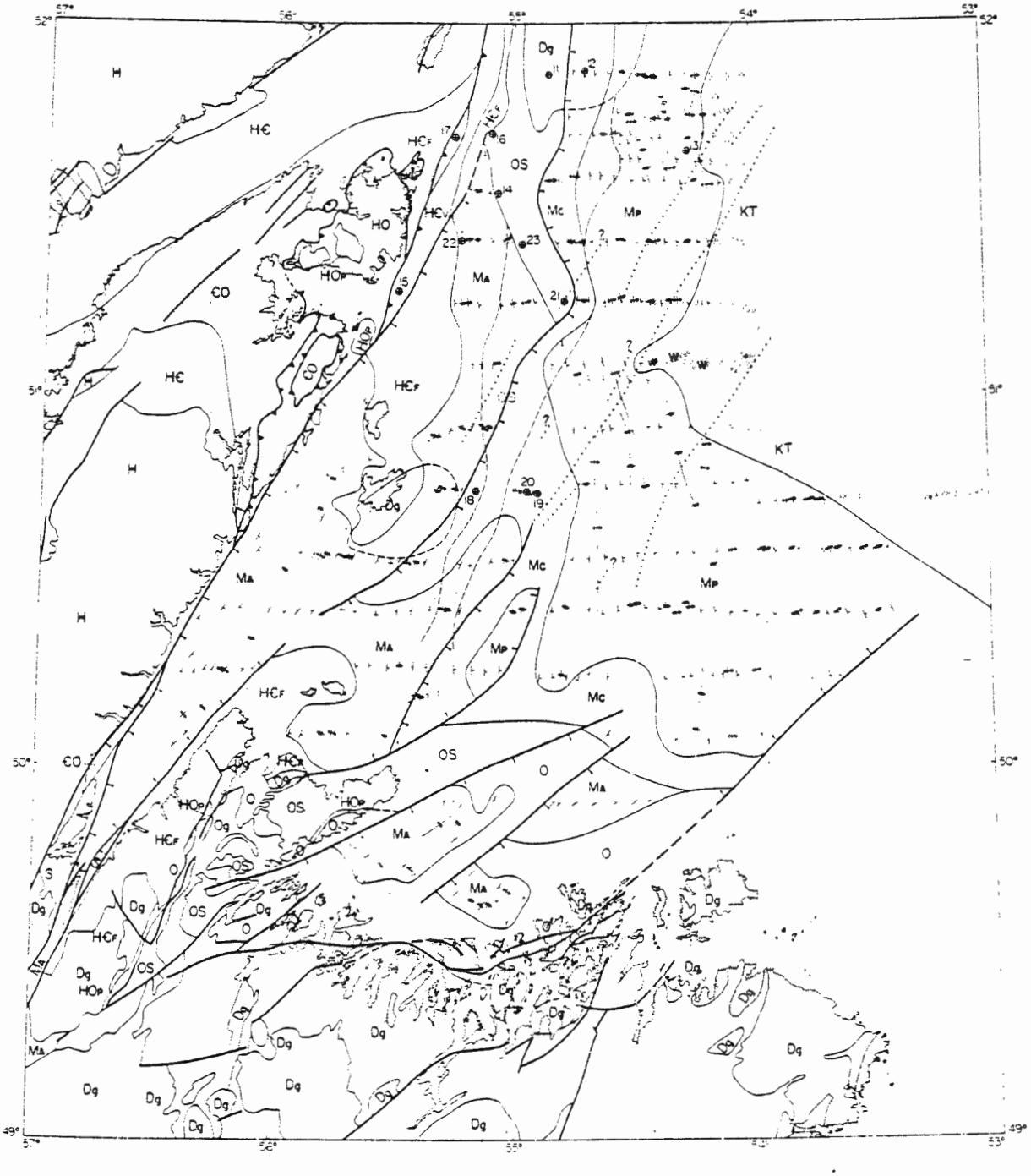

Fig. 2.3: Bedrock geology map of the northeast Newfoundland shelf area (after Haworth, 1976a).

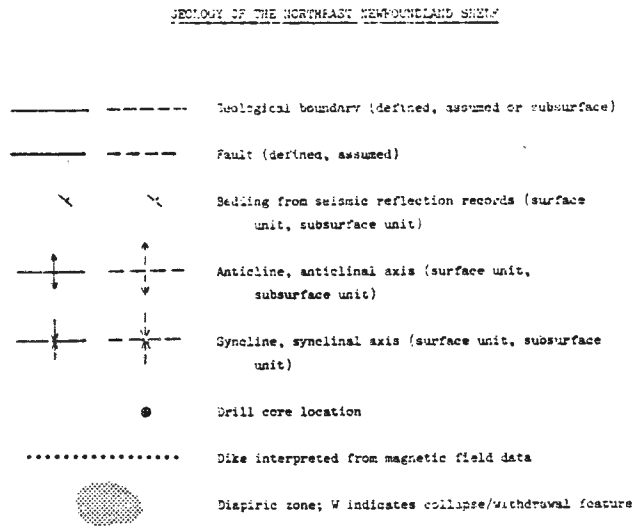

CRETACEOUS(?) AND TERTIARY

KT Siltstone, mudstone, sandstone

MISSISSIPPIAN AND PENNSYLVANIAN

Mp Grey, red and brown sandstone, conglomerate and shale (mainly Parachois Group) (may include some Permian and lower Mesozoic strata)

MISSISSIPPIAN

Mc Red and grey conglomerate, sandstone, siltstone, shale, limestone and evaporites (mainly Codroy and Windsor Groups)

Ma Grey, green and red conglomerate, sandstone, siltstone, shale (mainly Anguille, Grouse Harbour and Cape Rouge Formations)

DEVONIAN

Dg Granitic rocks (may include some Ordovician granites).

WESTERN AUTOCHTHONOUS ROCKS

SILURIAN

S Sedimentary and volcanic rocks southwest of White Bay

UPPER CAMBRIAN TO MIDDLE ORDOVICIAN

€O Limestone, dolomite, and in upper part, shale and slate (includes Doucers, St. George, Table Head and Goose Tickle Formations).

UPPER HADRYNIAN AND CAMBRIAN

H€ Quartzite, slate, limestone, dolomite locally minor basalt (includes Bateau, Lighthouse Cove, Bradore, Forteau and Hawke Bay Formations).

HELIKIAN AND OLDER

H Grenvillian rocks. Gneiss, schist, granitic and gabbroic rocks.

HARE BAY ALLOCHTHON

HADRYNIAN (?) TO MIDDLE ORDOVICIAN

HO Quartzose greywacke and slate; basalt, tuff, schist and amphibolite, structurally beneath peridotite sheets (HOp); Lower Ordovician basalt, tuff and black slate; Middle Ordovician melange locally at base of and within the allochthon (includes strata of Hare Bay Allochthon).

EASTERN AUTOCHTHONOUS ROCKS

ORDOVICIAN OR SILURIAN

OS Felsic and mafic volcanics, minor sedimentary rocks (includes Cape St. John Group)

LOWER ORDOVICIAN mainly

O Basalt, tuff, greywacke, slate, gabbro and peridotite; granites (Og) (includes Baie Verte, Mings Bight and Lushs Bight Groups).

HADRYNIAN AND CAMBRIAN mainly

H€A Psammitic and pelitic schists, locally basic schist and amphibolite derived from basalt (includes undifferentiated plutonic rocks); Hev, mainly chlorite schist derived from basaltic rocks and may include meta-gabbro and meta-peridotite (includes Fleur de Lys Supergroup).

Fig. 2.3 (cont.): Key to bedrock geology map.

tion. There are numerous constructional glacial features in the areas of thick drift deposition. These features are proposed as evidence for locating the glacial maximum position during the last significant ice advance. Other evidence will be presented in Chapters 4, 5 and 6. The position and character of these features indicate that water depth may have been important in determining the distance out onto the shelf that ice advanced. Further, the idea that ice may have built up independently offshore on shallower shoaling areas must be considered.

Huntec D.T.S. Seismic Data

The seismic facies analysis approach has been used in exploration seismology (Roksandić, 1978) and depends upon the identification of seismic facies or units of specific and areally distinguishable character which can be correlated and mapped. A knowledge of the actual geological cause of these units is not initially required, the continuity of individual seismic events and the facies they make up are utilized to produce a seismic facies map which can later be interpreted geologically once a knowledge of the geological nature of the seismic facies is had. This approach has been used on the D.T.S. graphic records. Limits are imposed, however, by the resolution of the seismic system and the ability of the seismic interpreter to distinguish accurately and objectively between the identified seismic facies.

Five seismic facies have been identified and mapped (Fig. 2.4). This map was initially prepared at 1:250,000 from all the available D.T.S. data (and airgun data where required) and later reduced to 1:2,000,000.

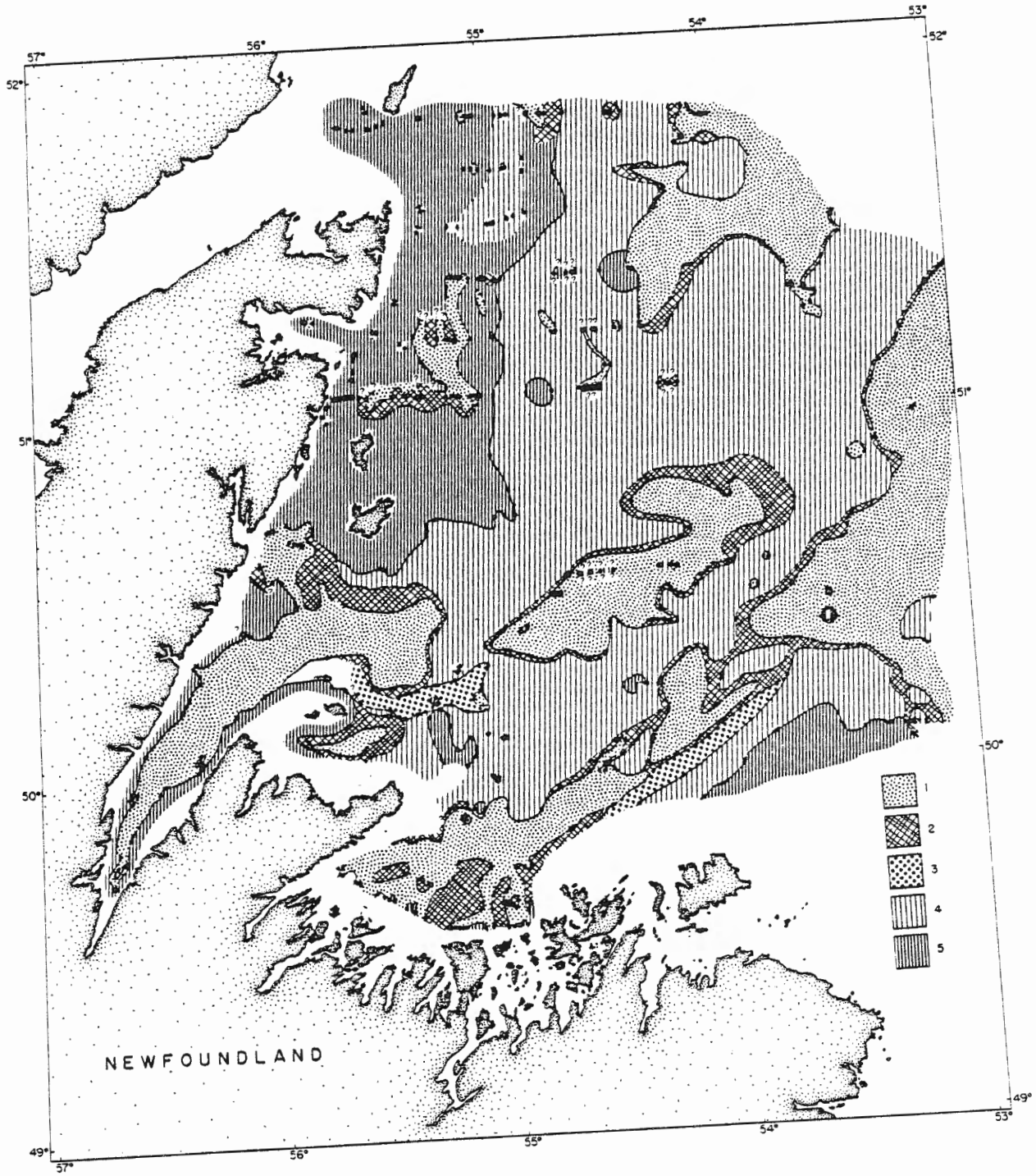

Fig. 2.4: Surficial seismic facies map. Briefly these are: Facies 1, acoustically transparent; Facies 2, seismically stratified; Facies 3, semi-stratified/scattering; Facies 4, scattering medium, interpreted as glacial drift, non-stratified; Facies 5, predominantly bedrock. Details are given in the text.

The facies distribution was mapped by locating the interfacies contacts observed on the seismic lines (Fig. 2.2 and identified by dots at the boundaries in Fig. 2.4) and then extrapolating between these points using bathymetry as a guide.

The D.T.S. seismic sections in Fig. 2.5 exhibits all five of these different units: Unit 1, an acoustically transparent layer, is generally found ponded in the basins and troughs of the study area (compare Fig. 2.4 with 2.1). Underlying this, and often appearing to outcrop around Unit 1, is a stratified seismic unit (Unit 2). In outcrop this unit thins appreciably, and appears of an intermediate character possibly marking a gradational change between units 1 and 4. Unit 4 is a non-stratified, highly scattering medium which is interpreted as a diamicton from its recovered sediment counterpart, and where deposited close to or in constructional bedforms, it can be interpreted as glacial till. This unit is widespread and of varying thickness throughout the shelf. Unit 3 has only been identified in two regions. It appears to be semi-stratified and allows only limited D.T.S. seismic penetration (Fig. 2.5). In close proximity to Unit 3 there is till-type material, as previously described, which may be genetically related to this stratified unit. Unit 5 is interpreted as bedrock and can be seen as outcrop on both D.T.S. and airgun seismic records. This unit, as mapped in Fig. 2.4, is predominantly bedrock outcrop but may be covered by 20-30 cm of other surficial sediment and have small hollows filled in with other sediment.

The seismic facies map is a simplification. Localized pockets and gradiations of sediment will exist, but on a regional scale it provides a

Fig. 2.5: Huntec D.T.S. seismic sections illustrating facies 1, 2, 3, 4 and 5.

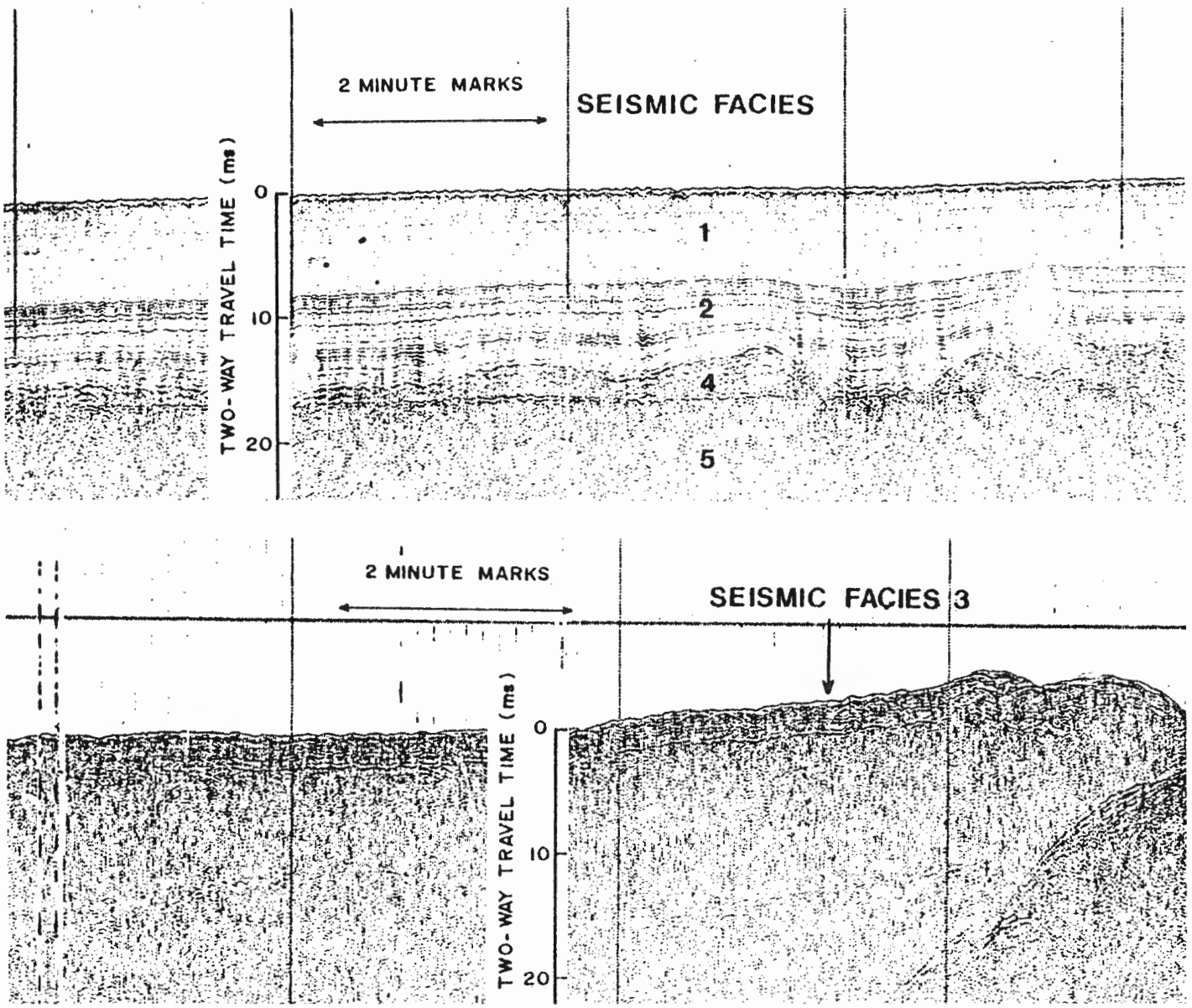
2 MINUTE MARKS
SEISMIC FACIES
TWO-WAY TRAVEL TIME (ms)
0
10
20
1
2
4
5
2 MINUTE MARKS
SEISMIC FACIES 3
TWO-WAY TRAVEL TIME (ms)
0
10
20

good basis for a geological interpretation when combined with the core control that is available.

Core Collection

In order to sample as many different seismostratigraphic units as possible, core sites were identified from D.T.S. survey data. Samples were generally obtained where a maximum number of seismic units (usually 3) could be samples in a 10 m section. Such locations were found at the edges of basins containing ponded sediments.

Of the 11 locations at which piston cores were collected using a Benthos piston corer, six have acceptable D.T.S. data (given the problems of digital playback and signal to noise ratios, see Chapter 5). The exact locations of these 6 cores (see Fig. 2.2) are given in Appendix 1. Plates 1 to 5 show the D.T.S. record sections for the cores (numbers 2, 5, 6, 7, 11 and 12). The cores vary in length between 5 m and 11 m and penetrate 5 distinct sedimentological facies. The geotechnical and sedimentological analyses of the cores are described in Chapters 3 and 4. In Chapter 5, the relationship between the seismic facies and sedimentary lithologies is discussed.

PLATES 1 TO 5

The following five pages are plates showing the D.T.S. records from the vicinities of core sites 2, 5, 6, 7, 11 and 12.

Note that the expected penetration of a piston corer is approximately 10 m or 14 ms two-way travel time.

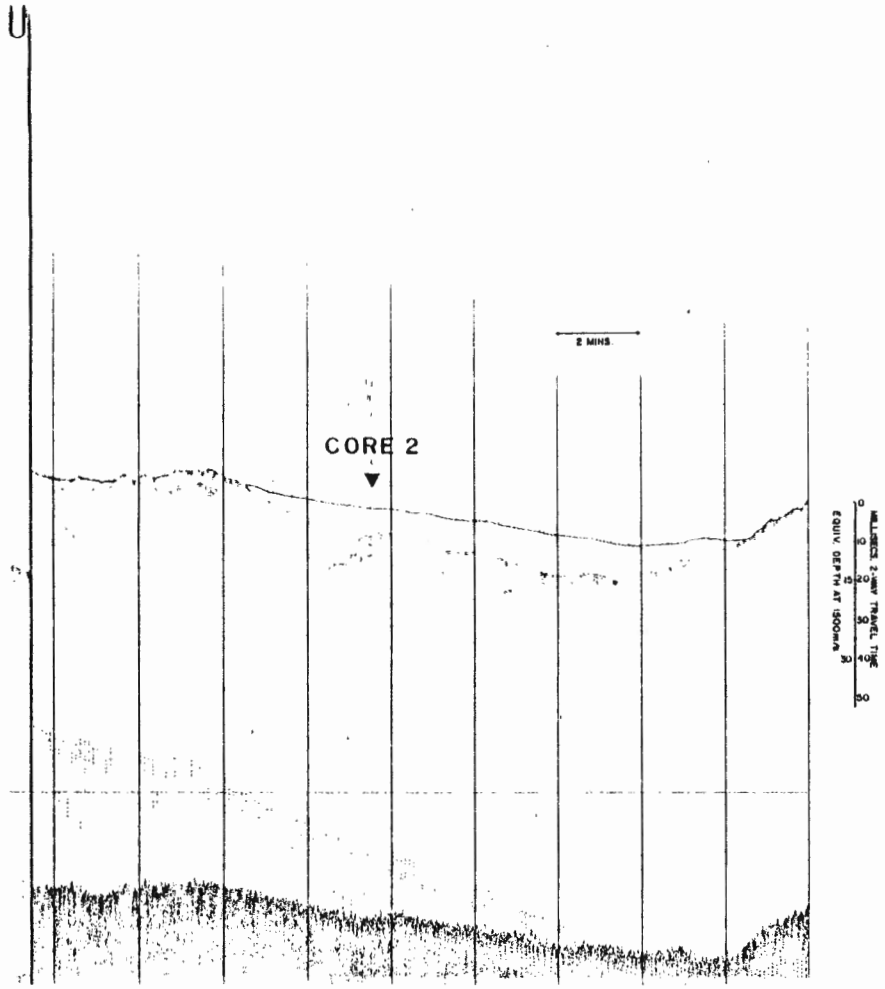
2 MINS.
CORE 2
MILLISECS. 2-WAY TRAVEL TIME
EQUIV. DEPTH AT 1500m/s
0
10
20
30
40
50
60
70
80
90
100
110
120
130
140
150
160
170
180
190
200
210
220
230
240
250
260
270
280
290
300
310
320
330
340
350
360
370
380
390
400
410
420
430
440
450
460
470
480
490
500
510
520
530
540
550
560
570
580
590
600
610
620
630
640
650
660
670
680
690
700
710
720
730
740
750
760
770
780
790
800
810
820
830
840
850
860
870
880
890
900
910
920
930
940
950
960
970
980
990
1000
1010
1020
1030
1040
1050
1060
1070
1080
1090
1100
1110
1120
1130
1140
1150
1160
1170
1180
1190
1200
1210
1220
1230
1240
1250
1260
1270
1280
1290
1300
1310
1320
1330
1340
1350
1360
1370
1380
1390
1400
1410
1420
1430
1440
1450
1460
1470
1480
1490
1500
1510
1520
1530
1540
1550
1560
1570
1580
1590
1600
1610
1620
1630
1640
1650
1660
1670
1680
1690
1700
1710
1720
1730
1740
1750
1760
1770
1780
1790
1800
1810
1820
1830
1840
1850
1860
1870
1880
1890
1900
1910
1920
1930
1940
1950
1960
1970
1980
1990
2000
2010
2020
2030
2040
2050
2060
2070
2080
2090
2100
2110
2120
2130
2140
2150
2160
2170
2180
2190
2200
2210
2220
2230
2240
2250
2260
2270
2280
2290
2300
2310
2320
2330
2340
2350
2360
2370
2380
2390
2400
2410
2420
2430
2440
2450
2460
2470
2480
2490
2500
2510
2520
2530
2540
2550
2560
2570
2580
2590
2600
2610
2620
2630
2640
2650
2660
2670
2680
2690
2700
2710
2720
2730
2740
2750
2760
2770
2780
2790
2800
2810
2820
2830
2840
2850
2860
2870
2880
2890
2900
2910
2920
2930
2940
2950
2960
2970
2980
2990
3000
3010
3020
3030
3040
3050
3060
3070
3080
3090
3100
3110
3120
3130
3140
3150
3160
3170
3180
3190
3200
3210
3220
3230
3240
3250
3260
3270
3280
3290
3300
3310
3320
3330
3340
3350
3360
3370
3380
3390
3400
3410
3420
3430
3440
3450
3460
3470
3480
3490
3500
3510
3520
3530
3540
3550
3560
3570
3580
3590
3600
3610
3620
3630
3640
3650
3660
3670
3680
3690
3700
3710
3720
3730
3740
3750
3760
3770
3780
3790
3800
3810
3820
3830
3840
3850
3860
3870
3880
3890
3900
3910
3920
3930
3940
3950
3960
3970
3980
3990
4000
4010
4020
4030
4040
4050
4060
4070
4080
4090
4100
4110
4120
4130
4140
4150
4160
4170
4180
4190
4200
4210
4220
4230
4240
4250
4260
4270
4280
4290
4300
4310
4320
4330
4340
4350
4360
4370
4380
4390
4400
4410
4420
4430
4440
4450
4460
4470
4480
4490
4500
4510
4520
4530
4540
4550
4560
4570
4580
4590
4600
4610
4620
4630
4640
4650
4660
4670
4680
4690
4700
4710
4720
4730
4740
4750
4760
4770
4780
4790
4800
4810
4820
4830
4840
4850
4860
4870
4880
4890
4900
4910
4920
4930
4940
4950
4960
4970
4980
4990
5000
5010
5020
5030
5040
5050
5060
5070
5080
5090
5100
5110
5120
5130
5140
5150
5160
5170
5180
5190
5200
5210
5220
5230
5240
5250
5260
5270
5280
5290
5300
5310
5320
5330
5340
5350
5360
5370
5380
5390
5400
5410
5420
5430
5440
5450
5460
5470
5480
5490
5500
5510
5520
5530
5540
5550
5560
5570
5580
5590
5600
5610
5620
5630
5640
5650
5660
5670
5680
5690
5700
5710
5720
5730
5740
5750
5760
5770
5780
5790
5800
5810
5820
5830
5840
5850
5860
5870
5880
5890
5900
5910
5920
5930
5940
5950
5960
5970
5980
5990
6000
6010
6020
6030
6040
6050
6060
6070
6080
6090
6100
6110
6120
6130
6140
6150
6160
6170
6180
6190
6200
6210
6220
6230
6240
6250
6260
6270
6280
6290
6300
6310
6320
6330
6340
6350
6360
6370
6380
6390
6400
6410
6420
6430
6440
6450
6460
6470
6480
6490
6500
6510
6520
6530
6540
6550
6560
6570
6580
6590
6600
6610
6620
6630
6640
6650
6660
6670
6680
6690
6700
6710
6720
6730
6740
6750
6760
6770
6780
6790
6800
6810
6820
6830
6840
6850
6860
6870
6880
6890
6900
6910
6920
6930
6940
6950
6960
6970
6980
6990
7000
7010
7020
7030
7040
7050
7060
7070
7080
7090
7100
7110
7120
7130
7140
7150
7160
7170
7180
7190
7200
7210
7220
7230
7240
7250
7260
7270
7280
7290
7300
7310
7320
7330
7340
7350
7360
7370
7380
7390
7400
7410
7420
7430
7440
7450
7460
7470
7480
7490
7500
7510
7520
7530
7540
7550
7560
7570
7580
7590
7600
7610
7620
7630
7640
7650
7660
7670
7680
7690
7700
7710
7720
7730
7740
7750
7760
7770
7780
7790
7800
7810
7820
7830
7840
7850
7860
7870
7880
7890
7900
7910
7920
7930
7940
7950
7960
7970
7980
7990
8000
8010
8020
8030
8040
8050
8060
8070
8080
8090
8100
8110
8120
8130
8140
8150
8160
8170
8180
8190
8200
8210
8220
8230
8240
8250
8260
8270
8280
8290
8300
8310
8320
8330
8340
8350
8360
8370
8380
8390
8400
8410
8420
8430
8440
8450
8460
8470
8480
8490
8500
8510
8520
8530
8540
8550
8560
8570
8580
8590
8600
8610
8620
8630
8640
8650
8660
8670
8680
8690
8700
8710
8720
8730
8740
8750
8760
8770
8780
8790
8800
8810
8820
8830
8840
8850
8860
8870
8880
8890
8900
8910
8920
8930
8940
8950
8960
8970
8980
8990
9000
9010
9020
9030
9040
9050
9060
9070
9080
9090
9100
9110
9120
9130
9140
9150
9160
9170
9180
9190
9200
9210
9220
9230
9240
9250
9260
9270
9280
9290
9300
9310
9320
9330
9340
9350
9360
9370
9380
9390
9400
9410
9420
9430
9440
9450
9460
9470
9480
9490
9500
9510
9520
9530
9540
9550
9560
9570
9580
9590
9600
9610
9620
9630
9640
9650
9660
9670
9680
9690
9700
9710
9720
9730
9740
9750
9760
9770
9780
9790
9800
9810
9820
9830
9840
9850
9860
9870
9880
9890
9900
9910
9920
9930
9940
9950
9960
9970
9980
9990
10000

PLATE I

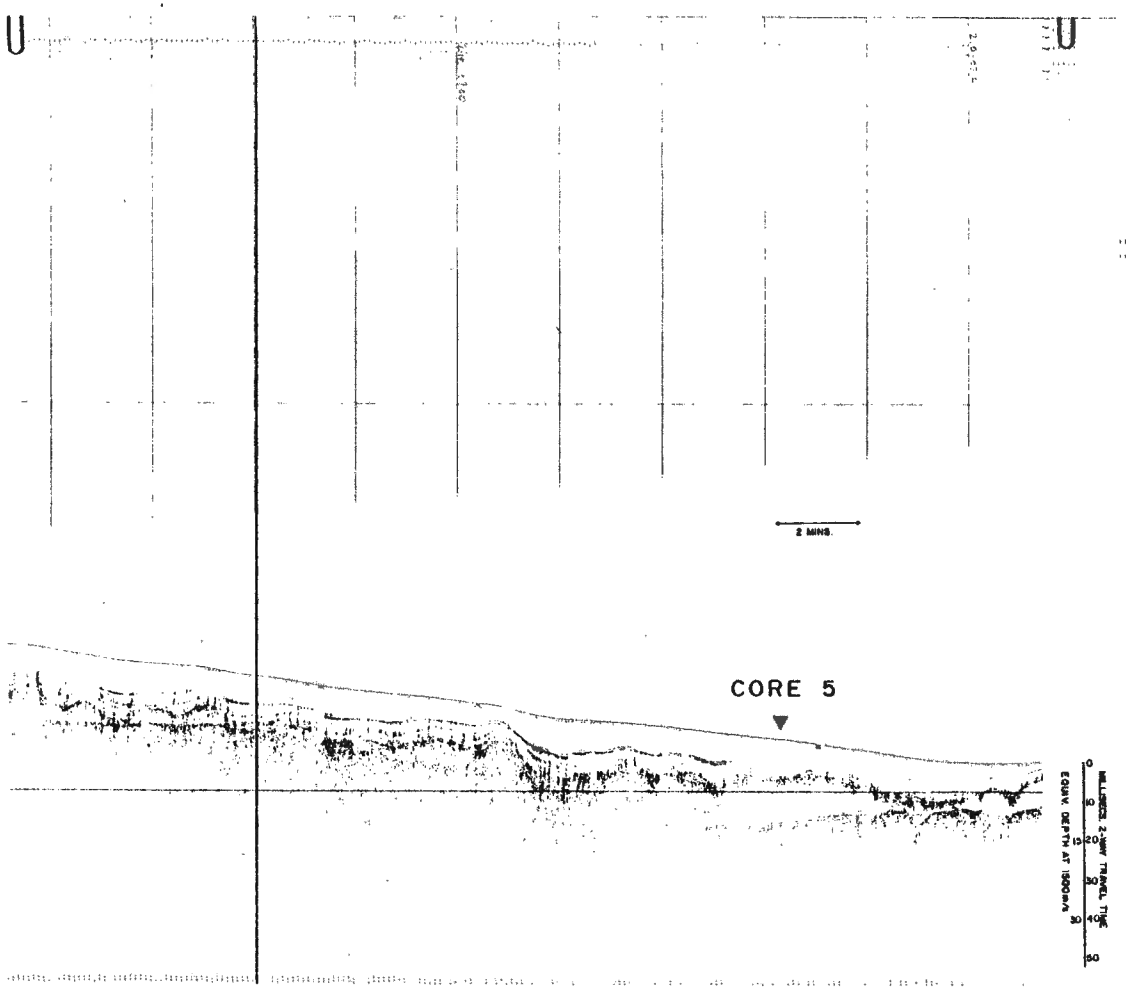

PLATE 2

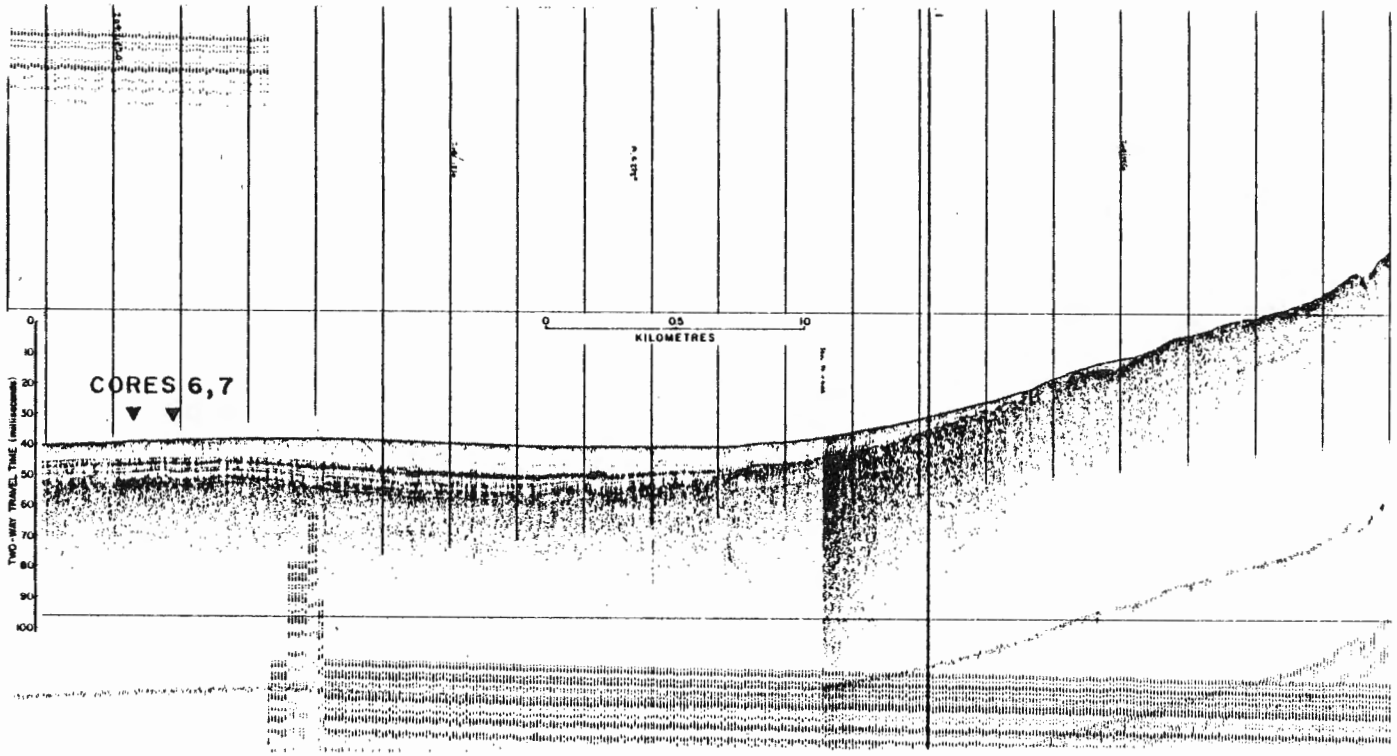
CORES 6,7
0
0·5
1·0
KILOMETRES
TWO-WAY TRAVEL TIME (milliseconds)
0
10
20
30
40
50
60
70
80
90
100

PLATE 3

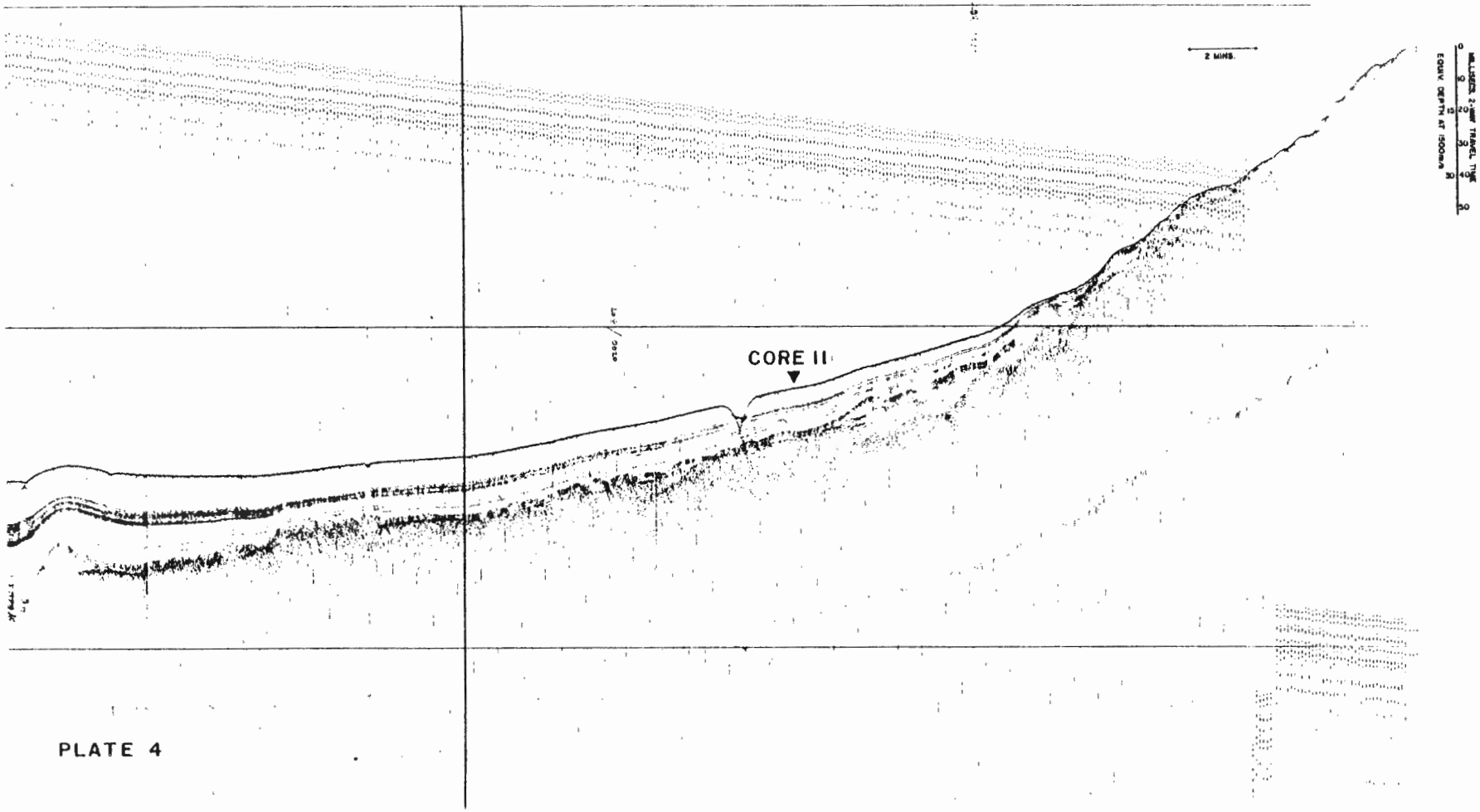
2 MINS.
CORE II
MILLISECS 2-WAY TRAVEL TIME
EQUIV DEPTH AT 1500m/s

PLATE 4

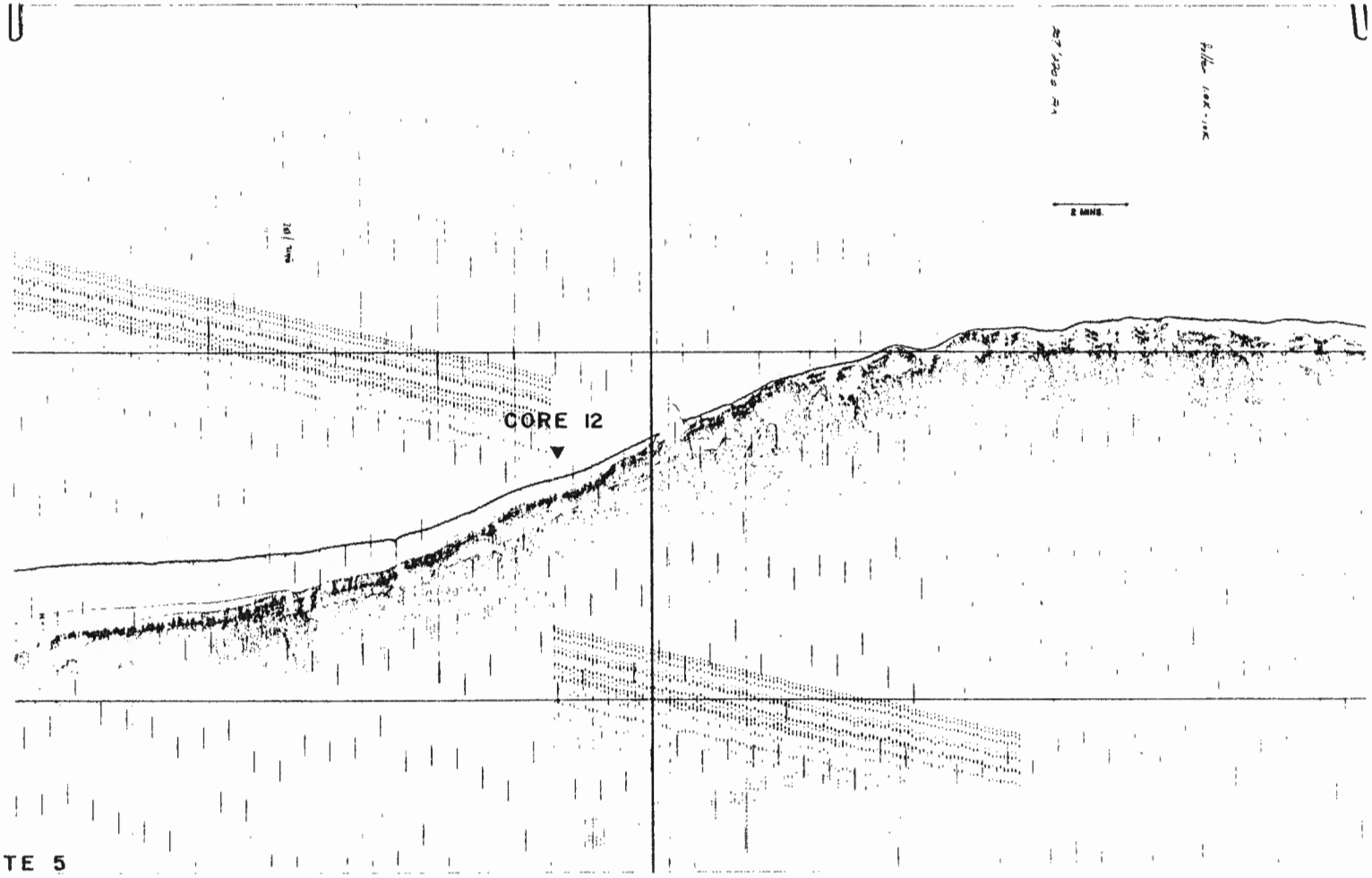

PLATE 5

CHAPTER 3

GEOTECHNICAL PROPERTIES OF THE SEDIMENTS

A detailed understanding of the seismic reflection process in the surface and near surface marine sediments requires measurements of the physical properties of those sediments that control seismic reflection.

The one-dimensional normal-incidence seismogram (i.e. a seismogram produced by an infinite and isotropic-layered elastic medium) is dependent upon variations in the acoustic impedance (the product of density and pressure-wave velocity, hereinafter termed velocity or sound velocity) within the medium of propagation (Zoeppritz, 1919), this is a fundamental assumption. Chapter 5 of this thesis is concerned with the details and the relationship of acoustically-reflecting horizons to actual sedimentary lithologies. Acoustic impedance and, therefore, sound velocity and bulk density, are of prime interest; in addition, porosity, water content, undisturbed and remoulded shear strengths (using a shear vane) have been measured so that inter-parameter correlations can be compared with the findings of other workers (e.g. Nafe and Drake, 1963; Jones et al., 1969; Hamilton, 1970; Akal, 1972).

Although methods have been devised for in-situ measurements of sound velocity while coring sediments (Anderson and Hampton, 1974; Tucholke and Shirley, 1979), the only practical method available for use in this study was to measure the sound velocity of the sediments after they had been collected using conventional piston-coring techniques. These measurements were made as soon as possible after recovery (within 1 to 2 hours),

to limit the possible effects that changes in temperature, biology, or chemistry may have had on the physical constitution of the sediment. After velocity scanning, the cores were carefully stored. The effects of drainage and desiccation are believed small and the bulk properties, which are less sensitive to a lag period before analysis, were measured later in the laboratory. Optimal sampling positions were determined with reference to the sound velocity data and X-radiographs of the unsplit cores. Disturbance is a problem when coring, but the cores used show little disturbance on X-radiographs. The correlations between geotechnical parameters further substantiate the observation that there has been little sediment disturbance. The apparent loss of sediment from approximately the top metre of some cores is a more serious problem and will be discussed in Chapter 5.

Methods

The definitions of geotechnical properties used here follow Jones et al., (1969).

Sound Velocity Determinations

A pulsed sound velocity measuring device was designed and constructed (e.g. Winokur and Chanesman, 1966). The apparatus operates in an "ear muff" configuration, capable of being slid along an aluminum bench on which the sediment core, enclosed in its liner, is placed (see Fig. 3.1). This enables scanning of core sections up to 3.5 m long, immediately after the cores are recovered from the seabed.

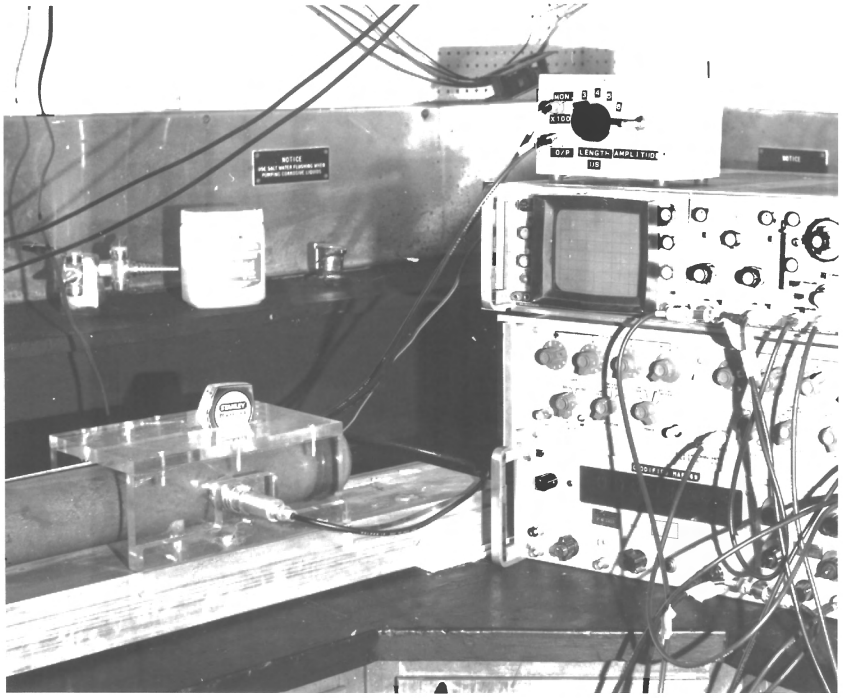

Fig. 3.1: Photograph of the acoustic scanning apparatus in operation

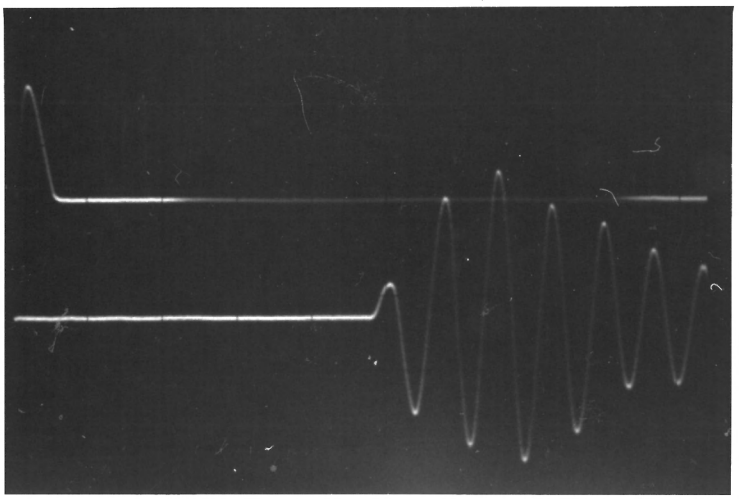

Fig. 3.3: Photograph of a typical oscilloscope display when measuring delay times. Trace 1 shows the outgoing pulse, trace 2 is the received signal. The delay between the outgoing and received signal equals the delay time.

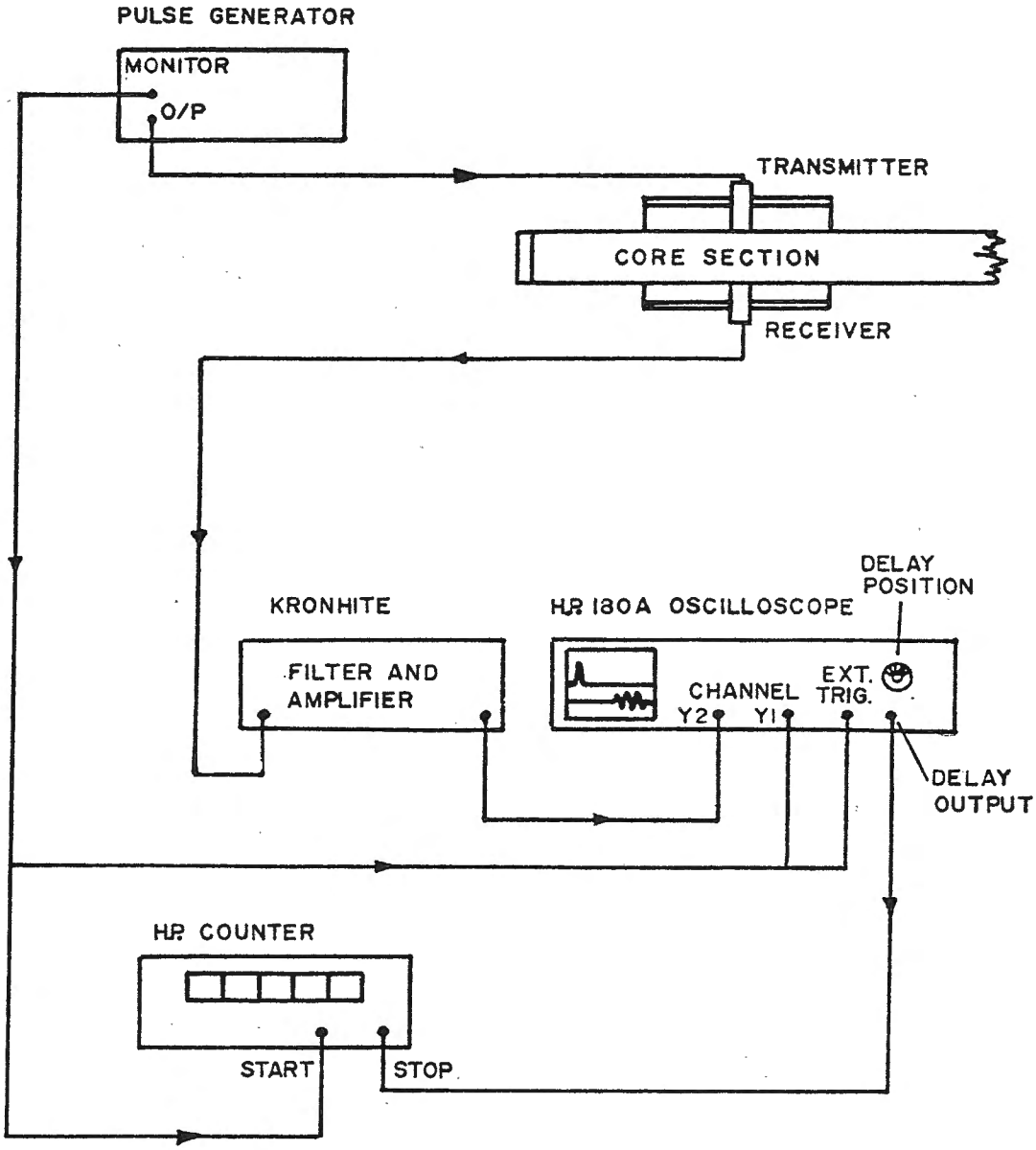

SCHEMATIC DIAGRAM OF THE SOUND VELOCITY MEASURING EQUIPMENT

Fig. 3·2

delays were converted into sound velocities with an accuracy of ± 5 ms^{-1} (Appendix 2). After these calculations, the distance down core and the velocities were digitized for further analysis.

Measurement of Shear Strengths

A standard Wykham Farrance shear vane was used to measure both "undisturbed" and "remoulded" shear strengths in the usual way (Lambe and Whitman, 1969). The angular torque, in a calibrated spring applied at a constant rotational speed on a vane of known dimensions, was recorded and converted into shear strength. The shear vane technique requires that the sediment be cohesive and undrained. The fine grained sediments in the upper part of the cores tested are believed to satisfy these criteria; however, the results in the more sandy and gravelly material lower in the cores should be viewed with caution since intergranular friction, and not cohesion, is the dominant strength mechanism in such sediments. This is further discussed in the results section of this Chapter. Sensitivity is the ratio of undisturbed: remoulded shear strength.

Measurement of Bulk Density, Porosity and Water Content

To minimize unwanted disturbance, the following sampling procedure was adopted: after careful splitting, the sampling locations were chosen with reference to lithology, X-radiographs and velocity-scanning data. Shear strengths (undisturbed and remoulded) were measured first by direct insertion of the shear vane into one half of the split core. Next, a small (~ 50 g) sediment sample was cut from the core adjacent to the location of the shear vane measurement. This was carefully trimmed to remove

sediment that had been close to the liner, where disturbance occurs, and kept in a cold box to prevent desiccation prior to weighing.

A simple buoyancy technique employing Archimedes principle was used to determine the bulk density of the sediment sample. Varsol was used as the displaced fluid because of its immiscibility with water, thereby leaving the samples intact after weighing them in the fluid. The samples were then dried in an oven for 24 hours, cooled, and weighed again to determine porosity (after a salinity correction) (see Hamilton, 1971a) and water content. The cores showed no tendency to crack or split, as do gassy cores, suggesting that the assumption that the sediments were saturated and gas free, as implied in these calculations, was justified. Grain size (% gravel, sand, silt and clay) measurements were made on a selected two-thirds of the geotechnical samples using standard techniques (Piper, 1974). In total, 156 geotechnical samples were taken and of these, 100 were analyzed for grain size.

Results and Discussions

The variations in geotechnical properties are plotted agains distance down core; detailed X-radiographic and lithological descriptions are included (Figs. 3.4 to 3.9) to show how the geotechnical variations correlate with the lithological changes. This will be of major importance later, when acoustically reflecting horizons are identified and compared with the sedimentary structure. To show the similarity of the geotechnical analyses to those of other workers (e.g. Hamilton, 1970) scatter-diagrams of the various parameters have been drawn (Figs. 3.10

Figs. 3.4 to 3.9: The following six figures show the down core variations in the measured geotechnical properties. The corresponding core number and cruise sample number is given as a heading on each diagram.

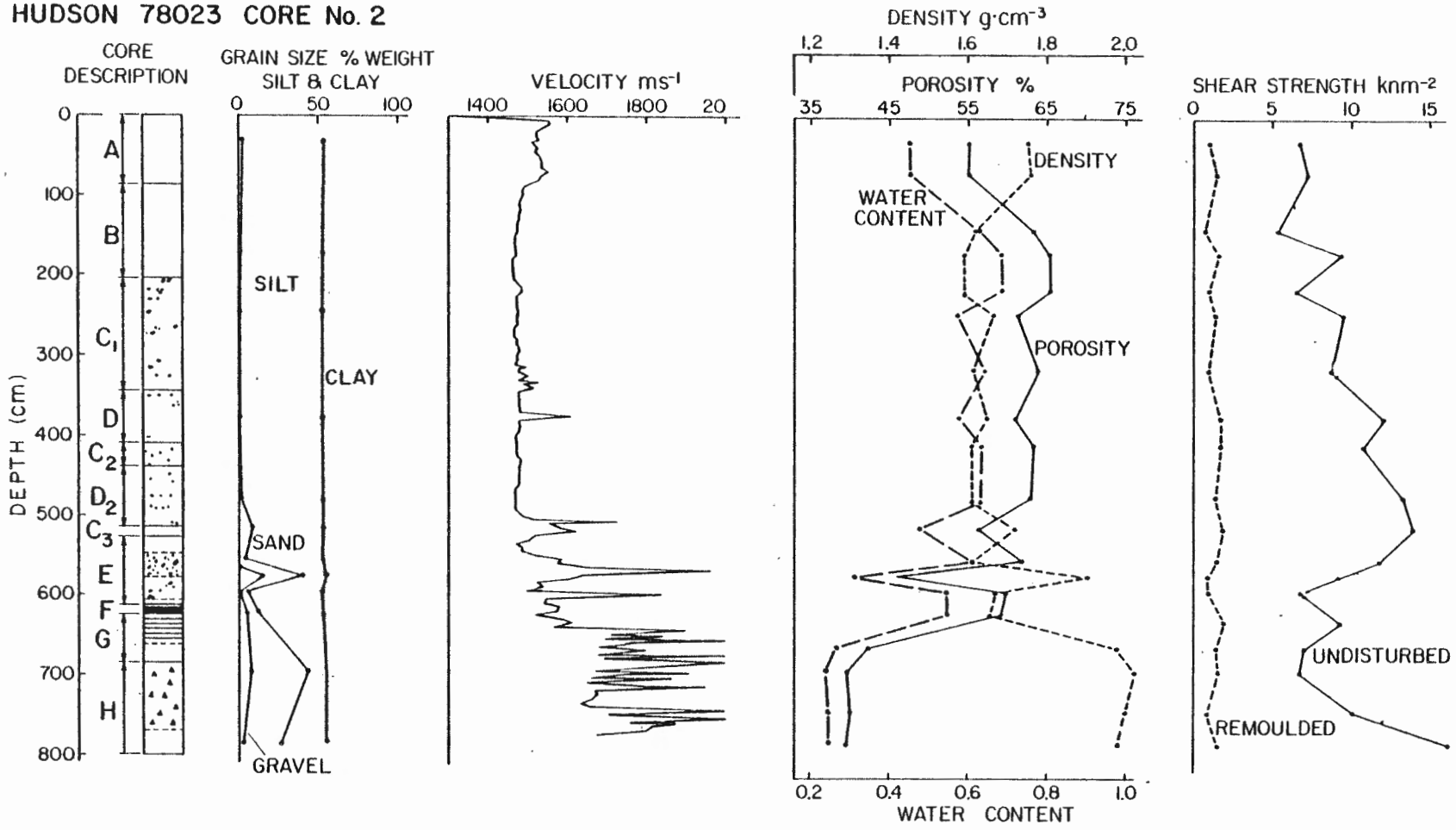
HUDSON 78023 CORE No. 2
CORE DESCRIPTION
GRAIN SIZE % WEIGHT SILT & CLAY
VELOCITY ms-1
DENSITY g·cm-3
POROSITY %
SHEAR STRENGTH knm-2
DEPTH (cm)
A
B
C1
D
C2
D2
C3
E
F
G
H
SILT
CLAY
SAND
GRAVEL
DENSITY
WATER CONTENT
POROSITY
UNDISTURBED
REMOULDED
WATER CONTENT

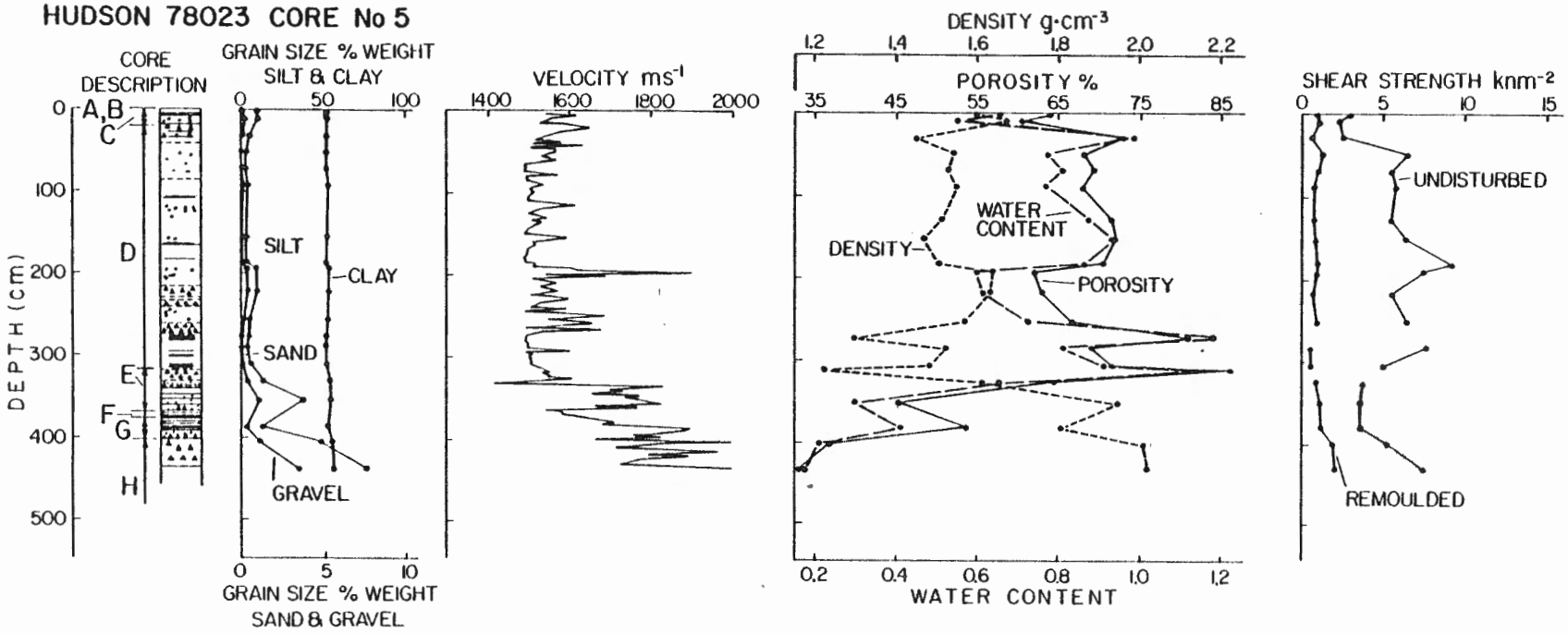
HUDSON 78023 CORE No 5
CORE DESCRIPTION
A,B
C
D
E
F
G
H
DEPTH (cm)
0
100
200
300
400
500
GRAIN SIZE % WEIGHT
SILT & CLAY
0
50
100
SILT
CLAY
SAND
GRAVEL
0
5
10
GRAIN SIZE % WEIGHT
SAND & GRAVEL
VELOCITY ms⁻¹
1400
1600
1800
2000
DENSITY g·cm⁻³
1.2
1.4
1.6
1.8
2.0
2.2
POROSITY %
35
45
55
65
75
85
WATER CONTENT
DENSITY
POROSITY
0.2
0.4
0.6
0.8
1.0
1.2
WATER CONTENT
SHEAR STRENGTH knm⁻²
0
5
10
15
UNDISTURBED
REMOULDED

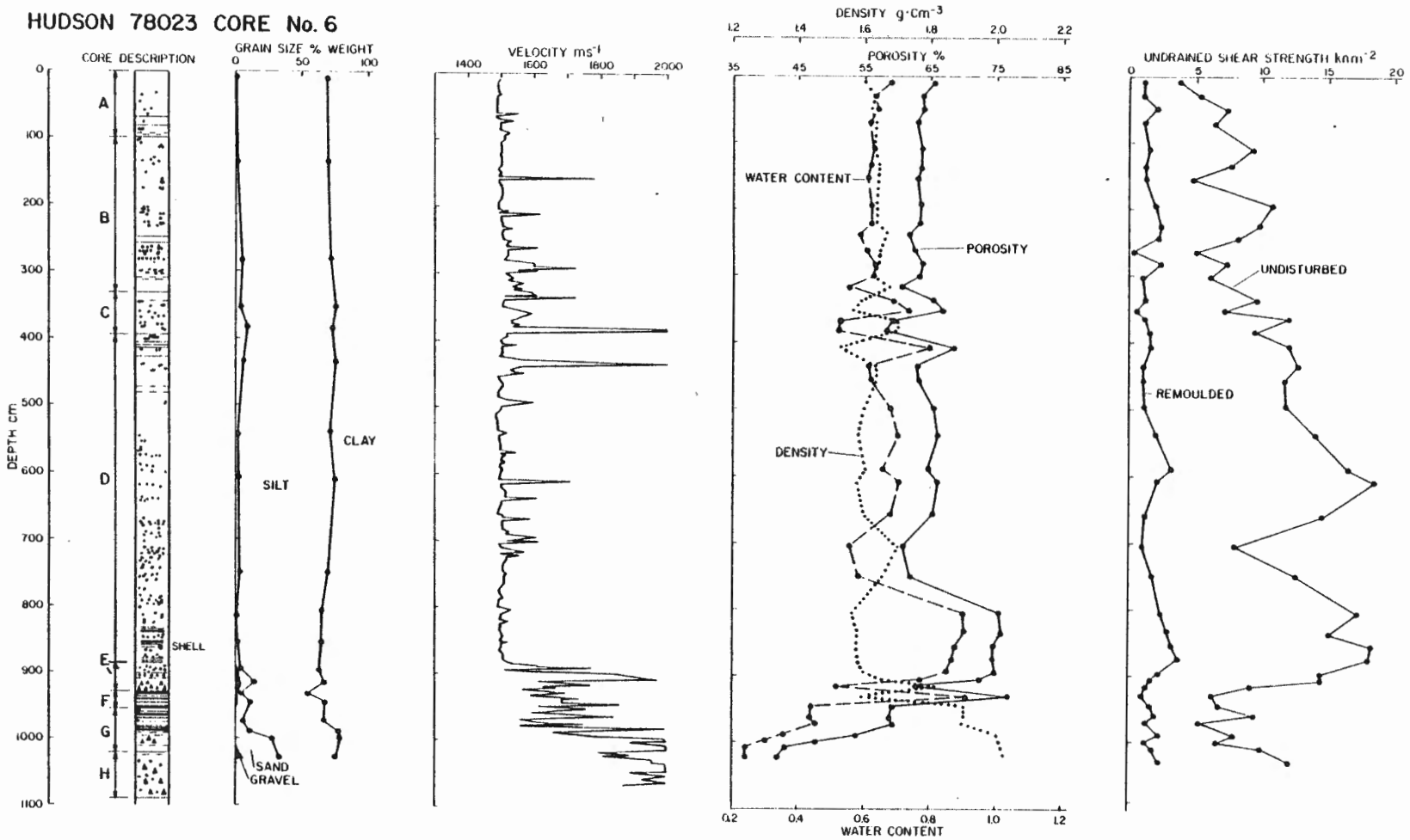
HUDSON 78023 CORE No. 6
CORE DESCRIPTION
GRAIN SIZE % WEIGHT
0
50
100
VELOCITY ms⁻¹
1400
1600
1800
2000
DENSITY g·cm⁻³
1.2
1.4
1.6
1.8
2.0
2.2
POROSITY %
35
45
55
65
75
85
UNDRAINED SHEAR STRENGTH kNm⁻²
0
5
10
15
20
DEPTH cm
0
100
200
300
400
500
600
700
800
900
1000
1100
A
B
C
D
E
F
G
H
SHELL
SILT
CLAY
SAND
GRAVEL
WATER CONTENT
POROSITY
DENSITY
UNDISTURBED
REMOULDED
0.2
0.4
0.6
0.8
1.0
1.2
WATER CONTENT

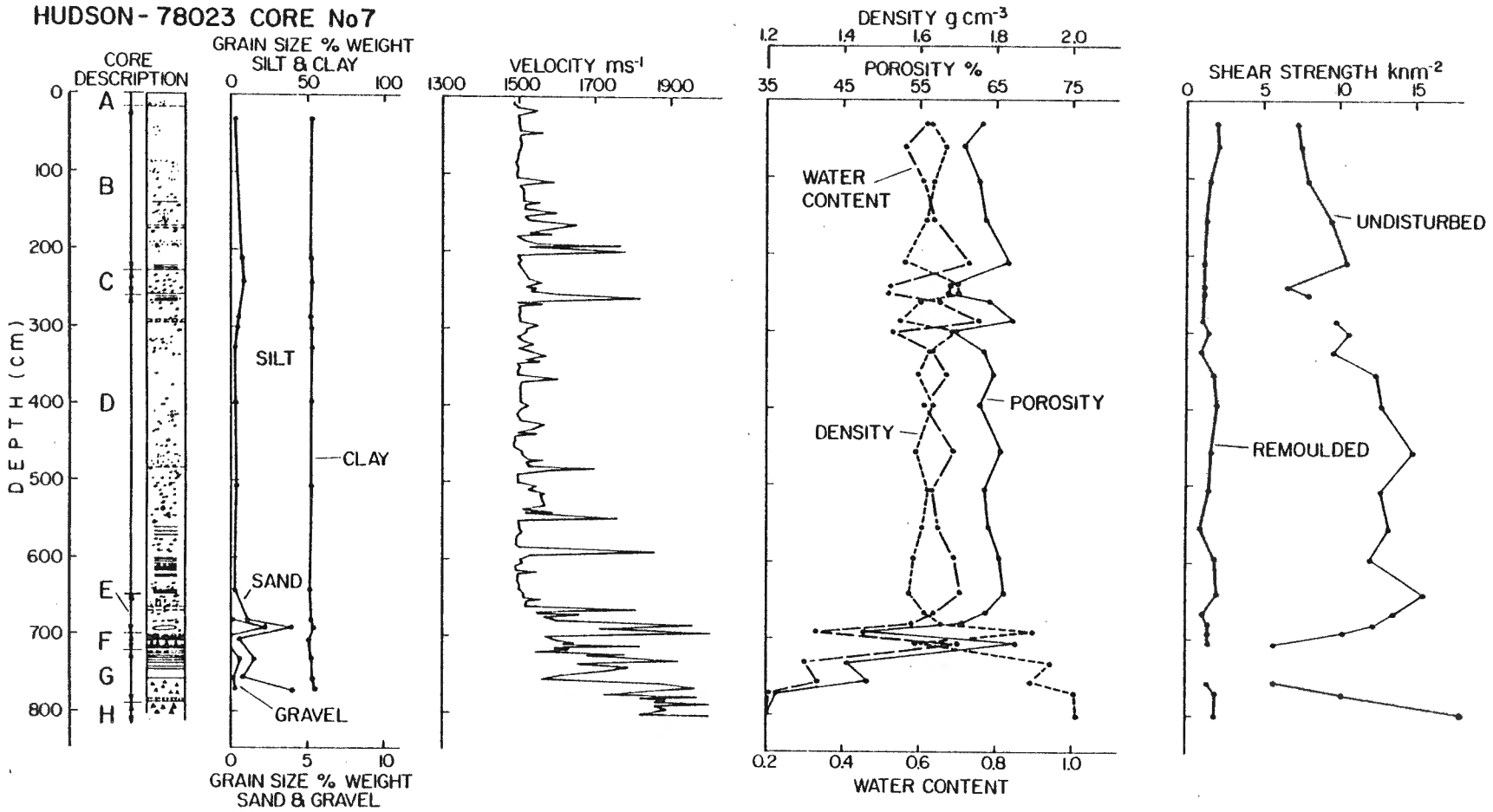
HUDSON - 78023 CORE No7
CORE DESCRIPTION
A
B
C
D
E
F
G
H
DEPTH (cm)
0
100
200
300
400
500
600
700
800
GRAIN SIZE % WEIGHT SILT & CLAY
0
50
100
SILT
CLAY
SAND
GRAVEL
0
5
10
GRAIN SIZE % WEIGHT SAND & GRAVEL
VELOCITY ms-1
1300
1500
1700
1900
DENSITY g cm-3
1.2
1.4
1.6
1.8
2.0
POROSITY %
35
45
55
65
75
WATER CONTENT
DENSITY
POROSITY
0.2
0.4
0.6
0.8
1.0
WATER CONTENT
SHEAR STRENGTH knm-2
0
5
10
15
UNDISTURBED
REMOULDED

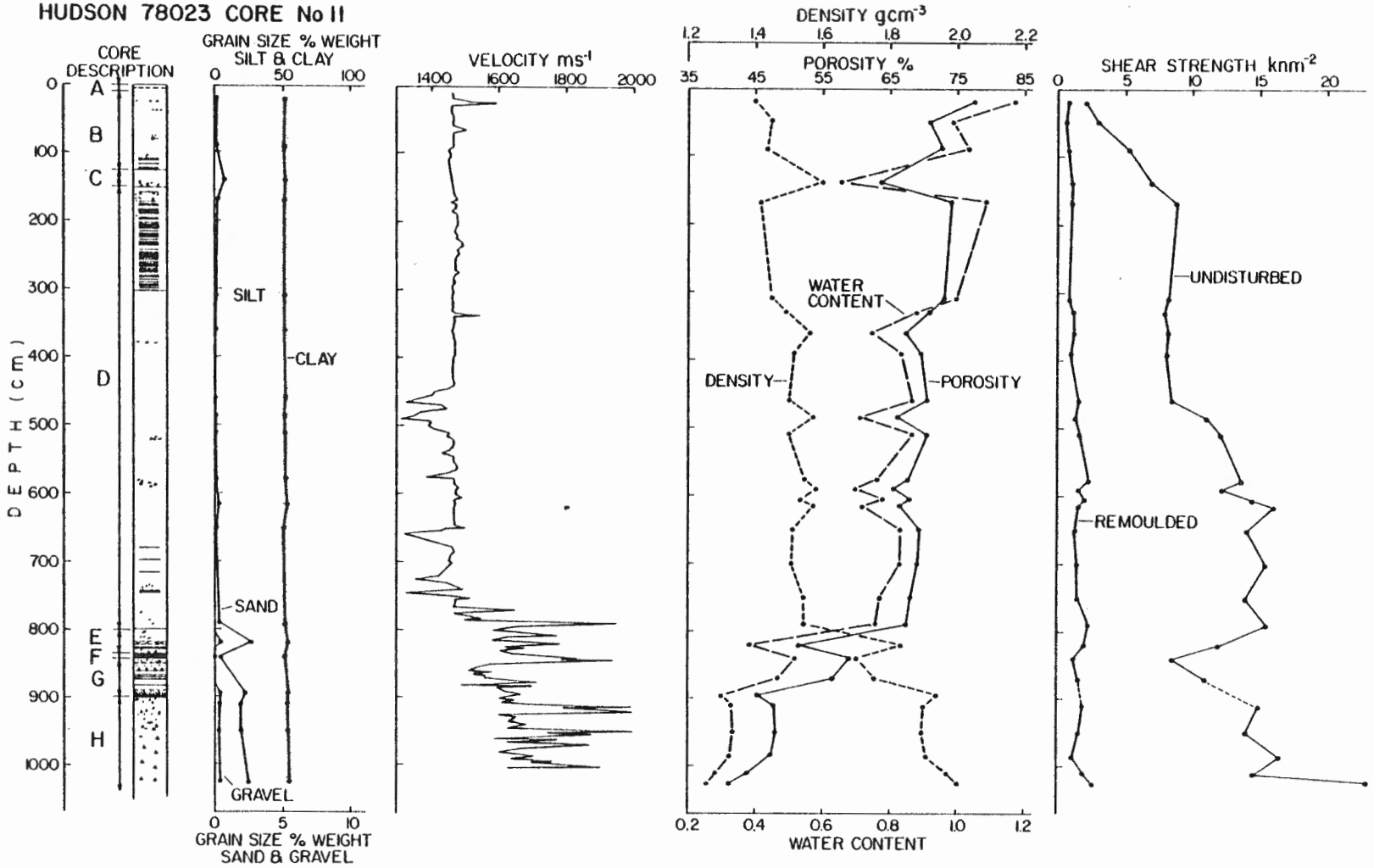
HUDSON 78023 CORE No 11
CORE DESCRIPTION
A
B
C
D
E
F
G
H
DEPTH (cm)
0
100
200
300
400
500
600
700
800
900
1000
GRAIN SIZE % WEIGHT SILT & CLAY
0
50
100
SILT
CLAY
SAND
GRAVEL
0
5
10
GRAIN SIZE % WEIGHT SAND & GRAVEL
VELOCITY ms-1
1400
1600
1800
2000
DENSITY gcm-3
1.2
1.4
1.6
1.8
2.0
2.2
POROSITY %
35
45
55
65
75
85
WATER CONTENT
DENSITY
POROSITY
0.2
0.4
0.6
0.8
1.0
1.2
WATER CONTENT
SHEAR STRENGTH knm-2
0
5
10
15
20
UNDISTURBED
REMOULDED

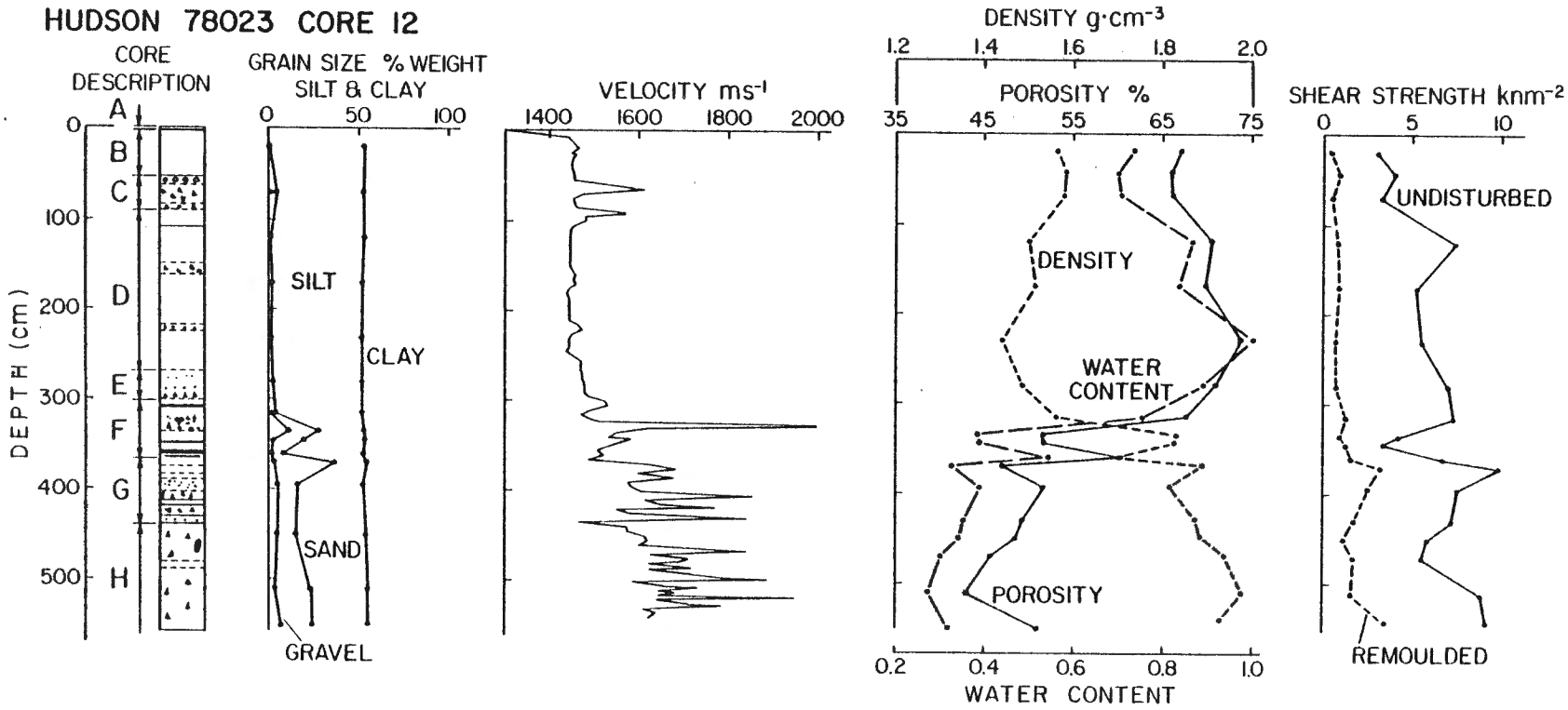
HUDSON 78023 CORE 12
CORE DESCRIPTION
A
B
C
D
E
F
G
H
DEPTH (cm)
0
100
200
300
400
500
GRAIN SIZE % WEIGHT SILT & CLAY
0
50
100
SILT
CLAY
SAND
GRAVEL
VELOCITY ms-1
1400
1600
1800
2000
DENSITY g·cm-3
1.2
1.4
1.6
1.8
2.0
POROSITY %
35
45
55
65
75
DENSITY
WATER CONTENT
POROSITY
0.2
0.4
0.6
0.8
1.0
WATER CONTENT
SHEAR STRENGTH knm-2
0
5
10
UNDISTURBED
REMOULDED

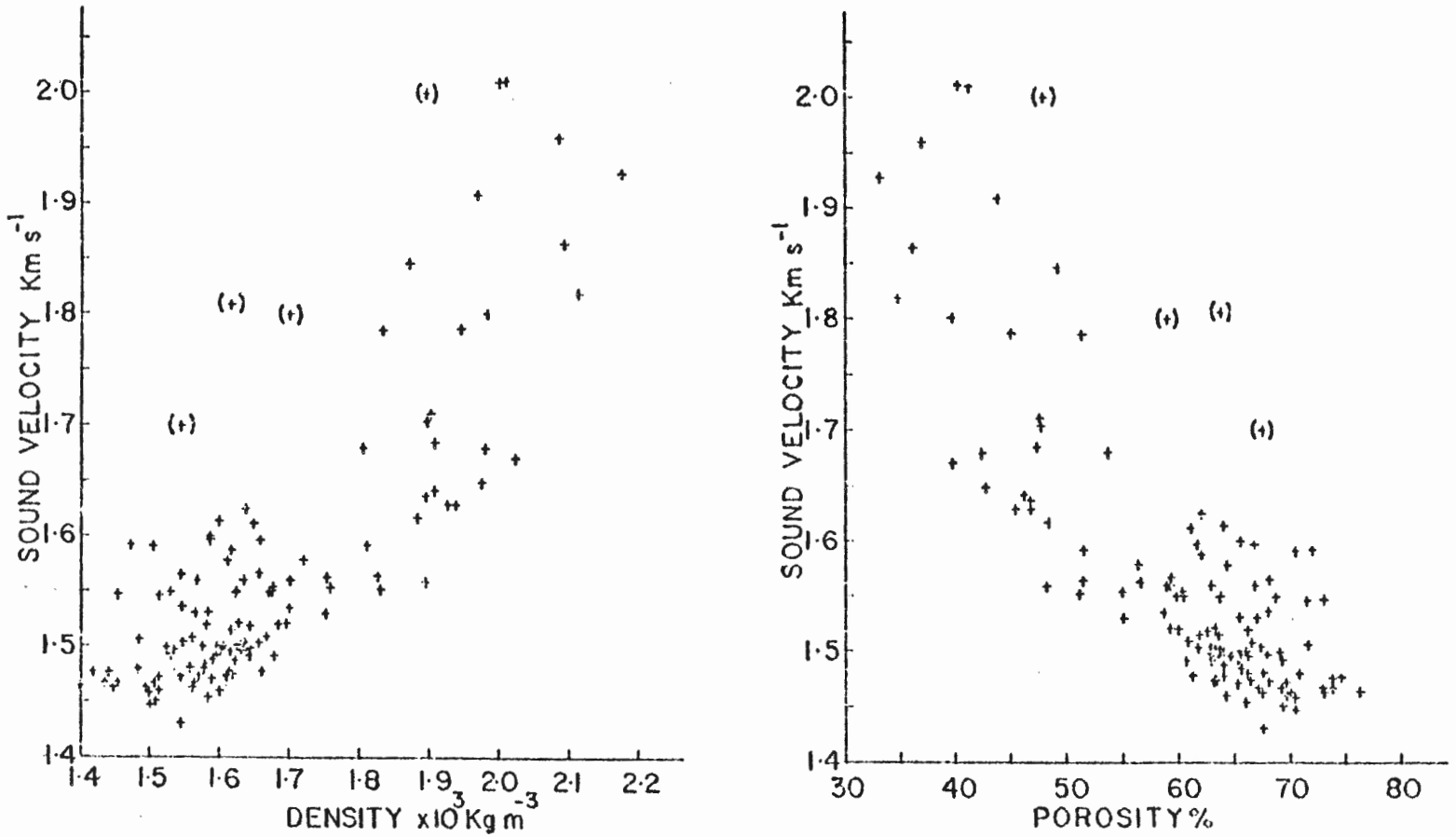

Fig. 3.10: Scattergrams of velocity versus bulk density and velocity versus porosity.

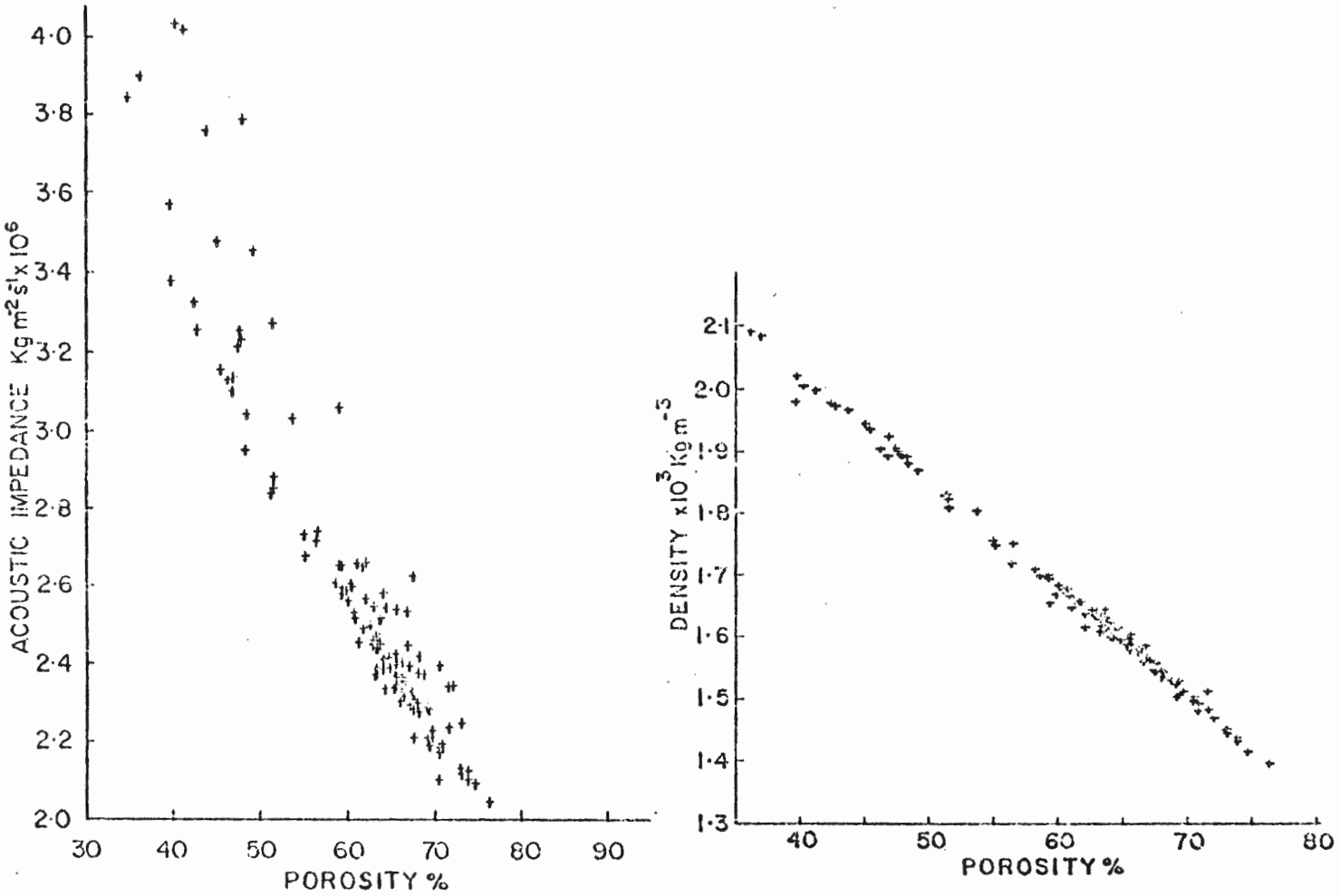

Fig. 3.11: Scattergrams of acoustic impedance versus porosity and density versus porosity.

and 3.11). Significant correlations between parameters were determined by submitting all the data to a statistical program for factor analysis (Nie et al., S.P.S.S. 2nd ed., 1975). The results are given in Tables 3.1 and 3.2. Digitized files of the geotechnical parameters for each core are given in Appendix 3; also, velocity and density variations down core are listed in Appendix 4. Note that the corresponding density data is the result of linear interpolation between measured values, (those in Appendix 3) to give a complete density profile corresponding to the velocity measurements.

Sound Velocity

In contrast with the other geotechnical properties, sound velocity is relatively quick and simple to measure. For this reason and the need for a quasi-continuous velocity profile, velocity variations are the most abundant of the measurements reported here. The estimated accuracy of the measurements is $\pm$ 5 ms^{-1}. Velocities are reported as measured and not corrected for temperature and pressure, contrary to Hamilton (1970, 1971) for the following reasons: for acoustic modelling purposes the in-situ velocities are preferable; the temperature of the sediments immediately after recovery, when scanned, were between 3°C and 7°C, compared with a bottom temperature of 3.2°C measured with an expendable bathythermograph. Since the sediments' temperatures did not change significantly during the velocity measurements, the velocities are thought to be representative of the in-situ seabed. (Note that at a salinity of 36°/$_{oo}$, a temperature change from 3°C to 7°C results in a velocity change of 16 ms^{-1} (Bark et al., 1964).) Pressure has little effect on velocity in

TABLE 3.1: Correlation matrix for geotechnical parameters (no. of cases = 151)

	DENSITY	POROSITY	WATER CONTENT	UNDISTURBED SHEAR STRENGTH	REMOULDED SHEAR STRENGTH	SENSITIVITY	VELOCITY
DENSITY	1.0						
POROSITY	-0.95	1.0					
WATER CONTENT	-0.94	0.96	1.0				
UNDISTRUBED S.S.	0.09	-0.06	-0.07	1.0			
REMOULDED S.S.	0.32	-0.26	-0.30	0.52	1.0		
SENSITIVITY	-0.21	0.18	0.20	0.43	-0.40	1.0	
VELOCITY	0.75	-0.68	-0.64	0.16	0.18	-0.03	1.0

TABLE 3.2: Mean and standard deviation of measured variables (no. of cases = 151)

VARIABLE	MEAN	STANDARD DEVIATION
DENSITY (gcm^{-3})	1.68	0.18
POROSITY (%)	61.23	9.76
WATER CONTENT	0.61	0.21
SOLID DENSITY (gcm^{-3})	2.78	0.18
UNDISTURBED SHEAR (KNm^{-2}) STRENGTH	9.37	4.14
REMOULDED SHEAR (KNm^{-2}) STRENGTH	1.43	0.63
SENSITIVITY = UNDISTURBED/REMOULDED	7.09	3.18
VELOCITY (ms^{-1})	1586.2	157.5

the water depths of the core sites (see Bark et al., 1964).

Some very large local velocity anomalies (Figs. 3.4 to 3.9) are correlated with either large pebbles or dense gravelly and sandy layers which are easily observed on X-radiographs. Other possible reasons for unusual velocities are:

(i) poor transducer coupling to the liner;

(ii) poor coupling between the core line and the sediment, due to air-filled gaps and/or gas bubbles;

(iii) internal disturbance of the sediment due to expansion-causing cracking or possible suck-in from the coring process;

(iv) Layers of high-velocity sediments thinner than the acoustic transducer elements.

Conditions (i) and (ii) can be readily seen during scanning and duly rectified. X-radiographic analysis provides acceptance guidelines for (iii). Interference caused by sound travelling at two different speeds has been investigated in the laboratory (Tucholke and Shirley, 1979). Their results indicate that received signal amplitudes can drop below measurement level, thereby causing errors in estimating the delay time.

In cases where received signal amplitude decreases were observed, improvements in the signal were first sought by replacement of the transducers; if no change was observed, further inspection for cracks, bubbles or disturbances were made and then the transducers were moved a small distance (~ 1 cm) along the core to seek an improved signal amplitude.

The validity, thickness and extent of sediment layers of anomalous velocities have a significant effect on acoustic propagation in the seabed (see Chapter 5).

Sound Velocity, Density and Porosity

The correlation matrix (Table 3.1) indicates that sound velocity is most highly-correlated with density and porosity.

The relationship between sound velocity versus porosity has received considerable attention in the past (Hamilton et al., 1956; Hamilton, 1970, 1971; Akal, 1972; Buchan et al., 1972) because porosity is an easily-measured property that can be determined routinely in standard sedimentological analyses. Velocity is largely dominated by the effect of the compressibility of pore water rather than the compressibility of the mineral grains; therefore, porosity provides a useful empirical index of sound velocity. Because solid density is almost constant (Table 3.2), density and porosity are linearly related to each other and to the sound velocity (Figs. 3.10 and 3.11).

The relationships illustrated in Figures 3.10 and 3.11 are similar to those of Hamilton (1970) (Figs. 6 and 8) from the North Pacific continental terrace environment. The velocities herein are approximately 50 ms^{-1} lower because they are not corrected from the in-situ temperature to 22°C (see Bark et al., 1964, for velocity tables). Several measurements (shown in brackets in Fig. 3.10) have higher velocities than the others of comparable densities and porosities. This effect is due either to the conditions mentioned previously, or to the sample sizes for porosity and

density being insufficient in the sparsely-gravelled sediment.

More figures and data relating acousting progagation to the elastic properties of marine sediments are given in Hampton (1967), Horn et al. (1968), Hamilton (1970, 1971), Buchan et al. (1972), Akal (1974).

Shear Strengths

The relationships between shear strength and the other measured parameters do not suggest that it can be used as an empirical index for other geotechnical properties (Table 3.1). This is in agreement with the findings of Horn et al., (1968); Shreiber, (1968a, b) and Hamilton, (1970).

Shear strength has two components: cohesion and friction. Shear strength in sandy sediment is essentially due to intergranular frictional contact and resistance. In fine grained sediments, cohesion, caused by physicochemical forces of an interparticle, intermolecular and intergranular nature, is considered to be the active force (Hamilton, 1971). Measurements using vane shear, triaxial (without normal stress) and fall-core penetrometers are all tests of cohesion only and the results vary with the testing method (Mitchell, 1964). Accordingly, the results of the vane shear tests on the sandy and gravelly sediments lower in the cores examined, do not accurately reflect the shear strength here. Static testing of cohesive sediments cannot be compared with dynamic rigidity (there is reasonable agreement in cohesionless soils) (Whitman and Richart, 1967). In sound propagation, dynamic rigidity is a control-

ling factor. The lack of correlation between the quasi-static rigidity testing of the vane shear strength measurements and velocity implies that vane shear-derived rigidity is not comparable to dynamic rigidity in cohesive sediments.

The data (Figs. 3.4 to 3.9) show a general increase in shear strength with depth down the cores to a discontinuity between units D and E. Aging of deposits may lead to increased sediment structural strength (cohesion) in response to increased intergrain bonding having the nature of cementation (Bjerrum and Lo, 1963). Age does not have to be a primary cause, but it allows time for changes to take place. Such an effect can be seen here, where there is increased shear strength without any significant change in porosity due to overburden pressure. The discontinuity between units D and E is possibly a reflection of a change in the sedimentary régime, and not only caused by the sediment size distribution.

Geotechnical Character of Lithologies

For ease of description and comparison with the seismic data, the cores have been divided into sections A to H (Figs. 3.4 to 3.9). These sections can be compared to the sedimentary facies interpretation of Chapter 4 (Table 3.3 below). The sedimentary facies have been divided into smaller units so that units having different geotechnical features can be more easily identified. We are only concerned with lithological changes observed geotechnically, and facies 3 (diatomite) is a biofacies and has no formal correspondence with the units shown. Where coherent beds of diatoms occur, they are indicated by solid lines that partly

span the core illustrations (Figs. 3.4 to 3.9).

TABLE 3.3: Correspondence between geotechnical sections and sedimentary facies

GEOTECHNICAL SECTIONS	SEDIMENTARY FACIES
A, B, D	1 (possibly 3)
C	2
E, F, G	4 (possibly 3)
H	5

The upper units (A, B and D) show variations in geotechnical parameters caused largely by the sporadic gravel content of the otherwise homogeneous mud. In may cases, the grain size data is biased towards the finer fraction, due to sample size: the acoustic scanning method illuminates a cross-section of several cm^2 through the core; the sound will be transmitted via the fastest path (i.e. through the coarsest sediments) and therefore, grain size samples cut from a small part of the sediment body may be unrepresentative. Future work of this nature should use at least one half of a core for sampling.

Unit C, corresponding to the carbonate mud facies (Number 2) (see Chapter 4), has a significant gravel content and this is reflected in both the velocity and density increases with respect to the surrounding sediment. Down to the boundary between units D and E, the shear strength shows a general increase with depth, supporting the hypothesis of Bjerrum

and Lo (1963), mentioned earlier.

The most obvious feature in the geotechnical data is the discontinuity between units D and E. The pattern is consistent: a sharp velocity increase occurs as the gravel content of the sediment increases. Concurrently, a density increase and corresponding changes in porosity and water content are evident. The sharp density and velocity increases produce a large increase in acoustic impedance which results in a high reflectivity from this subsurface boundary.

Within units F and G there is usually a decrease in velocity and density due to the layers of porous fine mud within the more gravelly matrix. Sampling practicalities would not permit as many density measurements as there are measurements of velocity, so the description of the physical variations accompanying the sedimentology is incomplete. The implication of this will be discussed in Chapter 5.

Unit H is a diamicton (see Chapter 4). It is composed of gravelly mud with a complete spectrum of grain sizes and contains no sedimentary structures. This results in a medium which has a high average velocity and density and acoustically behaves as an efficient scatterer and attenuator of sound.

After lithologic comparisons between the gravity trip cores and the tops of the piston cores in the laboratory, it became apparent that up to 1.5 m of sediment is missing from some cores. Geotechnical measurements were not made on the gravity cores because on ship it was thought that a complete sediment section had been recovered. Thus the density and

velocity variations at shallow depths (down to 1.5 m) in the seabed are unknown and limit the prediction of the reflected pressure-wave from the seabed described in Chapter 5 and also, the absolute correlation of the acoustic character down the core to the seismic record because the zero reference (the seabed) is missing.

CHAPTER 4

SEDIMENTOLOGY OF THE LATE QUATERNARY DEPOSITS

The sedimentological and stratigraphic data of this study, though somewhat restricted, are sufficient for an interpretation of the changing sedimentary and environmental conditions in the study area since the last (Wisconsin) glaciation. This, the first detailed work on the inner shelf, acts as a useful adjunct to the findings of workers in adjacent areas; (e.g. Drapeau and King, 1972; Slatt, 1974; Fillon, 1976; Piper et al., 1978).

Six piston cores have been chosen for their completeness of geological section and adequate D.T.S. seismic coverage (see Chapter 2). Of these, cores 6 and 7 from a basin seaward of Cape St. John (Fig. 2.1), have identical lithologies and are used as standards with which the other cores are correlated (Fig. 4.1).

The labeled sediment facies in Figure 4.1 and their characteristics are described below. Detailed X-radiograph descriptions are given in Chapter 3 (Figs. 3.4 to 3.9). With the exception of core 2, the cores were recovered from water depths of 280 m or greater. This is unusually deep for a continental shelf and may possibly have provided sedimentary environments relatively undisturbed by sea level changes, though the effects of bottom currents in shelf areas is poorly studied (Kulm, 1973).

Comparisons between the top of all piston cores with their gravity trip cores has shown up to 1.5 m of sediment were lost during coring.

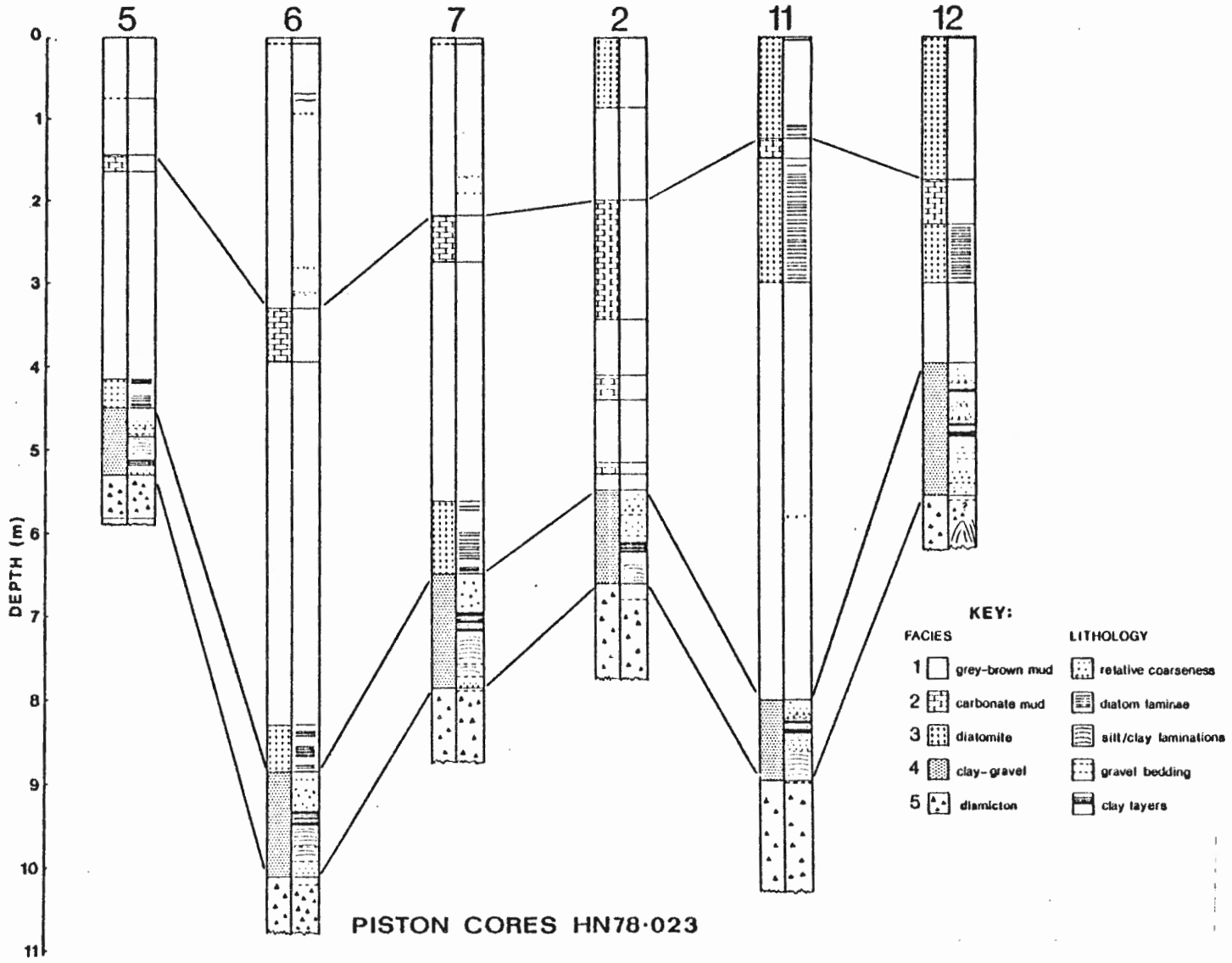

Fig. 4.1: Lithofacies correlation diagram.

In the facies diagram, total sedimentary sections synthesized from both the piston and trip cores are shown.

Facies Description

Five sedimentological facies have been identified on the basis of texture, colour (using the Munsell scheme, 1954 ed.) and X-radiography. The equivalence between these facies and the geotechnical units defined in Chapter 3 is given in Table 3.3.

Facies 1: Grey-brown Mud

A grey-brown mud (2.5 Y 4/1) is found in the upper part of all cores. It is structureless, but contains some ice-rafted pebbles which are more abundant low in the facies of the inshore cores (Numbers 5, 6 and 7). The top of facies 1 is usually slightly sandier and darker in colour (dark brown 7.5 YR 4/2) reflecting either low deposition or winnowing in recent times. The facies is characteristically poor in kaolinite (~ 10%) and rich in illite (~ 70%). It is probably the equivalent of the olive grey facies of Piper et al., (1978).

Facies 2: Carbonate Mud

Facies 2 is easily distinguished by its greyish-brown colour (10 YR 5/2) which is lighter than the other facies. X-radiographs show it to contain more gravel than the surrounding facies, the gravel content generally increasing in the facies with depth. Detrital carbonate is found throughout the range of grain sizes and other minerals are found in correspondingly diluted amounts, (see mineralogy, later in this Chapter).

Facies 3: Diatomite

A diatomite facies, composed of at least 75% diatoms, has been identified. This is a biofacies and, as such, differs from the other macrofacies described here. In the offshore cores (numbers 11 and 12) this facies is found at the top of the cores overlying facies 1 and is predominantly composed of diatoms of the Discus type. The inner shelf cores (numbers 5, 6 and 7) have a predominance of Chaetoceros fauna and the facies is found between facies 1 and facies 4. Depositional styles between the inshore and offshore cores also differ. Inshore, the facies consists of thick beds (up to 5 cm) of diatoms (> 75% sed. frac.) separated by more muddy sediments. The colour begins to grade towards the weak red of facies 4 from the grey-brown of facies 1 (i.e. from 2.5 Y 4/1 towards 10 R 4/2) even where diatom rich beds occur. Offshore, the bedding in the diatomite is developed to a lesser extent; the beds are much finer (~ 0.5 cm) and correspondingly more dispersion of the fauna throughout the sediment is found. This offshore diatomite is darker brown (7.5 YR 4/2) than facies 1.

Facies 4: Clay-gravel

This facies contains a large spectrum of sedimentary texture in discrete beds within the unit. The boundary between this and overlying facies is gradational, indicated by a gradual colour change over a metre or so from the grey-brown of facies 1 (2.5 Y 4/1) to weak red (10 R 4/2 to 7.5 YR 5/2). X-radiographs show an increasingly gravelly, more massive sediment with depth. The geotechnical data (Figs. 3.4 to 3.9) also show the variations expected to be associated with such a facies change. Four

different types of sedimentation are represented in this facies, typically in the following sequence:

(i) from the uppermost boundary a unit of sandy gravelly mud of approximately 20 cm to 50 cm in thickness is found;

(ii) underneath, and over an interval similar to 4(i), there are generally six thin (~ 2 cm) layers of fine, dusky red (10 R 3/2) clay sediment, separated by more gravelly material;

(iii) this subfacies is composed of finely interlaminated sands, silts and clays. It generally underlies 4(ii) but alternatively, as in core 5, it may overlie the clayey beds;

(iv) facies 4 finally grades into an increasingly coarse sand. The lower surface of this sand marks the boundary with facies 5.

Facies 5: Diamicton

The bottom of the cores sampled a poorly sorted gravelly sandy mud which is interpreted as a diamicton (definition of Flint et al., 1960). The unit exhibits better sorting and also greater microfossil abundances offshore, the significance of which is discussed later. Mineralogically, the facies is poor in illite (~ 45%) and rich in kaolinite (~ 30%).

Mineralogy

The clay and sand fraction mineralogy of 12 representative samples from the visually identified facies were analysed:

(1) to substantiate the visually identified facies described previously, and

(2) to provide data on facies provenance.

Core 6 was chosen as a standard for this analysis due to its length, position and completeness of section and, unless otherwise stated, all the data discussed is derived from this core.

Clay Minerals

The clay minerals (< 2μ sample fraction) were examined by X-ray fraction using the preparation and analysis techniques of Piper and Slatt (1977). The identified clay minerals are predominantly illite, chlorite, kaolinite and montmorillonite. Small amounts of mixed layer minerals may be present, but they were insignificant. Of the non-clay minerals, K-feldspar, plagioclase, quartz, amphibole, calcite and dolomite were significant. Table 4.1 gives the relative proportions of each mineral expressed as a percentage for both the clay and the non-clay mineral fractions.

The abundances of clay minerals are related to particular facies. Figures 4.2 and 4.3 clearly show the following trends: facies 1 is distinct from facies 5, being poorer in kaolinite and richer in illite. There is also a noticeable intermediate group of samples taken from facies 4 (numbers 30, 34, 36 and 38). This group could possibly represent mixing between the two major facies 1 and 5.

Sources and Provenance

Recent workers (Alam, 1976; Stow, 1977; Piper and Slatt, 1977) have suggested possible sources for clay minerals in Atlantic Canada, but they were generally dealing with more offshore situations. In this study, there is the possibility of placing more stringent restrictions on the possible

TABLE 4.1: Clay Mineralogy of Samples from Core 6 (Recalculated to 100%)

SAMPLE NUMBER	1	12	16	18	20	27	30	34	36	38	40	42	Averages and S.D.'s for Groups 1 → 27		30 → 38		40 → 42	
													Average	S.D.	Average	S.D.	Average	S.D
MONTMORILLONITE	1.52	1.54	4.54	1.89	1.66	6.15	4.59	4.31	2.98	1.61	3.01	2.97	2.88	1.98	3.37	1.37	2.99	0.03
ILLITE	77.27	74.59	72.89	75.03	69.39	70.77	62.72	63.80	56.71	61.62	50.24	49.83	73.30	2.90	61.2	3.13	50.0	0.29
CHLORITE	14.25	15.23	11.55	16.30	16.15	12.59	16.52	14.65	21.47	11.97	17.00	15.73	14.35	1.94	16.15	4.01	16.37	0.90
KAOLINITE	6.96	8.64	11.02	6.78	12.79	10.49	16.17	17.24	18.84	24.80	29.75	31.47	9.45	2.40	19.26	3.85	30.61	1.22

Non - Clay Mineral Clay Fraction (Recalculated to 100%)

QUARTZ	7.87	6.95	12.37	13.11	9.01	8.18	7.65	9.72	9.70	14.02	15.00	20.08	9.58	2.54	10.27	2.68	17.54	3.59
AMPHIBOLE	8.28	11.43	2.69	5.61	8.30	9.56	5.59	4.55	5.02	-	10.00	16.44	7.65	3.08	3.79	2.56	13.22	4.55
K-FELDSPAR	23.75	31.45	27.08	35.97	26.52	40.09	38.63	41.05	43.15	50.76	45.07	42.42	30.81	6.25	43.47	5.24	43.75	1.87
PLAGIOCLASE	43.30	46.07	42.20	37.40	34.86	42.17	39.69	38.95	35.32	24.10	26.00	21.06	41.00	4.11	34.52	7.2	23.53	3.49
CALCITE	10.05	2.00	9.47	2.53	13.69	-	2.96	2.40	3.25	8.11	2.05	-	6.29	5.50	4.18	2.64	1.03	1.45
DOLOMITE	6.76	2.10	6.19	5.38	7.62	-	5.48	3.33	3.56	3.01	1.88	-	4.68	2.98	3.85	1.11	0.94	1.33

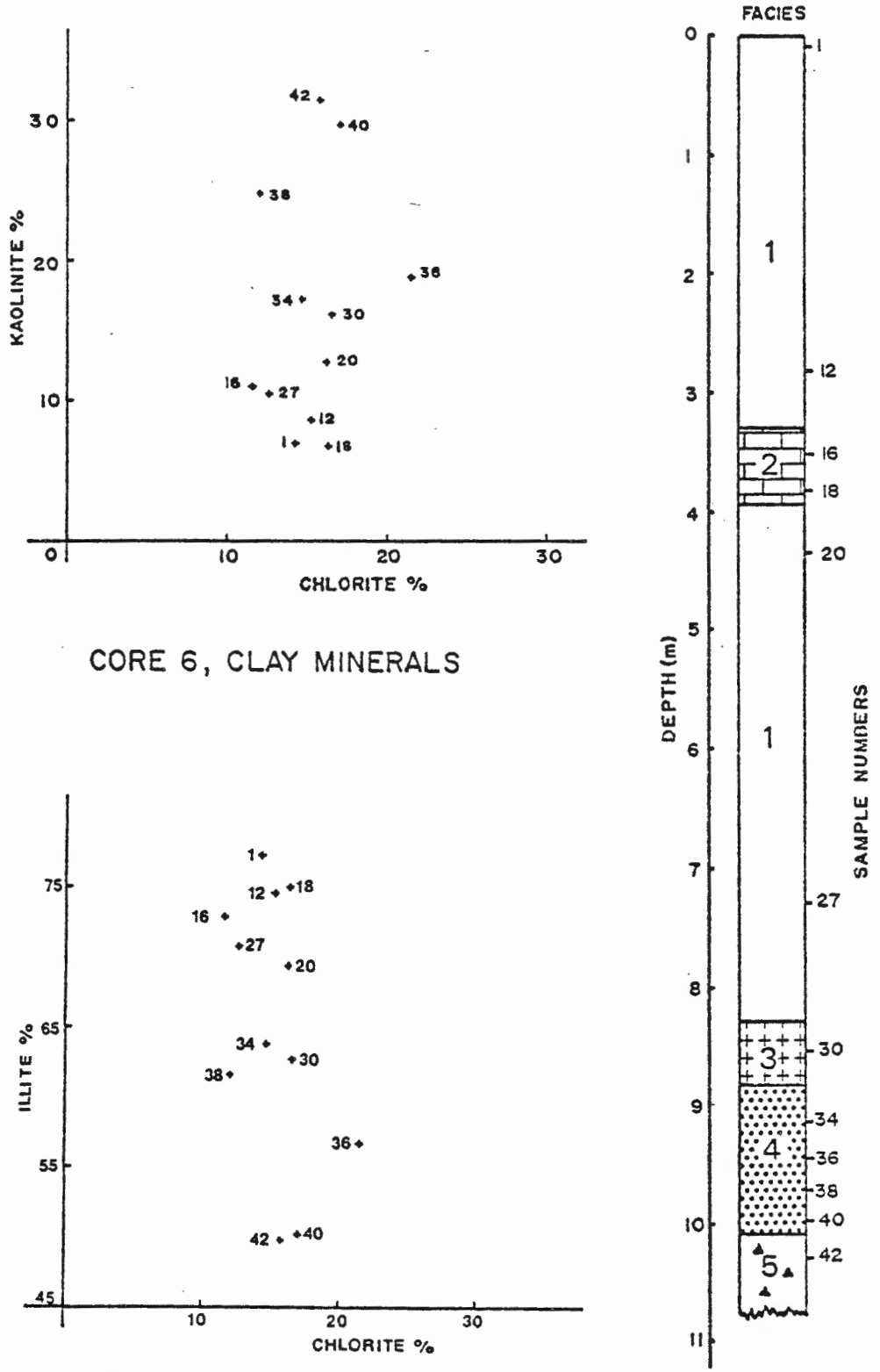

Fig. 4.2: Scattergrams of clay mineral data for core 6; the figures indicate a mineralogical polarization between the major sedimentological facies 1 and 5.

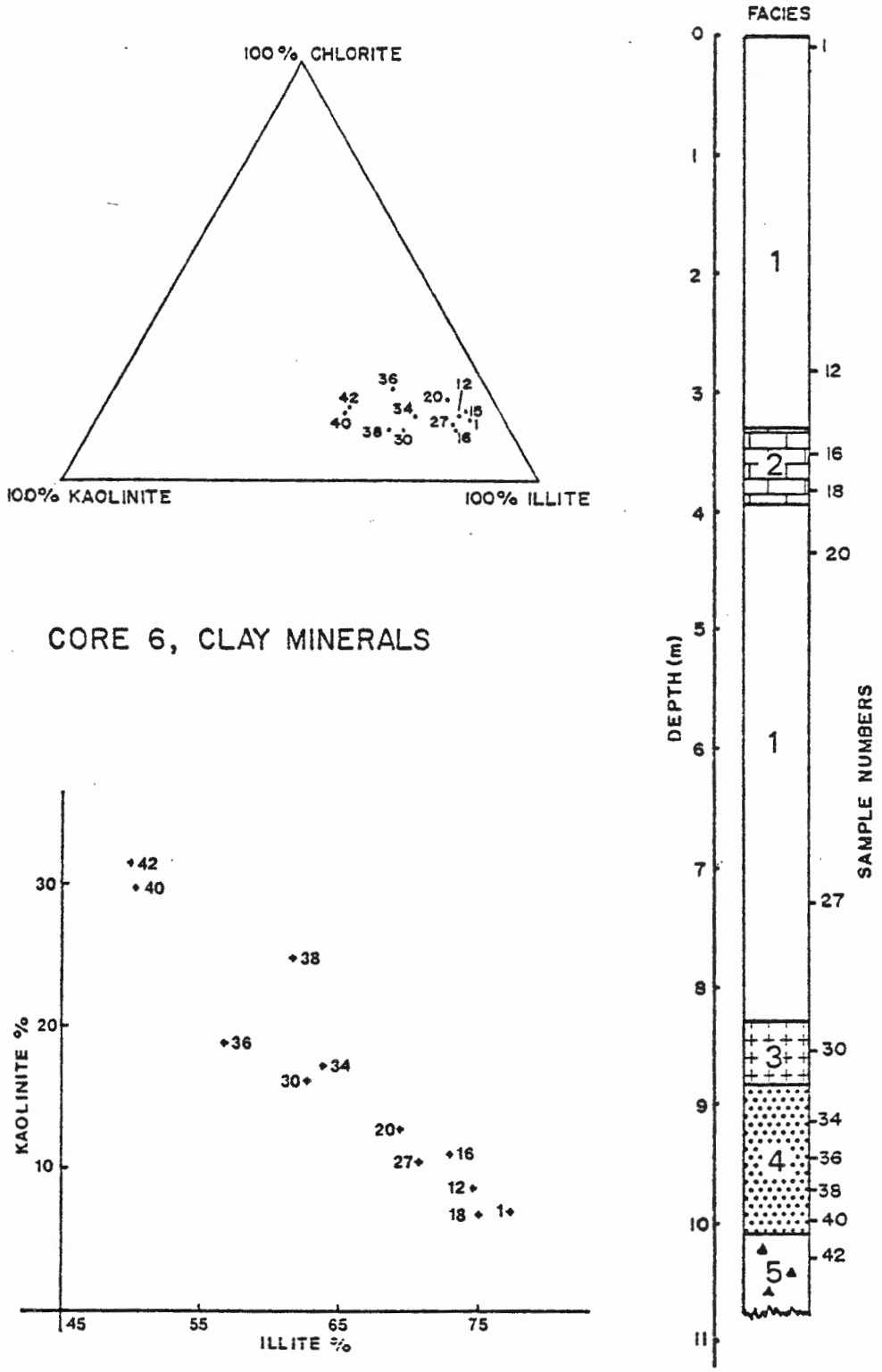

Fig. 4.3: Scattergrams of clay mineral data for core 6; the figures indicate a mineralogical polarization between the major sedimentological facies 1 and 5.

sources.

Kaolinite probably has its origin in the Carboniferous sediments that have been shown to occur extensively northeast of Newfoundland (Haworth et al., 1976a) and may also have equivalents in the Gulf of St. Lawrence (Loring, 1973; Haworth and Stanford, 1976). Coal fragments recovered from facies 5, which is the unit richest in kaolinite, have been dated using spore analysis techniques as Westphalian A age or possibly slightly older (S. Barss, Bedford Institute, pers. comm., 1979).

The presence of illite and chlorite probably reflects a predominance of the local Precambrian and lower Paleozoic igneous and sedimentary rocks, many of which have undergone low grade metamorphism, and also possibly land run off through the so-called "grey Newfoundland type till" (Alam, 1976).

Once again a tripartitioning between facies can be seen in the non-clay minerals (listed in Table 4.1). The most significant composition changes between facies 1 and 5 are an approximately 10% increase in K-feldspar and a 20% decrease in plagioclase. These changes also reflect the dominance of crystalline versus sedimentary sources for the sediment in facies 1 (Stow, 1977).

Sand Mineralogy

Heavy Minerals

Heavy minerals were separated using a floatation technique, employing tetrabromoethane (Carver, 1971). Only the 2.5 ø to 3 ø fraction was used to give a better comparison between samples and limit the problems of

selective sorting. The minerals were identified using a polarizing microscope after mounting on standard heavy mineral slides (A. Aksu, Dalhousie University, written comm., 1979).

Five types of minerals, garnet, amphibole, opaque minerals, ortho and clino pyroxene make up to 90% of the total heavy mineral suite, (this excludes altered grains) (Table 4.2). The discrimination between facies is generally good (see Figs. 4.4 and 4.5). There are slight variations between plots, but the overall pattern of grouping is consistent with a division placed between samples 20 and 27. Sample 27 is at a position of gradual colour gradation towards the weak red of facies 4, indicating that the colour changes may be representative of a mineralogical facies change. The figures also suggest further subdivisions: sample 16 (also possibly 18) and samples 30, 34 and 27 appear distinct from the sediments of the two end-member facies. The latter three samples probably represent a mixing between these end-members and samples 16 and 18 come from facies 2, the carbonate mud.

Light Minerals

Grain mounts of the 2.5 ø to 3 ø fraction were examined using a polarizing microscope (A. Aksu, Dalhousie University, written comm., 1979). The dominant minerals were quartz, K-feldspar, plagioclase, calcite and dolomite (Table 4.3). The light minerals show the poorest discrimination between facies but a general trend can be seen between facies 1 and facies 5.

TABLE 4.2: Heavy Mineral Counts of Sand Fraction (Recalculated to 100%)

Sample Number	1	12	16	18	20	27	30	34	36	38	40	42
Ortho. Pyroxene	3.08	3.85	14.13	8.33	4.44	1.66	1.60	1.80	1.18	1.10	1.83	1.78
Clino. Pyroxene	12.31	12.31	9.78	17.19	17.78	8.84	9.04	8.38	1.41	1.20	4.45	2.00
Tormaline	0.77	-	0.54	1.04	0.74	0.55	-	-	0.94	0.80	0.52	0.89
Zircon	0.77	0.38	1.09	-	0.74	-	-	-	0.71	0.70	0.52	1.11
Garnet	5.38	7.69	17.39	14.58	10.37	3.31	3.01	2.99	2.12	3.0	0.79	3.11
Cass. and Rut.	0.77	0.38	-	-	-	-	-	-	-	-	-	0.22
Titanite	0.77	-	-	-	1.48	-	-	-	0.24	0.20	-	0.44
Apatite	1.54	2.31	1.63	3.13	1.48	-	1.40	1.20	3.53	4.0	1.57	3.11
Staurolite	0.77	1.15	1.63	1.04	-	-	-	-	0.24	0.20	0.26	0.22
Andalusite	0.77	0.38	-	0.52	-	-	-	-	0.24	0.20	-	0.22
Amphibole	39.23	29.62	23.91	25.52	42.96	11.05	10.20	11.38	11.76	12.0	13.35	13.33
Opaques	20.77	31.92	24.46	16.15	10.37	56.91	52.10	53.29	45.41	45.5	48.43	43.78
Glauconite	-	-	-	-	-	0.55	-	-	0.71	0.30	-	0.67
Altered	12.31	6.92	3.26	10.42	7.41	14.36	18.65	16.77	29.88	30.80	26.18	26.66
Coal										*	*	*

* = present

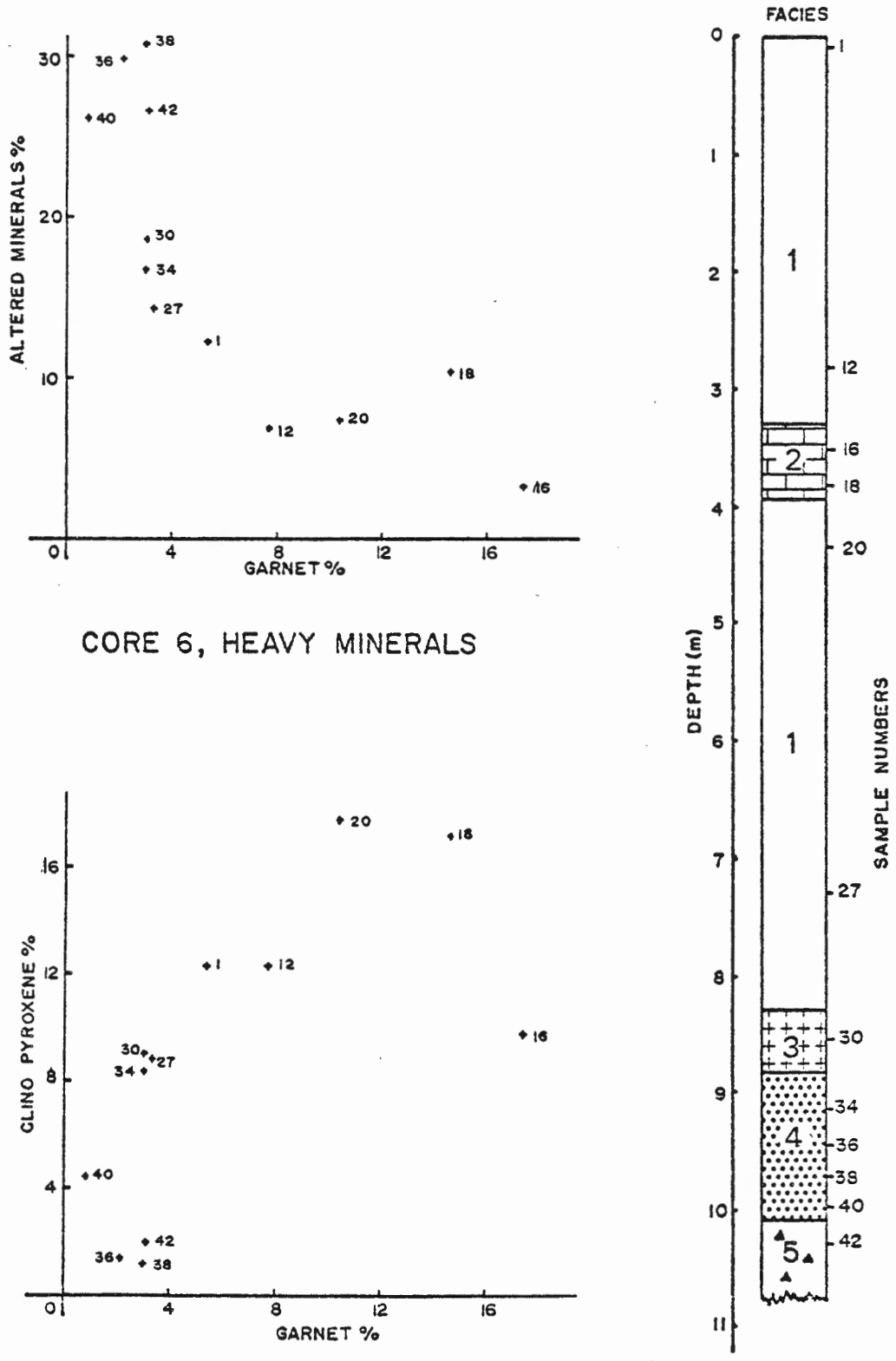

Fig. 4.4: Scattergrams of heavy mineral data for core 6; the figures indicate a mineralogical polarization between the major sedimentological facies 1 and 5.

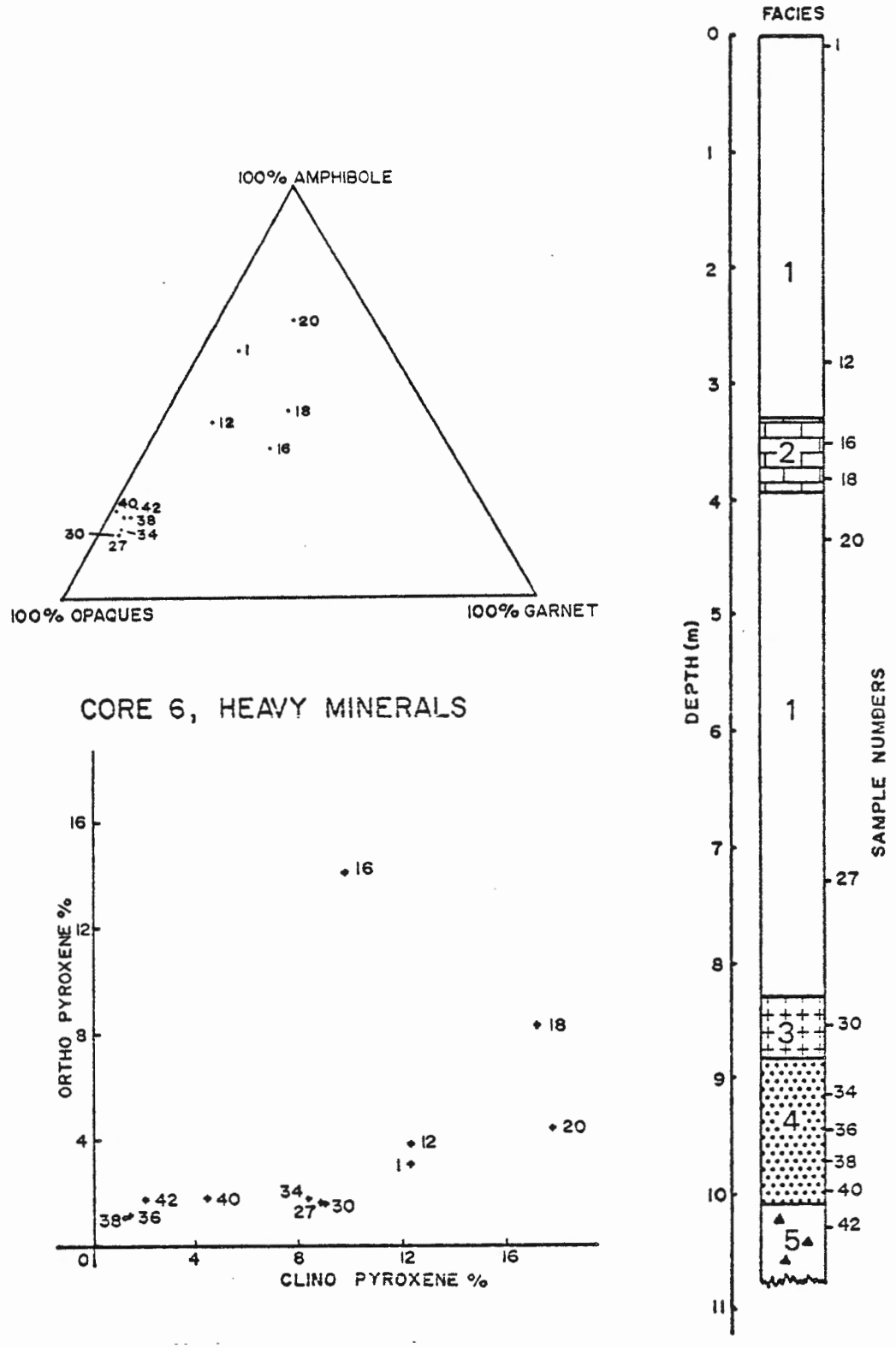

Fig. 4.5: Scattergrams of heavy mineral data for core 6; the figures indicate a mineralogical polarization between the major sedimentological facies 1 and 5.

SAMPLE NO.	1	12	16	18	20	27	30	34	36	38	40	42
QUARTZ	45.16	38.68	32.47	41.94	45.70	50.00	54.50	56.73	36.91	35.41	54.80	60.40
K-FELDSPAR	15.86	16.85	18.73	10.41	21.50	15.00	10.20	9.76	27.87	25.80	17.67	10.26
PLAGIOCLASE	27.98	33.50	43.30	33.43	32.81	25.00	24.40	23.30	31.07	33.01	21.17	23.44
CALCITE	8.67	7.66	4.08	10.93	0.00	6.00	5.40	6.74	2.31	3.06	3.08	4.45
DOLOMITE	2.33	3.31	1.42	3.29	0.00	4.00	5.50	3.47	1.84	2.72	3.27	1.45

TABLE 4.3: Light Minerals (Recalculated as percentages)

FACIES 1	FACIES 5
low quartz (~ 40%)	high quartz (~ 55%)
high calcite + dolomite (~ 10%)	low calcite + dolomite (~ 6%)

The carbonate mud facies has the highest calcite + dolomite percentage and also the lowest amounts of feldspar and quartz. Facies resulting from periods of detrital carbonate rich sedimentation have been observed by other workers throughout Baffin Bay (Aksu, 1977; Aksu and Piper, 1979), the northeast Newfoundland shelf (Piper et al., 1978) and the northwest Atlantic (Chough, 1978).

Marine Microfossils

Diatoms have been discussed previously in the description of facies 3. Benthonic and planktonic foraminifera have been examined in cores 6 and 11 at sampling intervals of approximately 20 cm and 30 cm respectively. These cores provide the longest sections and, therefore, the greatest resolution. Since they were taken respectively from the inner and outer parts of the shelf, the correlation between their results may indicate the possible linking of environmental events (recorded in the microfossils) across the shelf. Foraminifera were separated from the sediment by first sieving to collect the > 63 μ fraction of the sediment and then by floatation, using carbon tetrachloride (Piper, 1974). They were then counted using a binocular microscope (see Appendices 5 and 6; A. Aksu, Dalhousie University, written comm., 1979).

The foraminiferal assemblage is restricted: total number of planktonic forms are low and dominated by G. pachyderma with some G. bulloides. Benthonic species are more abundant and dominated by Cribroelphidium excavatum clavatum, Islandiella islandica and Islandiella teretis with minor numbers of Nonionella labradorica, Astrononion gallowayi, Nonion barleeanum and others. Appendix 5 gives the total counts for core 6. In core 11 only the dominant species were counted (i.e. numbers of G. pachyderma, C. ex. clavatum and total benthonics) and are given in Appendix 6.

Planktonic forms are less abundant inshore, but the data show consistent correlations with the offshore environment (Fig. 4.6). A similarly good down core correlation can be seen in the relative abundances of benthonic foraminifera in the two cores. Although the absolute numbers differ slightly, this agreement between the fauna of the inner and outer parts of the shelf with time suggests an open and similar sedimentary environment and sedimentation rate across the shelf, or at least in the basinal areas on the shelf.

Below the carbonate mud facies of both cores, the general abundance of C. ex. clavatum (as a percentage of total benthonics) is far higher than that found in modern assemblages which show a higher diversity of species (R. Fillon, Bedford Institute, pers. comm., 1979). Though the environmental significance of this is unclear, it does point towards conditions quite unlike those found today.

The correlation between microfossils in cores 6 and 11 (Fig. 4.6) also implies that sedimentation above the carbonate mud facies has been

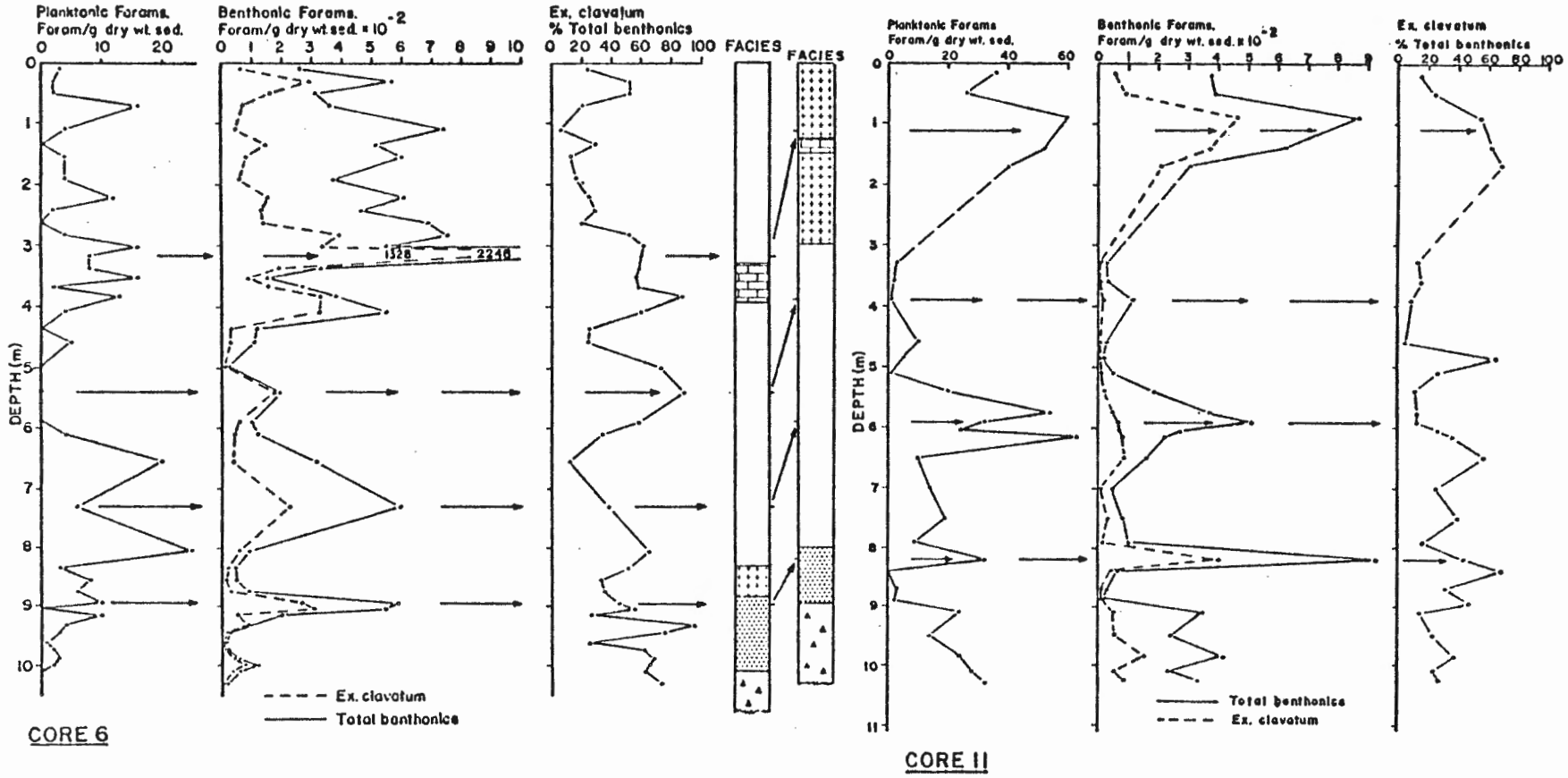

Fig. 4·6: Variations in and correlations between microfossil abundances in cores 6 and 11.

slower in the offshore; this may account, at least in part, for the high abundance of diatoms in recent sediments offshore.

Age Determinations

In this study, the following age determinations and estimates were made:

(1) Carbon 14 age determination on total clay/organic fraction of sediment sample from core 6 at a depth of 899 cm ± 12 cm (i.e. sample length was 24 cm). Age = 25,490 $\pm \begin{matrix}1570\\1310\end{matrix}$ ^{14}C yB.P. (Kruger Enterprises, Geochron. Labs. Div., sample no. GX-6404)

(2) Amino acid racimization age estimations (A.R. Nelson, Dalhousie University/University of Colorado, written comm., 1979) were made on small bivalve shell fragments.

(a) Core 6, HN78023-20, depth 860 cm

(b) Core 7, HN78023-21, depth 342 cm

(c) Core 11, HN78023-31, depth 660 cm

(d) Core 11, HN78023-31, depth 780 cm

Samples a, b and c all have amino acid ratio assemblages which are indistinguishable from modern samples and indicate ages no older than 15,000 yB.P. Sample d has an estimated age of between 15,000 and 20,000 yB.P.

(3) Palynological analyses estimated the ages of core catcher material from HN78023-13, Core 2 as Lower Eocene (G. Williams, Bedford Institute, pers. comm., 1979) and of coal in HN78023-20 (see Table 4.2) as Westphalian A in age (S. Barrs, Bedford Institute, pers. comm., 1979).

Discussion

Correlations

Lithostratigraphically, there is an excellent correlation from basin to basin across the shelf. These changes are paralleled by synchronous events in the microfossil record reflecting an open environment that was similar in both its sedimentary and oceanographic nature. This is thought to be mainly due to the anomalous depth of water on this shelf area.

The diamicton facies in the offshore cores exhibits relatively better sorting than in the inshore cores and also contain higher abundances of microfossil fauna. The offshore diamicton is interpreted as the distal equivalent of the same units further inshore.

An exception to this is found in Core 2: the usual diamicton is highly compacted and spore analysis has shown it to be of Lower Eocene age (G. Williams, Bedford Institute, pers. comm., 1979). Airgun reflection seismics show the sedimentary Carboniferous bedrock collapsed with dissolution of the underlying diapiric salt, creating what has been termed a "salt withdrawal structure" (Haworth et al., 1976a). The lower Eocene sediments which were deposited probably prior to the collapse, became protected from later erosion by the enclosing hard sedimentary bedrock . These Lower Eocene sediments are believed to be the youngest preglacial sediment left on the inner shelf (R.T. Haworth, Bedford Institute, pers. comm., 1979). Also in Core 2, the carbonate mud facies appears "stretched" and the equivalent of the lower part of facies 1, as seen in cores 5, 6 and 7 where it contains significant ice-rafted material, is

missing. The carbonate mud facies also provides us with a useful marker horizon, its significance is discussed in the Chronology section below. This core was collected in approximately 200 m of water as compared with 280 m or greater for the others. A plausible reason for the missing part of lower facies 1 in core 2 is that either such a depositional environment did not occur at site 2, or otherwise it was eroded due to reworking in its comparatively shallower water. (N.B.: relative sea level was probably lower than today, G. Quinlan, Dalhousie University, pers. comm., 1979).

Chronology

As mentioned earlier, a ^{14}C age determination at a depth of 9 m in core 6 gave an age of approximately 25,000 y B.P. An amino racimization age determination on a bivalve at approximately 8 m in the same core indicated an age of no greater than 15,000 yB.P. (A.R. Nelson, Dalhousie University, pers. comm., 1979). Is there a contradiction here? R. Fillon (Bedford Institute, pers. comm., 1979) finds that ^{14}C dates on similar sedimentary units cluster into 3 groups:

(a) 2,000 to 6,000 yB.P.

(b) 8,000 to 13,000 yB.P.

(c) 21,000 to 26,000 yB.P.

Therefore, the possibility of sedimentary hiatuses between periods of large sediment input are not out of the question. The age dating control obtained in this study, though limited, also supports recent evidence and hypotheses (Grant, 1977; Ives, 1978; Andrews and Barry, 1978; Nelson, 1978; R. Fulton, G.S.C., Ottawa, oral comm., 1979; and

other studies) that the classic late Wisconsin ice advance was indeed limited in extent on the eastern Canadian seaboard. These factors will be further discussed in the environmental interpretation which follows.

Environmental Interpretation

Mineralogically, there is a polarisation between the two end member facies (1 and 5). This provides good evidence that two sediment sources have existed. The sedimentary structures indicate a glaciomarine genesis for facies 4 and 5.

When compared with models of glaciomarine sedimentation (Carey and Ahmad, 1961; Reading and Walker, 1966; Overshine, 1970; Tucker and Reid, 1973; Gostin and Herbert, 1973) many commonalities in sediment types with outer, intermediate and distal zones are found in facies 4 and 5 (see Nelson, 1978); for a full description of these zones). Further, the abundance of kaolinite in the clay minerals and the associated coal fragments found in these facies supports a source in the offshore Carboniferous bedrock. The low abundances of microfossils indicates high deposition and/or possibly low biological productivity. The genesis of facies 4 and 5 is therefore interpreted to have involved both glacial erosion of local bedrock as well as ablation processes which gave rise to subfacies 4(i) to 4(iv).

Facies 1 has a mineralogical suite similar to the "grey Newfoundland tills" (Alam, 1976) suggesting that the surrounding land mass was a source for the structureless post-glacial sediments. These were probably input fluvially into the oceanic environment and then transported offshore. The gradational change between facies 1 and 4 suggests that a gradual change from glacial to post-glacial depositional styles occurred, although it is also possible that

TABLE 4.4

Average percentages of heavy minerals and clay minerals in the sample groupings shown

Dominant heavy minerals

Sample grouping	1 → 20 (ex16)	27 → 38	40, 42
Ortho pyroxene	4.9	1.5	1.8
Clino pyroxene	14.9	5.8	3.2
Garnet	9.5	2.9	2.0
Amphibole	34.3	11.3	13.34
Opaques	19.8	50.6	46.1
Altered	9.3	22.1	26.4

Clay minerals

Sample grouping	1 → 27 (ex16)	30 → 38	40, 42
Montmorillonite	2.5	3.4	3.0
Illite	73.4	61.1	50.0
Chlorite	14.9	16.2	16.4
Kaolinite	9.2	19.3	30.6

a hiatus in sedimentation occurred (as suggested by the age determinations). Such a hiatus would not necessarily be readily observable because of the deep water and probably low energy depositional environments in this area.

Piper et al. (1978) have a possible equivalent to the red-brown glaciomarine sediments of facies 4 further eastwards close to the Grand Banks in their facies H. A possible deep water equivalent of the same facies can be seen as far away as the Laurentian Fan, where Stow (1977) reports a "brick red" granular mud facies with a similar mineralogy of facies 4. Although this area is separated geographically from northeast Newfoundland the sediments were probably derived from similar Carboniferous and Triassic bedrock in the Gulf of St. Lawrence (Loring, 1973; Haworth and Sandford, 1976). Stow tentatively dates the facies at 22,000 to 23,000 yB.P. and the lower till at 26,000 to 28,000 yB.P. and notes that the origin of such sediment remains problematic. From his evidence, it appears that the effects of deglaciation may have been felt on the Scotian margin from about 28,000 yB.P. onwards; this also agrees with Nielsen's (1976) evidence, but is contrary to earlier investigations (Flint, 1943; Prest, 1969, 1970; see Tucker, 1976, for a review).

What, then, constitutes the Late Wisconsinan event in the cores analyzed in this study? A further examination of the detailed X-radiographic descriptions of Figures 3.4 to 3.9 clearly show the abundance of pebbles in the cores. Appreciable amounts can be seen in unit E and also in the lower part of unit D in cores 5, 6 and 7. In the offshore cores (numbers 11 and 12) only minor amounts can be seen in two zones, above unit E. If the cause of this deposition of pebbles was due to ice-berg ablation, a more uniform distribution of pebbles in these units might be expected across the shelf (the depth of water is great

enough that grounding is unlikely in either area). The apparent lack of ice rafted material offshore suggests that either the ice rafting was a localized effect, due to either a local source for the ice-bergs, or that the oceanographic circulation caused a massing of ice in the inshore regions. The latter is contrary to observations on ice-berg movements today along the Canadian east coast (Anderson, 1971; Harris and Jollimore, 1974). Large ice-bergs move almost totally under the influence of deeper currents (Bruneau and Dempster, 1972) which, in this case, would be the paleo-Labrador current; the former hypothesis is favoured. The local ice-berg source was probably the Newfoundland land mass. It appears that the glacial conditions were not extreme during Late Wisconsinan time and, therefore, the ice shelf probably advanced only a short distance offshore, as floating ice, due to the great nearshore water depths around the deep fjordic coast of northern Newfoundland.

The sediments of facies 1 probably correspond to the "olive grey and light tan sediment types" of Stanley et al. (1972), the uppermost facies of Piper (1975), Piper et al. (1978) and the "olive grey mud" of Stow (1977). In the recent past, differences between inshore and offshore sedimentation have occurred. The abundance of diatoms in the top of the offshore core has been produced by sedimentation more like that found by Alam (1976) off the Grand Banks, and is thought to be due to modified oceanographic conditions during the Late Holocene (Alam, 1979).

The carbonate mud facies can be correlated with a similar unit found by Piper et al. (1978) on the northeast Newfoundland shelf, and Aksu and Piper (1979) in Baffin Bay. This is thought to be of early Holocene age

(~ 8000 yB.P.) and provides a useful marker horizon.

The diatom bloom, producing facies 3 inshore, occurred during a transition from the depositional environment of facies 4 to that of facies 1. Recent studies concerned with the oceanography of ice shelves (Paquette and Bourke, 1979) and ice biota (Hoshiai, 1972; Horner, 1977) suggest that, close to and under ice shelves, areas of extremely high productivity may exist. Both large nutrient and silica input would be required to produce the numbers of diatoms found in these cores. The role of continental ice shelves in providing necessary conditions for such high productivity remains an important understudied area.

CHAPTER 5

COMPARISONS BETWEEN HUNTEC D.T.S. DATA AND SYNTHETIC SEISMOGRAMS

Introduction

To establish the nature of seismic reflection horizons and their relationship to the observed sedimentary lithologies, the measured acoustic impedances (i.e. the product of density and velocity) which control seismic propagation in the sediments need to be compared in a quantitative way to the recorded field seismic data. Because the D.T.S. data collected for this study has an unfortunately high noise component (discussed later in this Chapter) a forward modelling approach has been adopted: the synthetic or theoretical seismogram response (hereinafter termed synthetics) of the sediments has been computed from the measured velocity and density profiles made on the cores (see Chapter 3) for comparison with the replayed field seismic data.

The theoretical seismogram response (as a variation of pressure with time at a receiving hydrophone on the D.T.S. fish) has been computed by convolving the seismic pressure pulse shape of the D.T.S. boomer source with the impulse response of the sediment column. This simple filter theory approach is possible because of a knowledge of the temporal repeatability of the D.T.S. pulse, and the derivation of an impulse response for the sediments made possible by the velocity and density measurements.

Direct comparisons between the synthetic and field seismograms are facilitated if both data sets have the same format. Continuous variations of pressure with time at the hydrophone were chosen (wiggly traces) and normalised amplitudes and equivalent time scales were used. The forementioned noise on the field data is greater than the expected signal level in some cases, so a gross average measure of the seismic arrivals, the smoothed instantaneous energy, has been calculated for both the field and synthetic seismogram data, and compared with more success.

Recording Huntec D.T.S. Seismic Data

The reflection of sound from the seabed and subsurface physical discontinuities is due to variations of the acoustic impedance with depth. If areally continuous contrasts in acoustic impedance exist, then these surfaces will give rise to reflection horizons which, in simple cases, will be observed as continuous events on the analogue graphic records routinely collected using continuous subbottom profiling systems (van Overeem, 1978).

The principles of producing such records are well known (e.g. Dobrin, 1976); however, some of the features of the D.T.S. are uncommon and worth mentioning:

The D.T.S. (Hutchins et al., 1976) is a towed body "fish" containing an electrodynamic sound source (boomer) which produces a highly repeatable broad frequency band, impulse-like output (Fig. 5.1) directed downwards from the fish (McKeown, 1975). The seismic source is pressure compensated so that the acoustic pressure output is constant to a depth of 300 m.

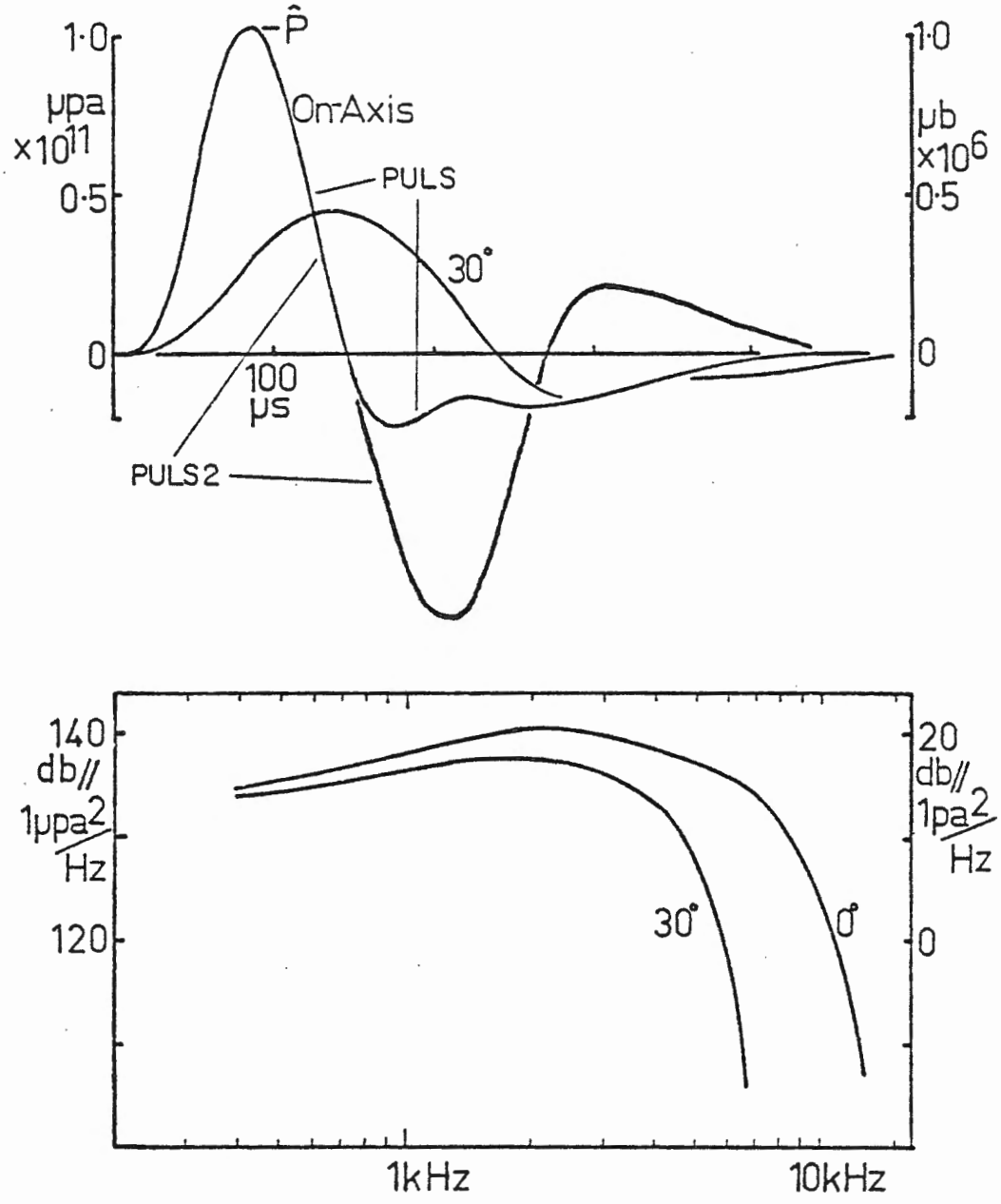

HUNTEC ED10C Boomer pressure pulse and spectra

Fig. 5.1: Huntec D.T.S. far field pressure pulse shapes. For an ED10C boomer PULS is the measured outgoing waveform; the lower figure gives the corresponding spectra both on- and 30° off-axis. PULS2 is explained in the text.

Reflections from the sea floor and subsurface physical discontinuities are sensed by either of two single element hydrophones mounted on the fish. An internal hydrophone is positioned directly beneath the transmitting boomer and an external hydrophone is mounted outside the rear end of the fish's side skin. The fish depth changes with time due to hydrodynamic motions and, more significantly, the heaving of the towing vessel. Heave causes the distance of the fish from the seabed to change with time. If a fixed interval firing rate were used, then the reflections from the seabed and subsurface seismic horizons would be recorded with significant shot to shot advances and delays. This would destroy the registration (coherence) and alignment of one seismic trace with the next, and produce a poor and inaccurate, continuous seismic record of the seabed topography, as well as scrambling any continuous (i.e. coherent) subsurface seismic horizons.

This limits an acoustic system approaching its theoretical maximum resolution (Tyce, 1977). To solve this problem, fish depth is continuously monitored to an accuracy of 0.1 m using accelerometer and pressure transducers, and the boomer firing time is slightly delayed or advanced to maintain a constant firing rate with respect to the crossing of a horizontal surface (Hutchins, 1978). In this study the firing rate was 0.75 seconds. An excitation voltage of approximately 5 kV was used, giving a peak on-axis intensity of 219 dB relative to 1 μPa at 1 m. The output from the transducers on the fish, and the power to the boomer are transmitted along a single, armoured, faired multiconductor towing cable. The hydrophone signals from the fish were monitored and recorded together with a calibra-

tion pulse, a 6.4 kHz reference signal and necessary timing information on a HP3960 4-channel instrumentation tape recorder at a tape speed of 3.75 inches sec^{-1}. At this speed the tape recording passband extends from 50 Hz to 15 kHz and the signal to noise ratio is 38 dB. The signal from one hydrophone is also used as input to an EPC graphic recorder to produce real-time analogue seismic records.

Playback of Huntec D.T.S. Data

The analogue tape recordings made at sea were processed for replay using an analogue to digital converter and digital output system built around a PDP-11 minicomputer (Parrott, 1978). The analogue tapes were transcribed at calibrated levels, filtered to reject frequencies outside the 1 kHz to 10 kHz source bandwidth (to eliminate unwanted low and high frequency ambient noise), digitized shot by shot and stored on conventional 9-track magnetic tapes.

A digitizing interval of 10 μs was used in this study. This corresponds to a Nyquist frequency of 50 kHz (outside the range of the boomer source) which, although unnecessary for fidelity alone, results in flexibility of scaling and smooth display of the data when output, using a digital graphics system (e.g. Fig. 5.2).

The digital D.T.S. echo was normalised to remove the effects of variable source energy, recording and playback gain and A/D converter gain (Dodds, 1976; Parrott, 1978). As the source pulse propagates spherical spreading losses through the water column occur; these are accounted for by multiplying the signal at each sample point by a linear

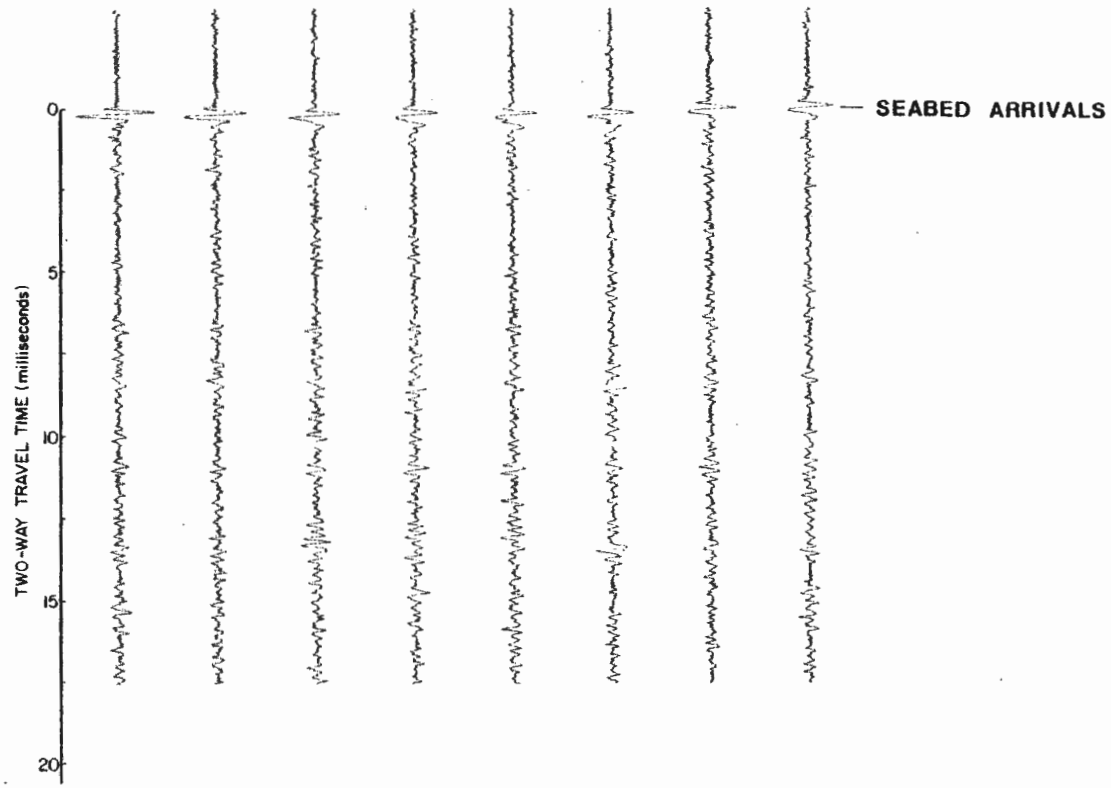

Fig. 5.2: An example of a typical "wiggly trace" digital replay of D.T.S. data.

function of time. The function is zero when the boomer is fired and has a slope chosen so that the energy in a pulse, reflected from a perfect plane reflector, is unity, independent of fish to bottom separation. The transmitted energy is assumed to be constant and equal to that measured in previous calibration trials made on the boomer used (Dodds, 1976).

Much of the D.T.S. data collected northeast of Newfoundland have been found in general to have poor signal to noise (S/N) ratios. One major reason for this was an operator error in setting recording levels too high for the low returned signal strengths in the deep water of the study area. However, the analogue graphic records exhibit continuous reflection horizons attesting to the gross spatial coherency of the data. It was therefore necessary to find a method of displaying the data so that the noise content was suppressed and the coherent seismic events could be seen and compared to the synthetic data.

One possible method would be to stack a number of individual seismic traces (i.e. align a number of traces, add the traces together point by point and, finally, normalise the result) to produce an average trace which would be made up of amplified coherent events and a reduced noise level because the incoherent noise contributions would cancel on the stacked traces. However, use of this technique was not possible because the noise content of the data generally prevented the precise tracking of the first arrival required to align adjacent shots before stacking. An alternative method is to look at the gross properties of the seismic traces and compare these results to similarly calculated properties of

the synthetics. Instantaneous energy is such a property.

Instantaneous Energy

Instantaneous energy has been calculated by squaring the digitized pressure amplitudes and has been plotted versus time, similar to the seismogram curves (Tucker and Gazey, 1966; Knott et al., 1977). The resulting values have been expressed as a fraction of the instantaneous energy theoretically obtained if a pulse from the D.T.S. sound source was reflected from a perfect reflector (e.g. Fig. 5.3).

The recorded field data are composed of both wanted signal and unwanted noise; we can, therefore, write the following expressions for any i'th digitized amplitude of the pressure-time seismogram.

$$S_m(i) = S_R(i) + N(i) \qquad (1)$$

where $S_m(i)$ = i'th digitized measured amplitude

$S_R(i)$ = i'th digitized amplitude without noise

$N(i)$ = noise component.

The instantaneous energy

$$E(i) = S_m^2(i)$$

$$= S_R^2(i) + N^2(i) + 2S_R(i)\, N(i) \qquad (2)$$

Since $S_R(i) >> N(i)$, which is the case for large seismic events, and if we assume N(i) has a reasonably constant variance, though random, then the cross-product and squared term involving N(i) will be observed as a minimum threshold level at times earlier than the seabed arrival in the

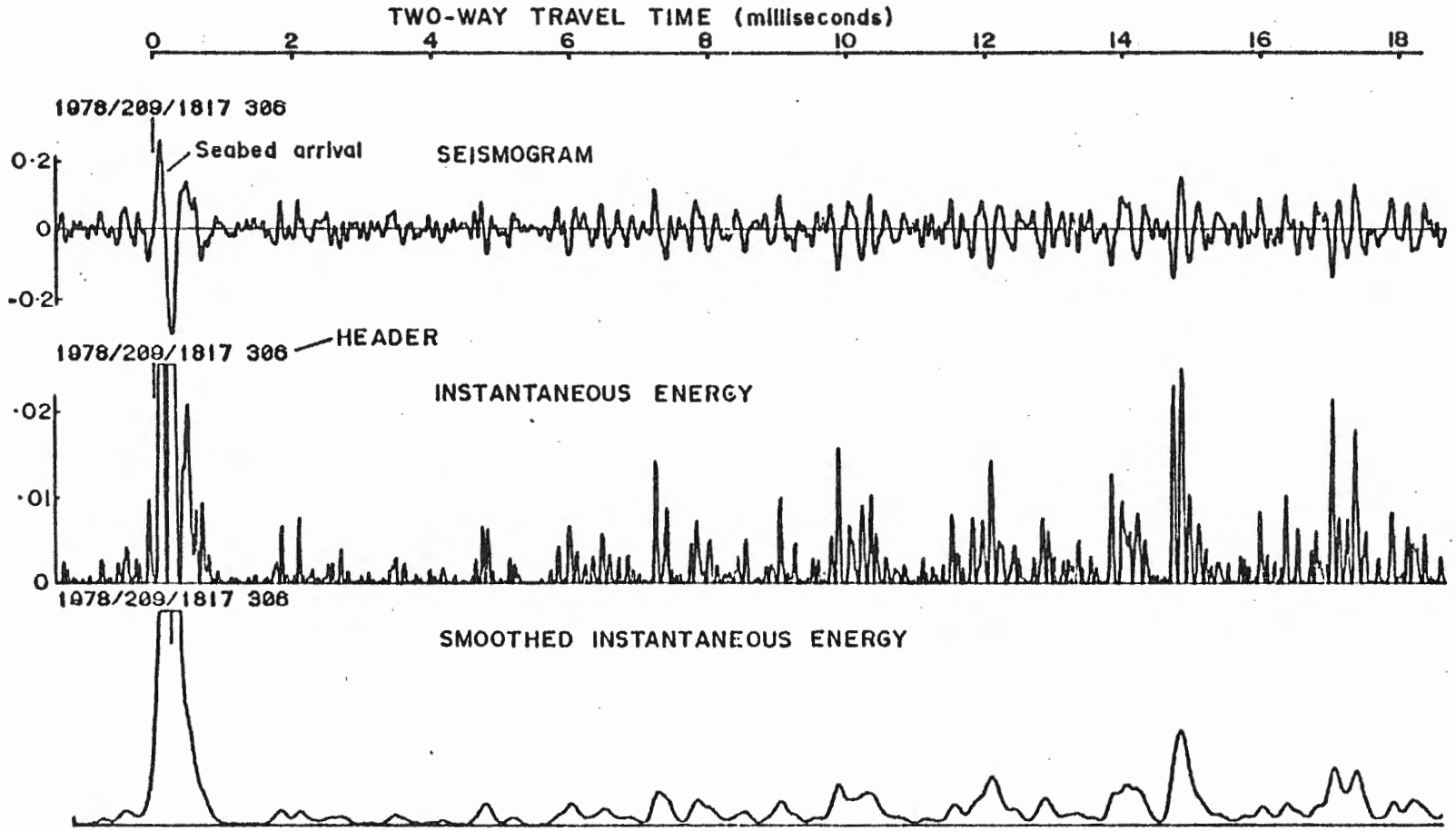

Fig. 5.3: An example of D.T.S. data replay including instantaneous and smoothed instantaneous energy. The seabed reflection is indicated as is the tape header which records the year, Julian day, Greenwich time and digitized shot number.

replayed instantaneous energy data (Fig. 5.3). This operator has the effect of suppressing the noise content of the seismograms; at the same time, it eliminates the phase information in the seismogram which, in the context of finding large coherent energy events between successive seismic records is a valid and useful technique. However, once the phase information is lost, there is no way of applying inversion techniques to the data to give properties dependent upon phase information (such as an average impedance profile).

Smoothed instantaneous energy has been calculated by convolving the instantaneous energy, E(i), with a Gaussian smoothing window (- 6 dB down-points at ± 83.4 μsecs, i.e. approximately 2 D.T.S. pulse peaks in width). The seismograms were replayed and their corresponding instantaneous energies were calculated (Fig. 5.3) with a PDP-11/60 minicomputer using programs developed by Dodds (Huntec '70, pers. comm., 1979) and modified by the author. Appendix 7 gives playback data from core sites 2, 6 and 7. These seismic data were chosen for comparison with the synthetic seismograms for two reasons: (1) at the site of core number 2, the D.T.S. data had the best S/N ratio of the entire suite of field data, and (2) at the sites of core numbers 6 and 7, which are close together and record very similar and laterally continuous geology, the synthetics can be compared critically with one another, as well as with the field data.

Appendix 7 contains replays of raw D.T.S. traces and their corresponding instantaneous energy plots over the 3 core sites.

Synthetic Seismogram Modelling

The development of normal incidence synthetic seismograms has been largely motivated by seismic exploration for hydrocarbons. The approach and techniques are, however, equally applicable to both deep-seismic investigations and shallow seismic studies of sediments under the ocean. The only difference is one of scale; in deep seismic work, frequencies of a few Hertz to a few tens of Hertz are utilized for penetration to depths of a few seconds in travel time, whereas herein, the frequencies are in the kilohertz range and the penetration depths are in microseconds of travel time. Although the actual seismic propagation process is three-dimensional, past experience has shown that a one-dimensional approach to wave propagation and reflections in a perfectly elastic and horizontally stratified earth is a good approximation to reality in most situations (Robinson and Treitel, 1978).

The basic method is to compute an impulse response for a layered earth model which, after convolution with an appropriate pulse shape, results in the required synthetic or theoretical seismogram. Computations have been made by both anologue and digital means, with and without multiple reflections, with and without absorption and by many different methods (Peterson et al., 1955; Wuenschel, 1960; Trorey, 1962; Darby and Neidell, 1966). The method has also been formulated in the frequency domain; this indicates the relevance of filter theory as applied in this context (Sherwood and Trorey, 1965; Treitel and Robinson, 1966; Claerbout, 1968).

One such approach used in exploration is to compute the impulse

response from well logs of density and p-wave velocity; this has been used here on surficial sediment cores. The relevant theory is given by Wuenschel (1960) and, rather than repeat that here, a practical approach indicating the assumptions and computational procedures used will be given.

In this study, the propagation of seismic waves is concerned with p-waves, energy transmission and reflection phenomena. In a three-dimensional medium this is described by the partial differential equations:

$$\text{div (grad } p) = \frac{1}{C^2} \frac{\partial^2 p}{\partial t^2} \tag{3}$$

$$\text{div (grad}\phi) = \frac{1}{C^2} \frac{\partial^2 \phi}{\partial t^2} \tag{4}$$

where $p(x, y, z, t)$ = the pressure variable

$\phi(x, y, z, t)$ = the scalar velocity potential

(x, y, z) = spatial co-ordinates

t = time

C = the p-wave velocity of the medium

Pressure and particle velocity are related to ϕ by:

$$p = \rho \frac{\partial \phi}{\partial t}$$

$$\underline{u} = - \text{grad } \phi$$

$\underline{u}$ being the particle velocity and ρ the density of the medium. At an interface between two media, the physics of the situation imposes the boundary conditions of compatibility of stress on either side of the boundary and

continuity of particle velocity across the boundary. The model assumed here has simple parallel interfaces, normal incidence and a perfectly elastic medium (i.e. one-dimensional). Thus, for a medium of infinite extent, the local pressure waveform will be a direct replica of the signal source pressure waveform (assuming the source waveform has been measured at a far field distance from the source) delayed by a time = DISTANCE/VELOCITY. If pressure pulses impinge on boundaries between media at normal incidence the energy is partially transmitted and partly reflected without conversions from pressure to shear waves occurring. Each reflection and multiple reflection contributes to the amplitude scaling of the respective incident pressure signal (which corresponds to a particle velocity in solid phases). No further primary reflections occur once the pulse has entered a "basement" medium.

The cumulative effect of the sum of all the reflections is a received pressure signal which consists of a sum of replica pulses of the source pulse in the water above the subsurface. Each replica pulse has an amplitude scaled by the product of respective reflection - transmission boundaries encountered and given by the well-known Rayleigh reflection and transmission coefficients (e.g. Mateker, 1965) which are boundary value solutions to equations (3) and (4) above:

$$R_{ij} = \frac{\rho_j v_j - \rho_i v_i}{\rho_i v_i + \rho_j v_j} \tag{5}$$

$$T_{ij} = \frac{2\rho_i v_i}{\rho_i v_i + \rho_j v_j} \tag{6}$$

where R_{ij} = reflection coefficient

T_{ij} = transmission coefficient

i = index of medium of initial propagation

j = index of medium receiving the propagating wave

ρ_i, ρ_j = densities of media i, j

v_i, v_j = pressure-wave velocities of media i, j.

The delay in time between recorded pulses is given by the respective propagation time for the media traversed. For the assumptions of plane waves impinging upon plane boundaries (where no wave-type conversions occur) in a lossless medium, the model can be formulated as a passive, linear, time invariant filter (Sengbush et al., 1961).

A further simplification is possible if it is assumed that the contribution of internal multiple reflection and transmission coefficients is negligible. In this case a reflectivity versus travel time profile is a good approximation to the impulse response of the model. Figure 5.4 gives three models which illustrate the applicability of the above simplification. Density has been chosen equal to unity so that reflectivity is a function of velocity alone. The velocity change across each boundary has been chosen as 250 ms^{-1}, which is a large change for surficial sediments and will point out above-average effects of multiple reflection and transmission amplitudes. The reflection coefficient into and out of each layer is given for the models and the corresponding reflectivity functions $r_1(\tau_1)$, $r_2(\tau_2)$, $r_3(\tau_3)$ have been evaluated from the equations given in Figure 5.4. A negative sign indicates that the reflected pulse

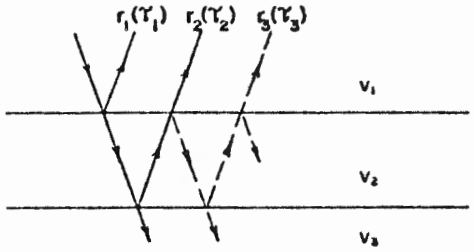

EVENT	TYPE	AMPLITUDE
$r_1(\tau_1)$	PRIMARY REFLECTION	$A_i \cdot (R.C.)_1$
$r_2(\tau_2)$	PRIMARY REFLECTION	$A_i \cdot (T.C.)_1 \cdot (R.C.)_2 \cdot (T.C.)_2$
$r_3(\tau_3)$	MULTIPLE REFLECTION	$A_i \cdot (T.C.)_1 \cdot (R.C.)_2^2 \cdot (-(R.C.)_1) \cdot (T.C.)_2$

NOTE: A_i = INCIDENT AMPLITUDE = 1
$(R.C.)_1$ = REFLECTION COEFFICIENT AT TOP BOUNDARY
$(R.C.)_2$ = REFLECTION COEFFICIENT AT BOTTOM BOUNDARY
$(T.C.)_1$ = TRANSMISSION COEFFICIENT INTO LAYER
$(T.C.)_2$ = TRANSMISSION COEFFICIENT OUT OF LAYER

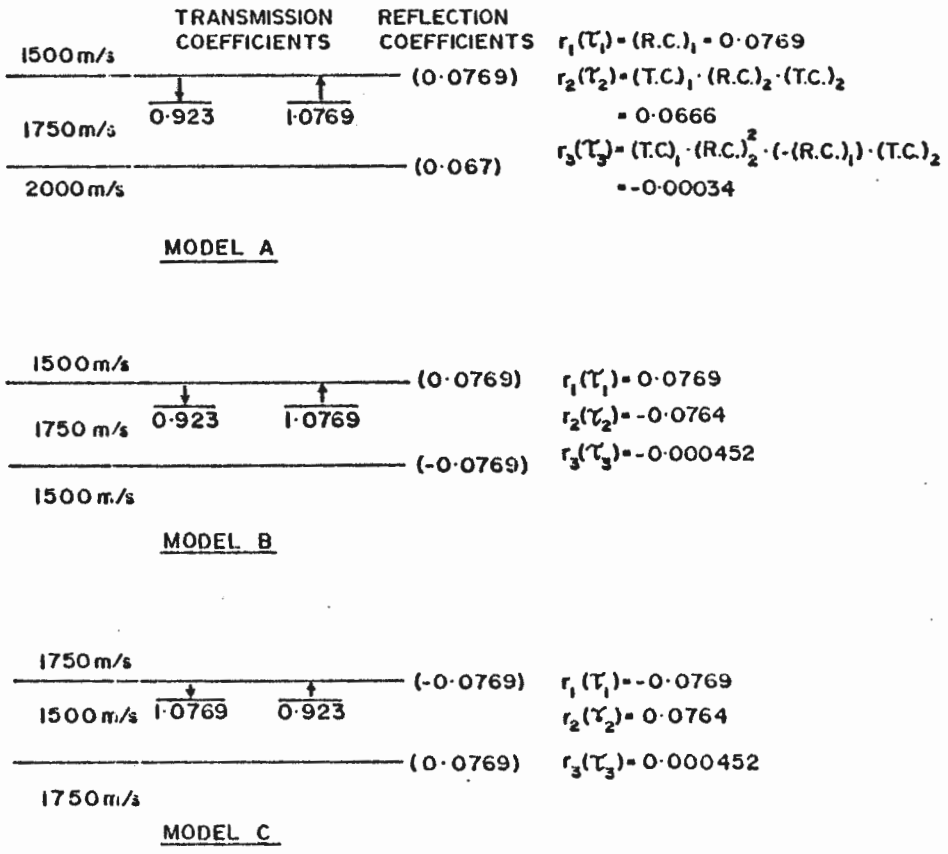

REFLECTIVITY FUNCTIONS FOR SINGLE LAYER MODELS

Fig. 5.4: Three reflectivity models to illustrate the magnitude effect of internal ray-path multiples. The reflection (R.C.) and transmission (T.C.) coefficients are given for each interface as are the received reflection amplitudes in layer 1 ($r_i(\tau_i)$).

is inverted (180° phase shift) with respect to the incident pulse.

Two important conclusions can be made from these models:

(1) The first-order multiple is less than 1% of the magnitude of the primary reflection, implying that internal multiples will be negligible for most realistic layered sediment models.

(2) The reflectivity function $r_2(\tau_2)$ is approximately equal to the reflection coefficient of the lower boundary.

In other words, the reflected energy is small and the impulse response is well approximated by the reflectivity function. Wuenschel (1960) and Robinson and Treitel (1978) have demonstrated, by modelling and theoretical studies of reflection synthetics, that the above is true when only small (< 0.2) reflection coefficients are present. Such is the case in this study, except where larger reflectivities are found at late travel times (Figs. 5.8, 5.9 and 5.10). However, the multiples from these horizons will be received at times too late to affect the primary reflected events. Thus, the impulse response has been calculated as the reflectivity versus travel time; this also makes the computation of the synthetics very much quicker than for the exact solution.

Once the impulse response has been calculated, the synthetic seismogram is produced by a convolution of the impulse response R(t) with the appropriate pulse shape p(t). The resulting output of this operation is given by:

$$s(t) = \int_0^t R(\tau)\, p(t - \tau)\, d\tau$$

where τ = lag

$s(t)$ = output = synthetic seismogram

$R(\tau)$ = impulse response

$p(t)$ = pressure pulse shape.

This integral operation is often written formally as

$$s(t) = R(t) * p(t)$$

where * denotes convolution.

Two different pulse shapes PULS and PULS 2 (Fig. 5.1) have been used in producing the synthetic seismograms. PULS is the outgoing pulse of the Huntec EDIOC boomer (as measured by Simpkin, 1977) and should therefore give a synthetic in best agreement with the field data collected using the external hydrophone on the D.T.S. fish. However, the seabed, which to a good first approximation acts as a plane reflector at the core sites, has produced reflections recorded in the D.T.S. data, which imply that the received pulse was more like PULS 2. This pulse modification is either an artifact of the seabed or the D.T.S. If the seabed were responsible, there would have to be a continuous acoustic impedance contrast comparable, in size, to that of the seawater/seabed interface, but negative in sign (to produce the large negative reflectivity) very close to the seabed. No evidence has been found supportive of this, so the pulse shape is thought to be due to either interference effects of the boomer plate on the incident reflected wave and/or changes in the boomer charac-

teristics (J. Dodds, Huntec '70, pers. comm., 1979). This is a major problem that deserves attention in the future.

Computational Procedures

In these calculations, a minimum basic travel time interval has to be chosen because each sediment layer in the synthetic seismogram computations must be an integer multiple of this travel time interval. A minimum one-way travel time layer thickness of 10 μs one-way travel time was chosen; this limits unwanted aliasing and means that 1000 layers correspond to a sedimentary section of 15 m at 1500 ms^{-1}.

A computer program (Appendix 8) was written to compute synthetic seismograms from measurements of velocity and density versus distance down core (Chapter 3, Figs. 3.4 to 3.9; Appendix 3 for listings). The impedance profile was initialized for propagation through the seawater and into the seabed. Thus, on plots of variables versus travel time, the seabed contrast always appears at 1 ms (millisecond) two-way travel time. Next, acoustic impedances were calculated (density x velocity) for the whole profile, followed by reflection coefficients (using equation (5) above) between adjacent values of the calculated acoustic impedances. Then, starting at the top of the core, distances were converted to two-way travel time using weighted average interval velocities. These travel times were accumulated and then rounded off to the nearest 10 μs so each set of velocity, density, impedance and reflectivity was given an assigned layer in the model. The final step in the computation of a synthetic seismogram was to convolve the reflectivity function with the pulse shape

(Fig. 5.1). Appendix 9 gives an example of the final output from a run of the program. Such data were plotted and stored for further calculations and plotting of instantaneous energy.

A diagramatic outline of the computation methods used for both the synthetic and field data is given in Figure 5.5. Once the seismograms are normalised and ready for output, the calculation of instantaneous energies are equivalent for both field and synthetic data and their plots have equal scaling.

Results and Discussion

It is impossible to determine the exact position of the cored samples with respect to individual "shots" from the D.T.S. It is therefore necessary to compare the synthetic seismogram and its instantaneous energy computed from core data with a number of similarly processed D.T.S. shots taken in the vicinity of the core site.

Consider a hypothetical survey in which a "perfect" noise-free D.T.S. emits plane pressure waves over a seabed composed of planar, homogeneous, perfectly elastic, isotropic stratified layers, each with a characteristic acoustic impedance. The seismic returns in this situation would be composed entirely of reflection events, 100% coherent from trace to trace. In reality, such hypothetical properties are only approximated. At the scale of the sub-bottom profiles the reflection horizons appear spatially coherent, attesting to the constant characteristics of the D.T.S. and the general spatial coherency of the physical layers which cause the reflection events. However, on a fine (shot to shot) scale, the coherency of the

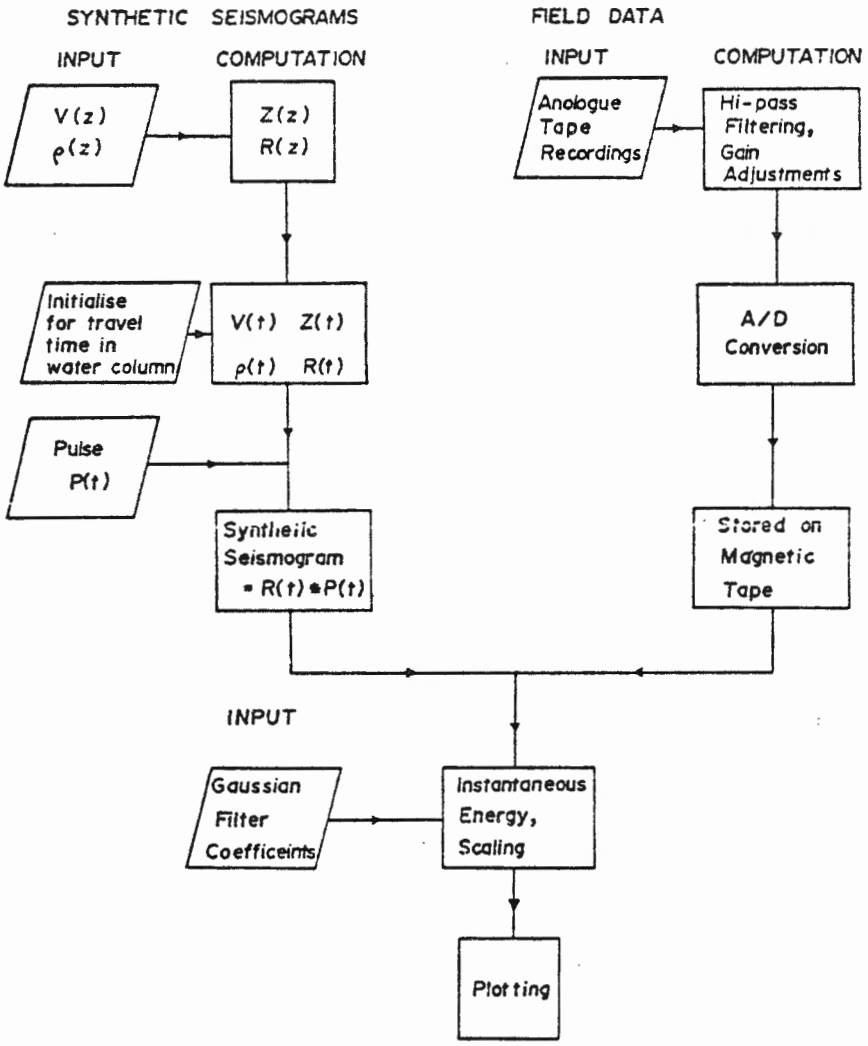

Fig. 5.5: Schematic diagram to show D.T.S. processing steps and synthetic seismogram computations.

field data is questioned.

When the seismic data were expanded into single shot format (Figs. 5.6 and 5.7) coherence between individual shots was difficult to observe, especially on data from core sites 6 and 7, where more complex seismograms were observed and higher noise levels existed. Displays of instantaneous energy alleviated this problem to some extent, although events on the processed seismograms still vary considerably in amplitude from shot to shot. This shot to shot incoherency makes it difficult to make a direct comparison between the field and synthetic data. What, then, is the significance of the synthetics and how can they be compared to the field data without a biased selection of shots which show the best match to the corresponding synthetic? The aim of this section of the thesis is to try and explain in some detail the nature of the seismic events observed; since the recorded seismograms on an individual basis appear incoherent, how can the synthetics help? First consider the possible, though inseparable, reasons for the incoherencies:

(a) the inhomogeneous nature of the sediments may have caused differential shot to shot reflections and scattering. Further, the effects of topographic focusing and roughness of layer interfaces would add to the variability of individual seismic returns.

(b) D.T.S. hardware problems add "non-geological" noise to the data. The boomer source has a fixed aperture (~ 60 cm diameter) which produces a directional outgoing wavefront so that the pulse shape and frequency spectrum change with

Fig. 5.6: Diagram showing the equivalence of digital replays to the analogue D.T.S. data in the vicinity of core 2. The equivalent instantaneous energy is shown beneath the seismogram. The synthetic energy is included, the corresponding synthetic seismogram is given in Fig. 5.12.

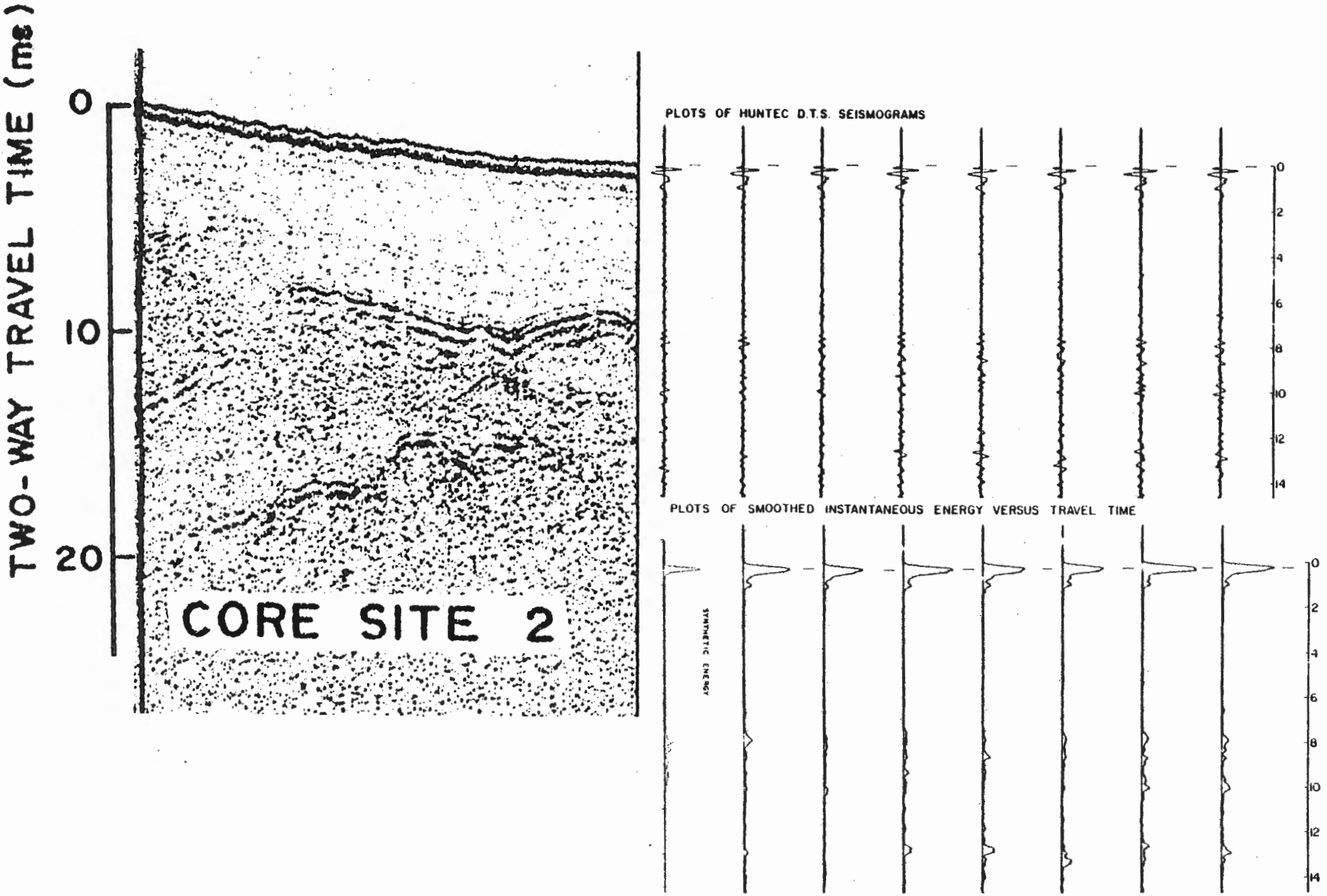
TWO-WAY TRAVEL TIME (ms)
0
10
20
CORE SITE 2
PLOTS OF HUNTEC D.T.S. SEISMOGRAMS
0
2
4
6
8
10
12
14
PLOTS OF SMOOTHED INSTANTANEOUS ENERGY VERSUS TRAVEL TIME
SYNTHETIC ENERGY
0
2
4
6
8
10
12
14

Fig. 5.7: Diagram showing the equivalence of digital replays to analogue D.T.S. data in the vicinity of cores 6 and 7. The equivalent instantaneous energy is shown beneath the seismograms. The synthetic energy from core 7 is included, the corresponding synthetic seismogram is given in Fig. 5.15.

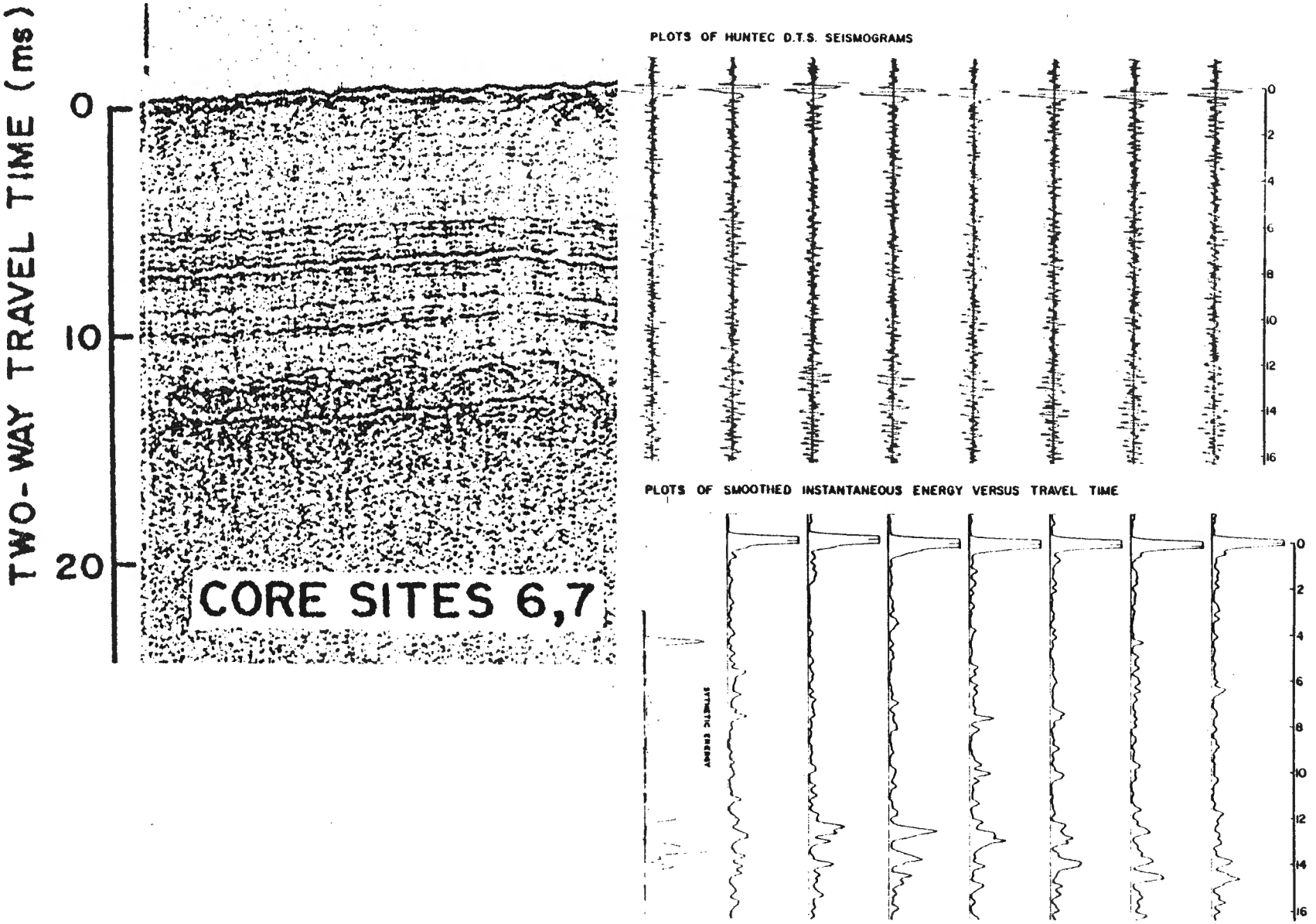
TWO-WAY TRAVEL TIME (ms)
0
10
20
CORE SITES 6,7
PLOTS OF HUNTEC D.T.S. SEISMOGRAMS
0
2
4
6
8
10
12
14
16
PLOTS OF SMOOTHED INSTANTANEOUS ENERGY VERSUS TRAVEL TIME
SYNTHETIC ENERGY
0
2
4
6
8
10
12
14
16

beam angle (MacIssac and Dunsiger, 1977; Simpkin, 1977). Consequently, pitching and rolling of the fish could cause the sediments directly beneath the fish to be ensonified by varying pulses and cones of acoustic illumination depending upon the attitude of the fish. Also, in some early data sets, electronic noise was a problem because the acoustic decoupling of the hydrophone from the body of the fish was found to be insufficient (MacIssac, 1977).

The problem of separating geological from hardware incoherencies with this data set is unanswered at the present time. However, on other data sets the shot to shot coherency has been successfully used as a remote classifier of sediment type (MacIssac, 1977; MacIssac and Dunsiger, 1977).

The synthetic seismograms may be able to indicate a geological reason for the incoherencies in the field data. The results of the computation of synthetic seismograms for cores 2, 6 and 7 are shown in Figures 5.8, 5.9 and 5.10. The velocity profiles versus travel time (a) are included so that a direct comparison can be made between seismic events and the causative sediments (i.e. compare with Figs. 3.4, 3.6 and 3.7). Traces (b) and (c) are the impedance and reflectivity profiles calculated as described above.

Traces (d) and (e) are the synthetic seismograms computed by convolving the reflectivity model with the two pulse shapes PULS and PULS 2. Recall that up to 2 m of the surface sediment were not collected by the

Figs. 5.8, 5.9, 5.10: The following three diagrams show the results of computations of the synthetic seismograms for cores 2,6 and 7 respectively. The computational steps are described in the text.

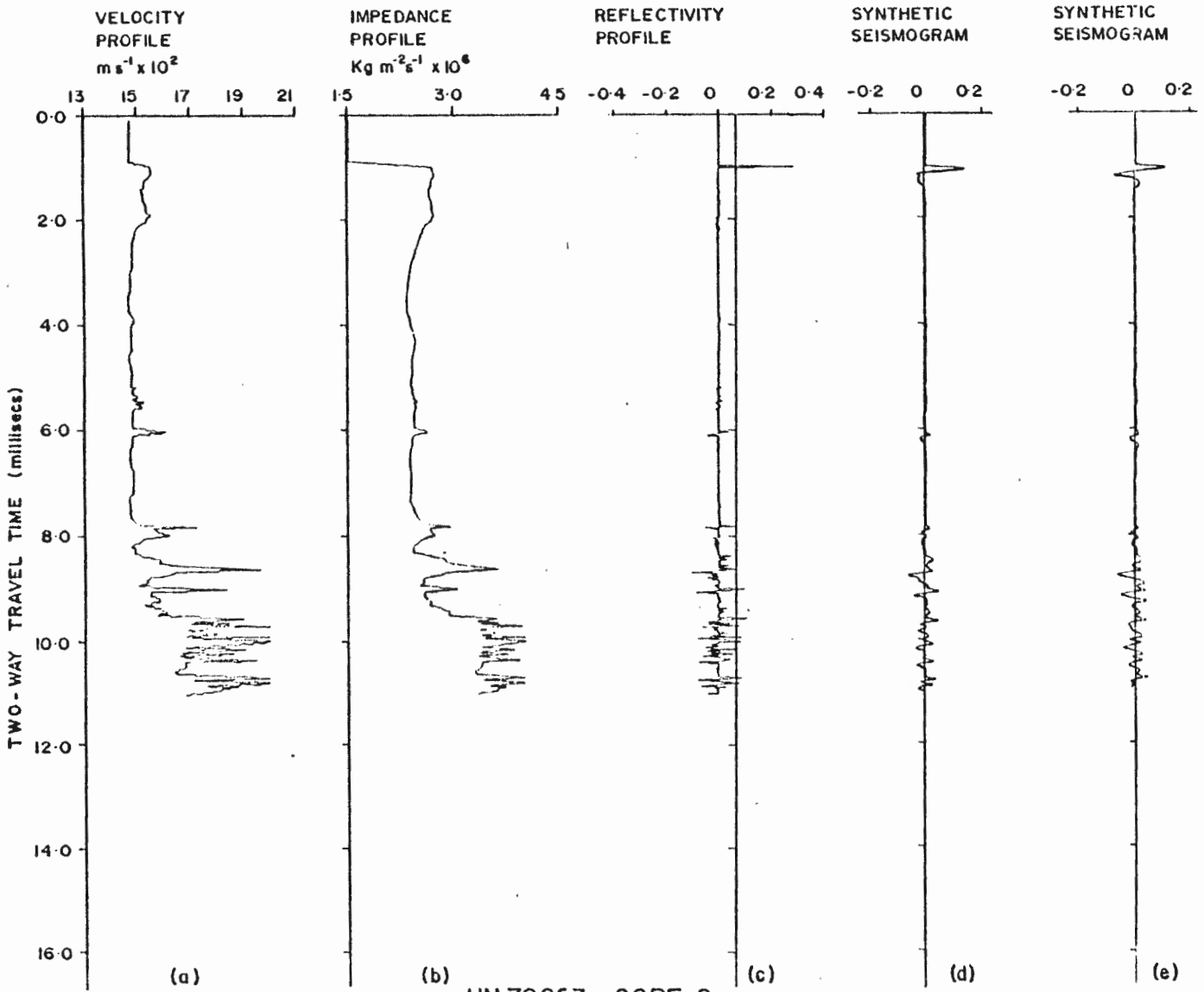

HN 78023, CORE 2

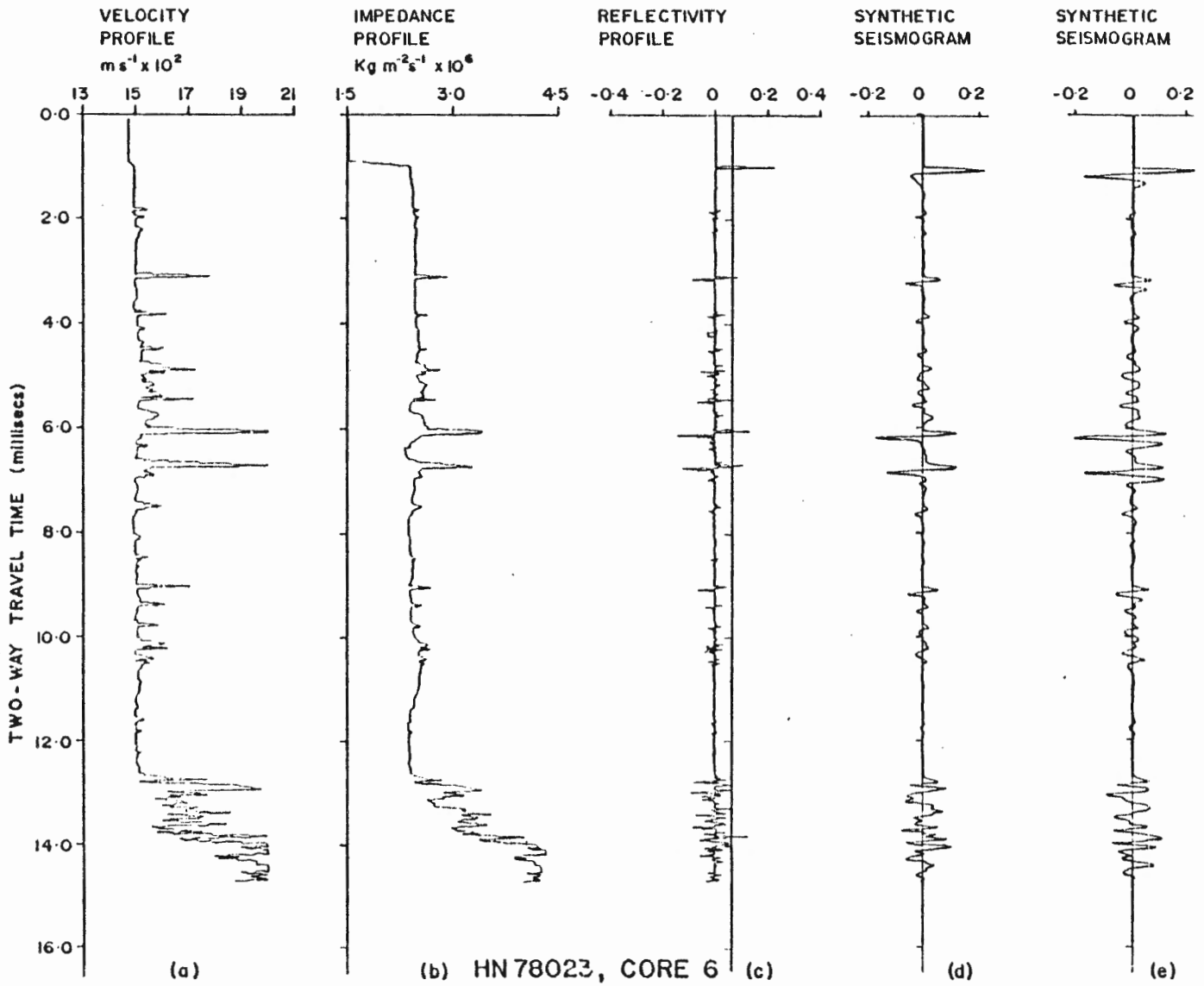
VELOCITY PROFILE
m s⁻¹ x 10²
13 15 17 19 21
IMPEDANCE PROFILE
Kg m⁻²s⁻¹ x 10⁶
1·5 3·0 4·5
REFLECTIVITY PROFILE
-0·4 -0·2 0 0·2 0·4
SYNTHETIC SEISMOGRAM
-0·2 0 0·2
SYNTHETIC SEISMOGRAM
-0·2 0 0·2
TWO-WAY TRAVEL TIME (milliseconds)
0·0
2·0
4·0
6·0
8·0
10·0
12·0
14·0
16·0
(a)
(b) HN 78023, CORE 6
(c)
(d)
(e)

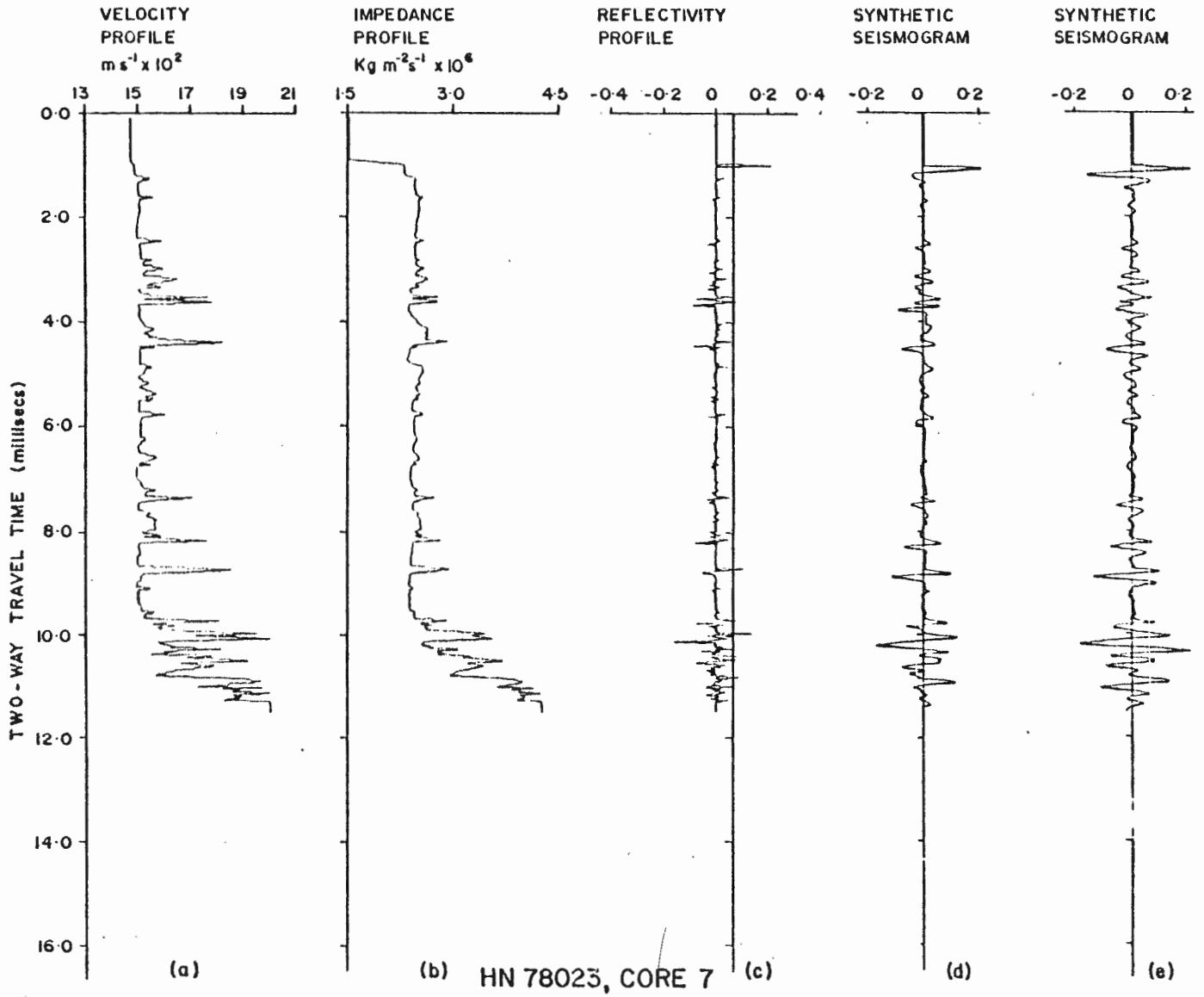

HN 78023, CORE 7

the piston cores; therefore, the positions and waveforms of the first arrivals of the synthetics should be disregarded and only the lower seismic arrivals should be correlated.

Consider the results from cores 6 and 7, which were collected approximately 1 km apart and are sedimentologically identical. The synthetics have a similar overall pattern (Fig. 5.11), although there are many detailed differences in amplitude and phase. These discrepancies are caused by pebbles. However, it is apparent that layers of pebbles have to be responsible for the seismic stratification (Fig. 5.7) and therefore, they must have been deposited as spatially continuous layers. Between core sites seismic horizons can be followed; therefore, the sedimentary counterparts of the seismic horizons should be present in the cores. However, the corer has a small diameter (~ 7 cm) and the probability of sampling any particular pebble horizon will depend on the density distribution of the pebbles on that horizon. A further complication is that some of the pebbles in the core may not be part of a pebble layer. The differences in the velocity profiles (Fig. 5.11) indicates the relative sampling success, and each profile gives synthetic response which is different in detail.

The synthetic seismogram calculated from core 2 data is simpler in character than those for cores 6 and 7, due to the geology lacking in the dropstone layers mentioned above. The D.T.S. record over the site of core 2 shows an acoustically transparent layer underlain by a partially stratified, scattering medium (Fig. 5.6). These data have the best signal to noise ratio of the data used and also the best overall match to the

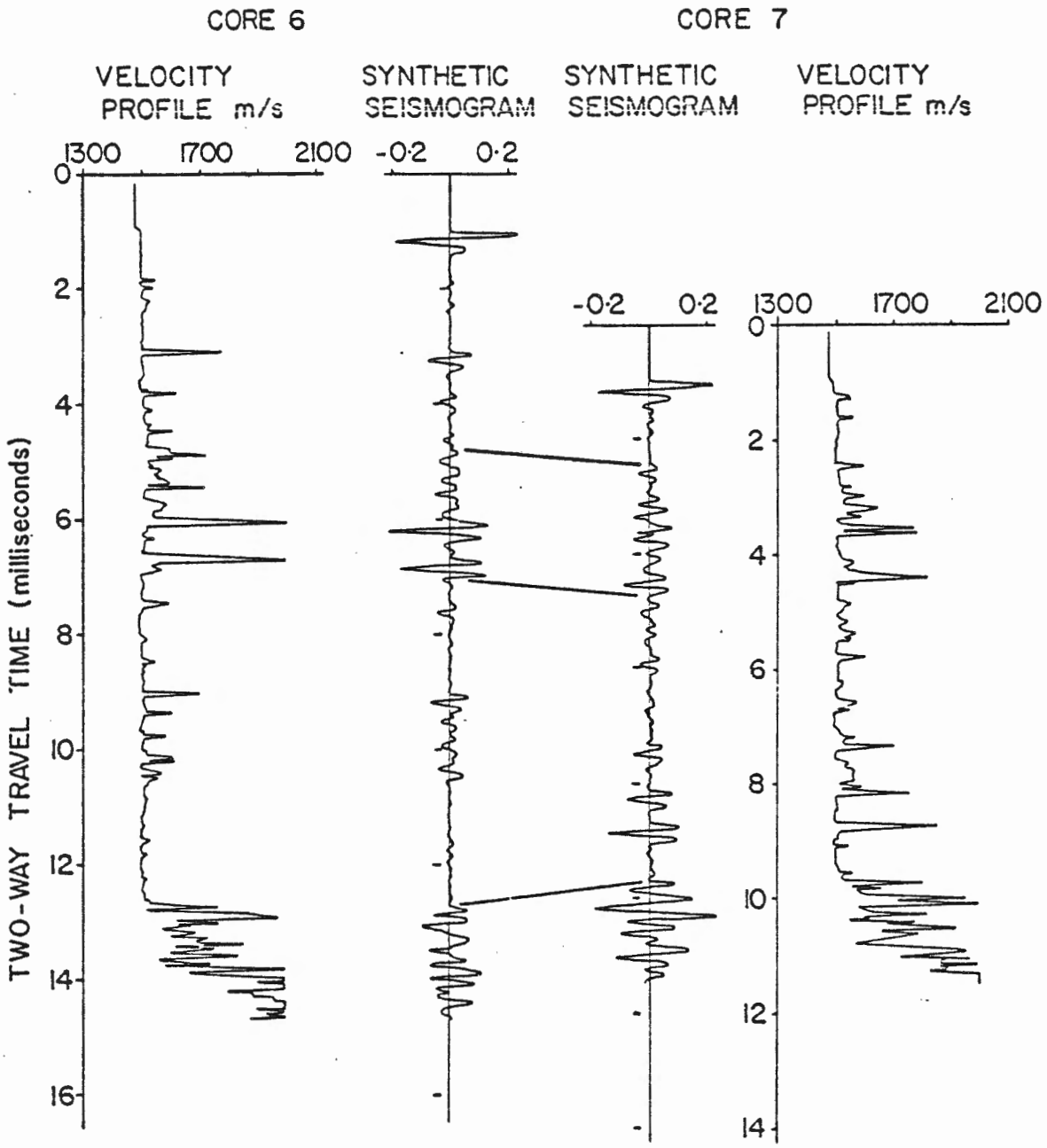

Fig. 5.11: Comparisons between the synthetic seismograms calculated from geotechnical data from cores 6 and 7. The velocity profiles are included so that the synthetics can be compared with the core descriptions in Figs. 3.6 and 3.7.

synthetic data (Fig. 5.12). This raises the possibility that incoherent events found in the seismic data collected over core sites 6 and 7 are simply due to noise. However, if we consider the seismic trace prior to the first arrival to contain a representative noise sample, then the level of this noise can be used as a threshold below which the signal level is insignificant. The significant seismic events have amplitudes greater than the noise level (compare instantaneous energies) and incoherencies can be seen between these seismic events (Fig. 5.7). Therefore, it is possible that lateral variations in geology exist and are "seen" by the D.T.S. The seismic returns from the seabed are dependent upon the area of acoustic illumination which corresponds to the first Fresnel zone of the sound source (Clay and Medwin, 1977). If the D.T.S. is represented as a point source and receiver occupying the same space at a given separation from the seabed, the radius of the first Fresnel zone is given by:

$$r = \frac{\lambda d}{2} + \frac{\lambda^2}{16} \quad \text{(see Fig. 5.13)}$$

and $$\lambda = \frac{c}{\nu}$$

where λ = wavelength of the energy generated

d = distance from the source to the interface

c = velocity of medium of propagation

ν = frequency of the energy generated.

At 3 kHz (approximate peak power) with 100 m between the fish and the seabed, the first Fresnel zone has a radius of 5 m, giving a total sonified area of 78.6 m^2. At 6 kHz the radius and corresponding area decrease

to 3.5 m and 38.5 m^2 respectively. Clearly, the speed of the ship towing the D.T.S. fish has an effect on the amount of overlap of the frequency dependent Fresnel zones. A ship travelling at 2 ms^{-1} (~ 5 knots) with the D.T.S. 100 m above the seabed, firing at every 0.75 sec, has a 3 kHz Fresnel zone which overlaps 75% the 78.6 m^2 of insonified seabed (i.e. 59 m^2 shot to shot overlap), whereas the 6 kHz Fresnel zone overlaps by only 65% the 38.5 m^2 of insonified seabed (i.e. 25 m^2 shot to shot overlap). This overlap will decrease as either the fish moves closer to the seabed or as the ship's speed increases. If the subsurface geology varies enough outside these areas of Fresnel zone overlap between each successive shot, then clearly incoherencies will be observed on the seismic returns. The incoherencies will be more pronounced in the high frequency signal content because the Fresnel zones are smaller and scattering increases with frequency (Clay and Leong, 1974).

The large amplitude arrivals seen late in the synthetic seismograms have counterparts in the real data (Figs. 5.12, 5.14 and 5.15). Once again, shot to shot correlation is not high but these seismic arrivals are produced by the physical properties and layering of diamicton and glacial outwash sediments, which are deposited in highly irregular beds. Therefore, the assumption of plane coherent depositional layers required for strong seismic correlations are violated, and the returns are made up of components of scattering from the rough surface and point reflectors making up continuous travel time horizons in the sediments.

In summary, the major incoherencies in the D.T.S. data are believed to be due to geology. The field data is a record of the acoustic response

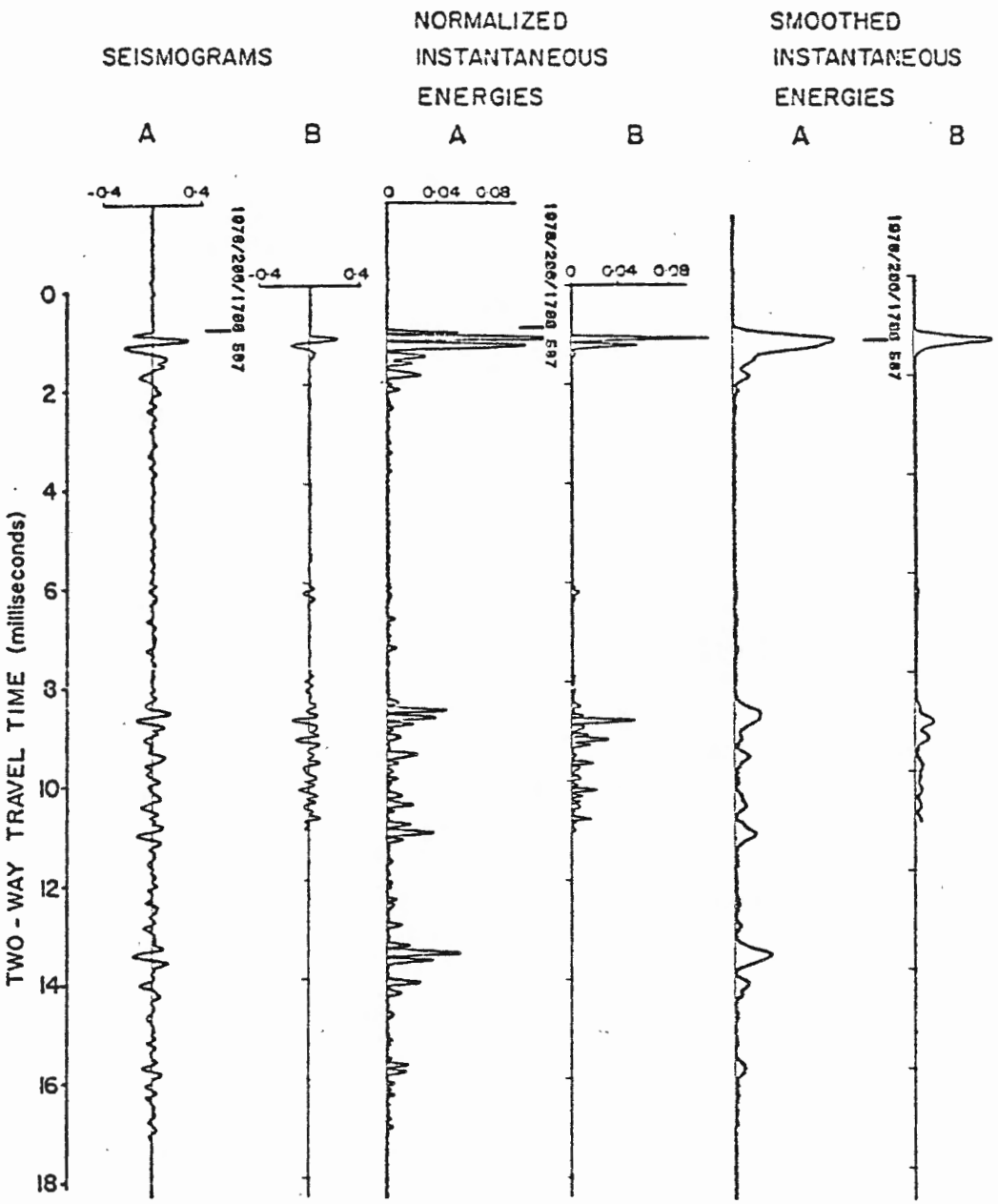

Fig. 5.12: A comparison between field D.T.S. data (A) and synthetic seismogram data (B) including energies for core 2. The reflectivity and energy are expressed as a fraction of that expected from a 100% reflector.

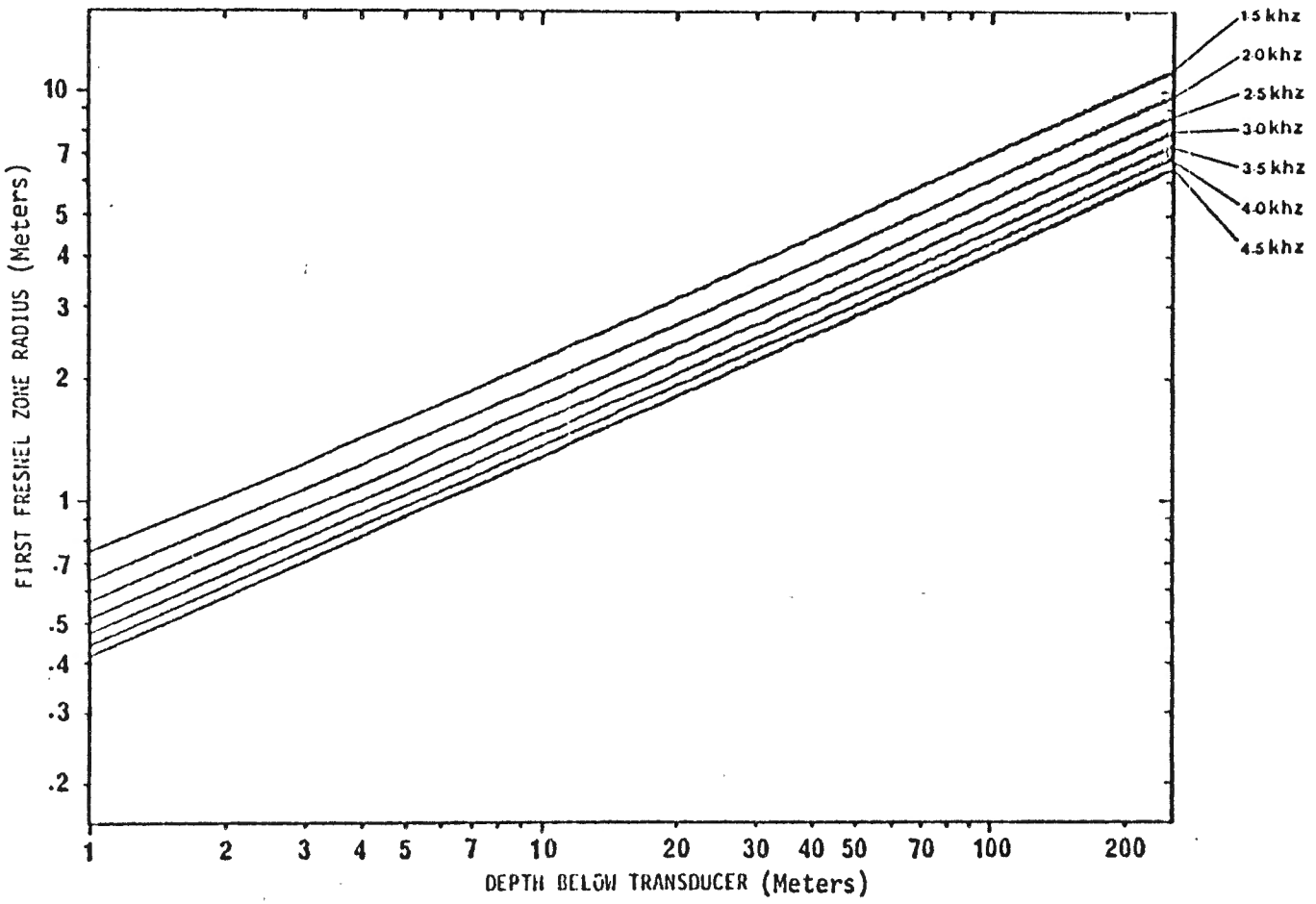

Fig. 5.13: Fresnel zones for a point source as a function of frequency and depth beneath the source (after MacIssac,1977).

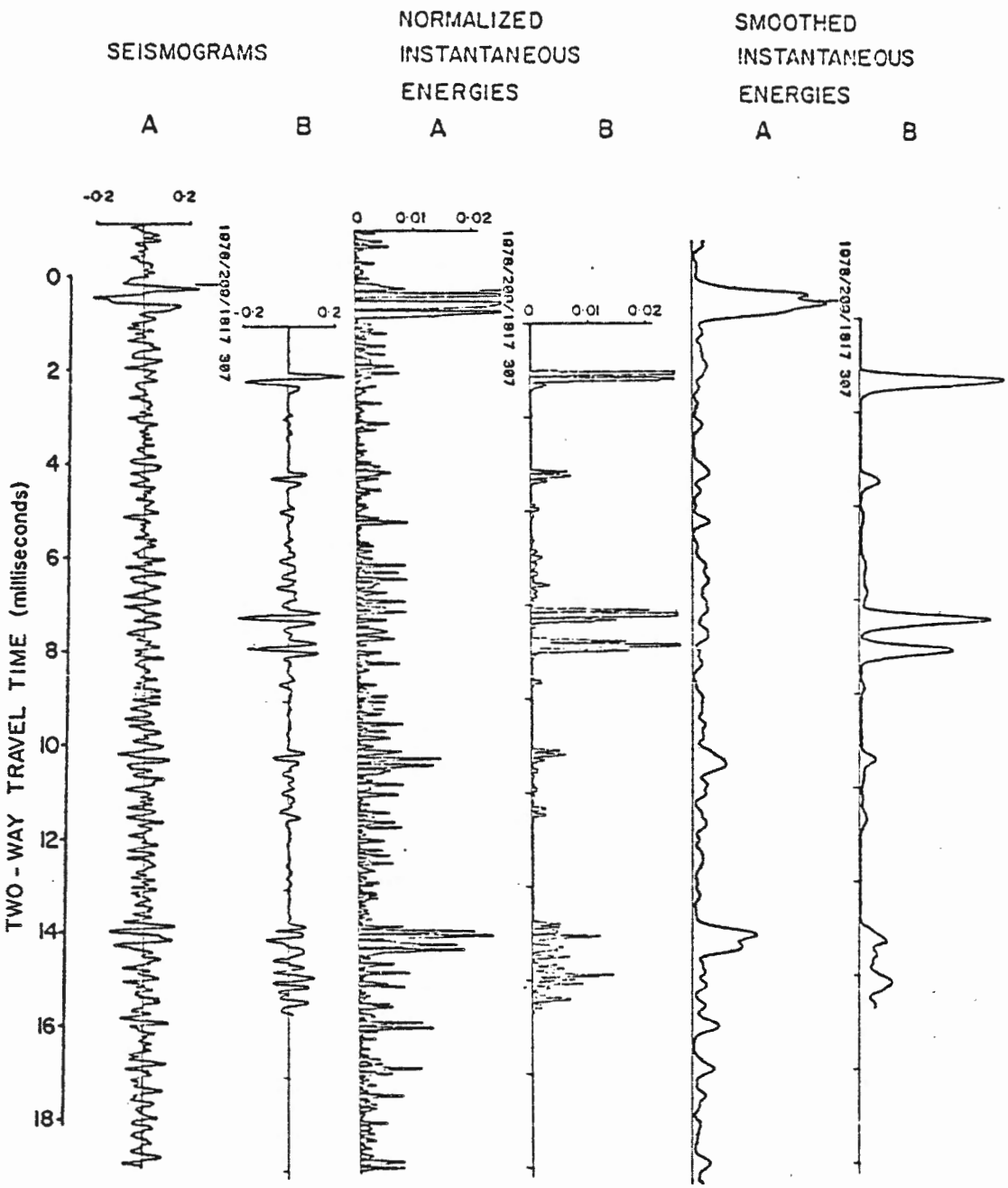

Fig. 5.14: A comparison between field D.T.S. data (A) and synthetic seismogram data (B) including energies for core 6. The reflectivity and energy are expressed as a fraction of that expected from a 100% reflector.

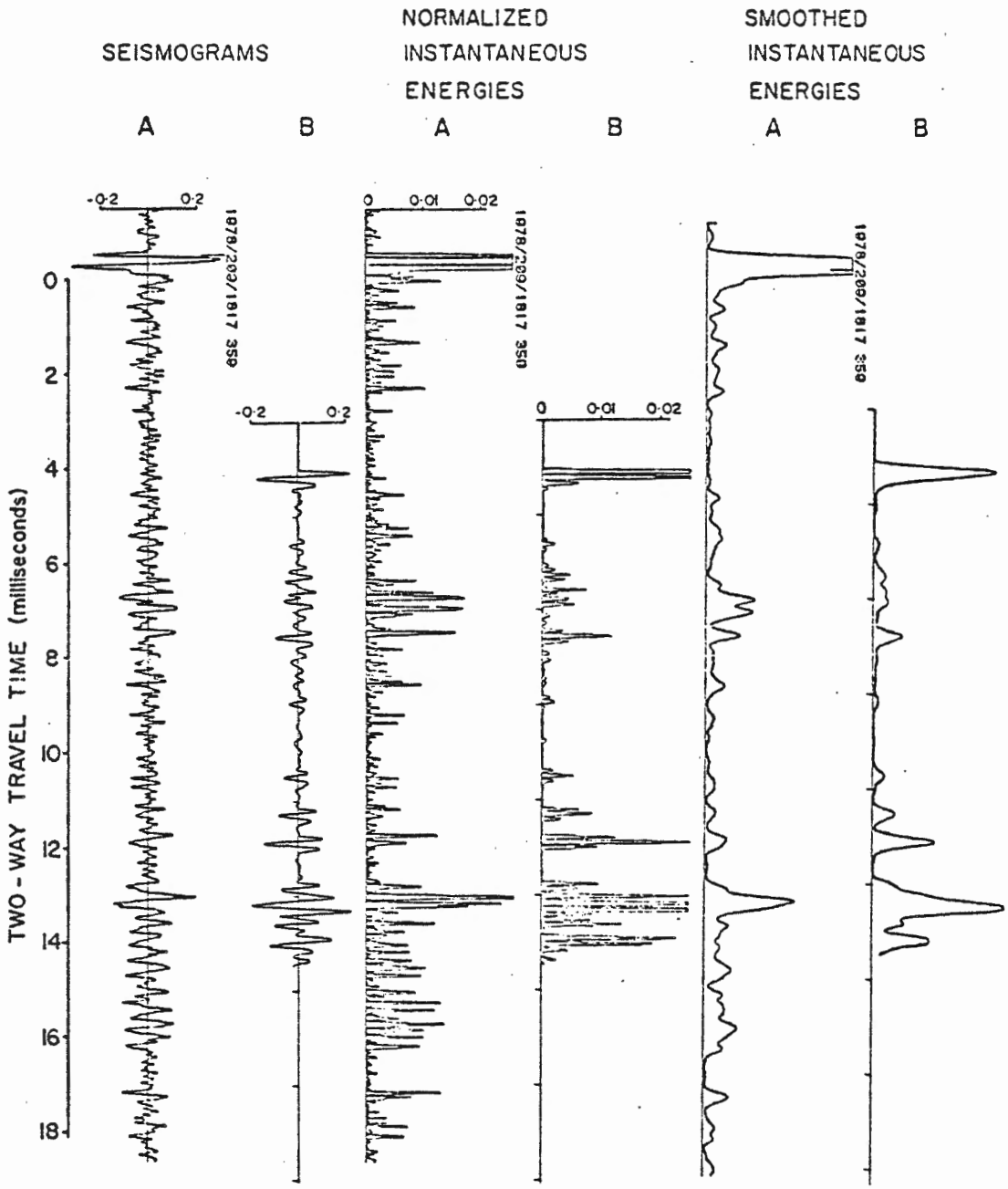

Fig. 5.15: A comparison between field D.T.S. data (A) and synthetic seismogram data (B) including energies for core 7. The reflectivity and energy are expressed as a fraction of that expected from a 100% reflector.

of a weakly-stratified sediment (due to pebble layers) underlain by a scattering medium with a rough, irregular surface. The synthetic seismograms are computed from a small sediment sample taken from a spatially inhomogeneous sedimentary section. It is clear that this sample is too small to be an accurate average, making the synthetics only an approximation to reality.

This study of synthetic seismograms and their relation to the field D.T.S. data does provide some valuable results:

(1) That seismic arrivals which appear coherent on the scale of the usual graphic recorder outputs are not necessarily so on a shot to shot basis;

(2) It has been found that shot to shot incoherencies in this study are probably due to geological causes. This suggests that shot to shot coherency may be usable as a classifier of the type of subsurface physical horizon, causing the reflection (i.e. there should be a gradation between a perfectly horizontal stratified sediment to a purely scattering medium). This would be an extension of MacIssac's work (1977).

(3) This study has shown that single cores from an area are insufficient for comparison to this type of seismic data. The problems of navigation may also cause ambiguities in correlating cores to the seismic data. Future studies should concentrate on a number of different geological environments with both varying lithologies

coherent over large areas and areas similar to this study area, where subtle lithological variations produce coherent seismic horizons. This is necessary to investigate the nature of subsurface seismic propagation in different sediment types and assess the possibility of remotely identifying sediments of different litho and textural characteristics. A valuable acquisition would be a suite of cores from a small site area taken while simultaneously running the D.T.S. off the stationary research vessel. Changes in the seismic returns over small distances could be observed and related to the geological variations. Such site specific procedures would eliminate the ambiguities of navigational positioning and enable a realistic measure of the coherency of the subsurface sedimentary structure and its variability to be made.

(4) Piston coring is not the best method of obtaining sediment samples for this type of work, apart from losing velocity and density measurements from the missing portion of the surface sediment (which would have to be replaced by either core nose velocimetry or in-situ techniques; e.g. Kepkay, 1977). There are problems obtaining a meaningful sample of the "average" geology, as observed with a seismic system. A wider barrel corer is recommended for any work involving

measurements of physical properties of sediments to obtain both a larger and less disturbed sample. If scattering due to bottom roughness is believed important in an area, then bottom photographs are required to estimate these effects around the core site.

(5) Further investigations are required into the detailed nature of the observed reflectors in sediments and the associated possibilities of deconvolving the seismic data to give a comparable layered model for surficial sediments.

(6) Any future studies which attempt to collect a large suite of cores (as suggested in item 3 above) to sample for seismic modelling purposes (similar to what has been done in this thesis) should bear in mind the necessity of frequent sampling (an interval no greater than 5 cm for velocity is suggested). This requires a large sampling effort which would clearly escalate as the number of cores increases.

(7) It has been shown that in this area the observed seismic stratification is not caused by such physical changes in the sediments as depositional or transgressional uncomformities. The stratification is due to periods of large-scale ice rafting, causing spatially coherent and extensive horizons of dropstones which can be observed on the anologue D.T.S. data. This illustrates well the necessity of a knowledge of the acoustic

impedance profile (or at least velocity) of the sediments, even in geological studies, if misinterpretation of this type of seismic data is to be avoided.

CHAPTER 6

SUMMARY OF CONCLUSIONS AND RECOMMENDATIONS FOR FUTURE WORK

Summary of Conclusions

This study has been concerned with three aspects of the Late Quaternary sedimentary geology of the northeast Newfoundland continental shelf. These aspects are the basic sedimentology, the geotechnical properties of the sediments and the expression of these sediments on Huntec D.T.S. seismic cross-sections. As such, this has been the first stratigraphic interpretation for this inner shelf region as well as the first study relating D.T.S. seismic horizons directly to the subsurface geology in a quantitative manner. The study has been based on stratigraphic, sedimentological and geotechnical data from six-piston cores, whose sites were chosen from D.T.S. data, and approximately 5,000 line-km of analogue D.T.S. and small airgun reflection seismic data (see Chapter 2).

The northeast Newfoundland continental shelf is a glacially overdeepened area with large fjord-like bathymetric features characterized by White Bay and Notre Dame Bay. These features were probably formed during pre-late Wisconsin glacial ice advances and mirror the areas of more easily eroded offshore bedrock. Glacial till deposits have been identified using reflection seisimology records and generally occur at depths greater than the present day 200 m isobath. This is probably due to grounded glacial ice advancing as far offshore as the equivalent of this depth (which was a lesser depth) during the last major ice advance and some, though limited, later reworking of the sediments above this

200 m isobath.

The sedimentological data, though limited, provides enough data for a working hypothesis: mineralogical and marine microfossil evidence indicates that glacial and post glacial sediments have been recovered.

The glacial sediments (till and outwash deposits) overlie bedrock and are found at the bottom of all six piston cores. The mineralogical data suggest that a large component of these deposits originates from the Carboniferous sedimentary rocks of the northeast Newfoundland shelf.

In contrast, the postglacial sediments appear to have been formed by fluvial land run-off followed by seaward dispersal and are probably derived from Newfoundland and the continental land mass close-by (see Chapter 4).

The ^{14}C date of approximately 25,000 yBP on sediments just above the diamicton (see Chapter 4) and the distribution of till as observed on the airgun seismic data (see Chapter 2) suggests that grounded ice-shelf conditions existed at about this date and earlier. This is an earlier estimate for the last maximum ice advance than anticipated in earlier studies. The geological equivalent of the classic Late Wisconsinan period in this area was a period of enhanced ice rafting hypothesised as the result of minor ice-shelf conditions around the Newfoundland coast.

The geotechnical analyses of the cores were carried out prior to the geological work to avoid undue disturbance of the sediments. This involved the measurement of p-wave velocities (carried out immediately after core recovery on the ship), density, porosity, water content, undisturbed and remoulded shear strengths. The geotechnical results are in

agreement with those of other workers, substantiating the techniques that were developed for and used in this study, and gave accurate down core profiles of acoustic impedance, the controlling factor of seismic propagation in the sediments. This enabled the identification of sedimentary lithologies corresponding to D.T.S. seismic facies (which were identified and mapped, see Chapter 2).

The upper acoustically transparent unit (seismic facies 1) corresponds to the grey-brown mud above the carbonate mud facies and represents sedimentation since approximately 7,000 yBP. The sediments from the top of the carbonate mud facies to just above the diamicton (see Chapter 3, Figs. 3.4 to 3.9) gave rise to the stratified seismic facies (2) and the diamicton produces the scattering signature of seismic facies 4. Seismic facies 3 was not cored and therefore no rigid interpretation applies, although it appears to be a semi-stratified/scattering medium probably genetically related to the diamicton facies found close-by. Seismic facies 5 has been interpreted as predominently bedrock.

Despite noise problems on the seismic data, it has been shown that seismic arrivals which appear to be coherent on the scale of the usual graphic recorder output, are not necessarily so on a shot to shot basis. It is concluded that the geology in this area, being only a poor approximation to a planar, elastic, stratified medium, is probably the major cause of the incoherencies (see Chapter 5).

Synthetic seismograms, modelled from the down core profiles of velocity and density, have indicated that using singular piston core data for

such modelling is problematic: the geological sample obtained is too small to be an accurate "average" of the geology as "seen" by the D.T.S. Larger barrel coring devices and a suite of cores from each site of interest are recommended for future work (see Results and Discussions, Chapter 5).

Finally, it is apparent that a knowledge of the acoustic impedance profile (or at least a velocity profile) through the sedimentary section is required in geological studies which employ high resolution seismic data if the geological interpretation is to be believed with confidence.

Recommendations for Further Work - Questions to be Answered

(1) What are the geological signals that correspond to cold- and warm-based ice-sheet conditions? To what extent do ice sheets enhance silica and/or nutrient input into the ocean?

(2) Why was the Late Wisconsinan event a minimum along the eastern Canadian seaboard, given that the oxygen isotope data available in the literature indicates a maximum uptake of ocean waters, implying an overall larger scale ice sheet, during this time period?

(3) Has the C.ex. Clavatum fauna any useful environmental significance? If so, what?

(4) Has the northeast Newfoundland "red" sediment source contributed significantly to the offshore western North Atlantic Quaternary sedimentation?

(5) Do the problems of locally changing physical properties of shelf

sediments pose too great a problem for investigating the nature of high resolution seismic reflections?

(6) Is it realistic to try to develop sophisticated and expensive signal processing approaches to remotely sense the seabed using systems such as the D.T.S.? If such processing can be developed, is it feasible to incorporate as an on-line package for analysis of the data as it is collected?

(7) There are problems associated with our knowledge of the D.T.S. received pressure pulse signature, a study is needed to solve this problem.

(8) Future studies pertaining to the nature of D.T.S. seismic reflectors would be better suited to an easily accessible study area (or areas) with as wide a variety of sedimentary types as possible in that area.

13. Boulton, G.S., Glacial history of the Spitsbergen archipelago and the problem of a Barents Shelf ice sheet. (Boreas, v. 8, 1979, pp. 31-57.)

14. Bruneau, A.A. and Dempster, R.R., Engineering and economic implications of icebergs in the North Atlantic. (Oceanology International '72 Conference, Soc. Underwater Technol., 1972, pp. 176-180.)

15. Buchan, S., McCann, D.M. and Taylor Smith, D., Relations between acoustic and geotechnical properties of marine sediments. (Q. Jl. Engng. Geol., v. 5, 1972, pp. 265-284.)

16. Carey, S.W. and Ahmad, N., Glacial marine sedimentation. (Arctic Geology, v. 2, edited by G.O. Raasch, Toronto University Press, Toronto, 1961, pp. 865-894.)

17. Carver, R.E., Procedures in Sedimentary Petrology. (Wiley-Interscience, N.Y., 1971, 653 p.)

18. Chough, S.K., Morphology, sedimentary facies and processes of the Northwest Atlantic Mid-Ocean channel between 61° N and 52° N, Labrador Sea. (Unpubl. Ph.D. thesis, McGill University, 1978, 167 p.)

19. Claerbout, J.F., Synthesis of a layered medium from its acoustic transmission response. (Geophysics, v. 33, 1968, pp. 264-269.)

20. Clay, C.S. and Leong, W.K., Acoustic estimates of the topography and roughness spectrum of the sea floor southwest of the Iberian Peninsula. (Physics of Sound in Marine Sediments, edited by L. Hampton, Plenum Press, N.Y., 1974, pp. 373-446.)

21. Clay, C.S. and Medwin, H., Acoustical Oceanography: Principles and Applications. (Wiley-Interscience, N.Y., 1977, 544 p.)

22. Darby, E.K. and Neidell, N.S., Application of dynamic programming to the problem of plane wave propagation in a layered medium. (Geophysics, v. 31, 1966, pp. 1037-1048.)

23. Dobrin, M.B., Introduction to geophysical prospecting. (McGraw-Hill, N.Y., 1976, 630 p.)

24. Dodds, J., Report on Digital analysis of deep towed seismic system reflections. (Internal company report for Huntec ('70) Ltd., March 31st, 1976.)

25. Drapeau, G. and King, L.H., Surficial geology off the Yarmouth-Browns Bank map area. (Marine Science Paper 2, Geol. Surv. Can., Paper 72-24, 1972.)

26. Fillon, R.H., Hamilton Bank, Labrador Shelf: postglacial sediment dynamics and paleo-oceanography. (Marine Geol., v. 20, 1976, pp. 7-25.)

27. Flint, R.F., Growth of the North American Ice Sheet during the Wisconsin Age. (Geol. Soc. Am. Bull., v. 54, 1943, pp. 352-362.)

28. Flint, R.F. et al., Diamictite, a substitute term for symmictite. (Geol. Soc. Am. Bull., v. 71, 1960, p. 1809.)

29. Fulton, R.J., Oral comm. GAC/MAC Joint Annual Meeting, Quebec City, May 23-25, 1979.

30. Gostin, V.A. and Herbert, C., Stratigraphy of upper Carboniferous and lower Permian sequences in the South Sydney Basin. (Geol. Soc. Australia Jour., v. 20, 1973, pp. 49-70.)

31. Grant, A.C., The continental margin off Labrador and eastern Newfoundland - morphology and geology. (Unpubl. Ph.D. thesis, Dalhousie University, 1971, 131 p.)

32. Grant, A.C., The continental margin off Labrador and eastern Newfoundland - morphology and geology. (Can. J. Earth Sci., v. 9, 1972, pp. 1394-1430.)

33. Grant, D.R., Glacial style and ice limits, the Quaternary stratigraphic record and changes of land and ocean level in the Atlantic provinces of Canada. (Géogr. phys. Quat., v. XXXI, 1977, pp. 247-260.)

34. Hamilton, E.L., Sound velocity and related properties of marine sediments, North Pacific. (J. Geophys. Res., v. 75, 1970, pp. 4423-4446.)

35. Hamilton, E.L., Elastic properties of marine sediments. (J. Geophys. Res., v. 76, 1971, pp. 579-604.)

36. Hamilton, E.L., Prediction of in-situ acoustic and elastic properties of marine sediments. (Geophysics, v. 36, 1971a, pp. 266-284.)

37. Hamilton, E.L., Shumway, G., Menard, H.W. and Shipek, C.J., Acoustic and other physical properties of shallow-water sediments off San Diego. (J. Acoust. Soc. Am., v. 28, 1956, pp. 1-15.)

38. Hampton, L.D., Acoustic properties of sediments. (J. Acoust. Soc. Am., v. 42, 1967, pp. 882-890.)

39. Harris, I.M. and Jollimore, P.G., Iceberg furrow marks on the continental shelf northeast of Belle Isle, Newfoundland. (Can. J. Earth Sci., v. 11, 1974, pp. 43-52.)

40. Haworth, R.T., Cruise report, Hudson 78-023. (Internal report, Atlantic Geoscience Centre, Bedford Institute of Oceanography, 1978.)

41. Haworth, R.T. and Stanford, B.V., Paleozoic geology of northeast Gulf of St.Lawrence. (Report of Activities, Part A, Geol. Surv. Can., Paper 76-1A, 1976, pp. 1-6.)

42. Haworth, R.T., Poole, W.H., Grant, A.C. and Sanford, B.V., Marine geoscience survey northeast of Newfoundland. (Report of Activities, Part A, Geol. Surv. Can., Paper 76-1A, 1976a, pp. 7-15.)

43. Haworth, R.T., Grant, A.C. and Folinsbee, R.A., Geology of the continental shelf off southeastern Labrador. (Report of Activities, Part C, Geol. Surv. Can., Paper 76-1C, 1976b, pp. 61-70.)

44. Horn, D.R., Horn, B.M. and Delach, M.N., Correlation between acoustical and other physical properties of deep-sea cores. (J. Geophys. Res., v. 73, 1968, pp. 1939-1957.)

45. Horner, R.A., History and recent advances in the study of ice biota. (Polar Oceans, edited by M.J. Dunbar, Arctic Institute of North America, Calgary, 1977, pp. 269-283.)

46. Hoshiai, T., Diatom distribution in sea ice near McMurdo and Syowa Stations. (Antarctic Journal, v. 7, 1972, pp. 84-85.)

47. Hutchins, R.W., Removal of tow fish motion noise from high resolution seismic profiles. (SEG-US Navy Symposium on Acoustic Imaging Technology and On Board Data Recording and Processing Equipment, National Space Technology Laboratories, Bay St. Louis, Mississippi, Aug. 17-18, 1978.)

48. Hutchins, R.W., McKeown, D.L. and King, L.H., A deeptow high resolution seismic system for continental shelf mapping. (Geoscience Canada, v. 3, 1976, pp. 95-100.)

49. Ives, J.D., The maximum extent of the Laurentide Ice Sheet along the east coast of North America during the Last Glaciation. (Arctic, v. 31, 1978, pp. 24-53.)

50. Jollimore, P.G., A medium range side scan sonar for use in coastal waters. Design criteria and operational experiences. (Proceedings of the IEEE Conference on Engineering in the Ocean Environment, Halifax, N.S., v. 2, 1975, Institute of Electrical and Electronic Engineers Inc., N.Y., pp. 108-114.)

51. Jones, A.S.G., Dewes, F.C.D., Buchan, S. and Taylor Smith, D., North Atlantic cores: an interim report. (University College of North Wales Marine Science Labs, Geological Report no. 69-4, 1969.)

52. Kepkay, P.E., Preliminary investigation of free gas as the control of a sub-bottom acoustic reflector in the fine-grained sediments of Halifax Harbour and St. Margaret's Bay, Nova Scotia. (Unpubl. M.Sc. thesis, Dalhousie University, 1977, 86 p.)

53. King, L.H., Use of a conventional echo-sounder and textural analyses in delineating sedimentary facies - Scotian Shelf. (Can. J. Earth Sci., v. 4, 1967, pp. 691-708.)

54. King, L.H., Submarine end moraines and associated deposits on the Scotian shelf. (Geol. Soc. Am. Bull., v. 80, 1969, pp. 83-86.)

55. King, L.H., Surficial geology of the Halifax - Sable Island map-area. (Dept. of Energy, Mines and Resources, Marine Sciences Branch, Ottawa, Paper no. 1, 1970, 16 p.)

56. King, L.H. and Fader, G.B., Application of the Huntec deep tow high resolution seismic system to surficial and bedrock studies - Grand Banks of Newfoundland. (Report of Activities, Part C; Geol. Survey Can., Paper 76-1C, 1976, pp. 5-7.)

57. Knott, S.T., Hoskins, H. and LaCasce, E.O., Jr., The energetics of normal-incident marine seismic profiles and estimation of the acoustic impedance structure of the seabed. (Proceedings of the International Symposium on Computer-Aided Siesmic Analysis and Discrimination, I.E.E.E. Computer Society, 1977)

58. Kögler, F.C. and Larsen, B., The West Bornholm basin in the Baltic Sea: geological structure and Quaternary sediments. (Boreas, V. 8, 1979, pp. 1-22)

59. Kulm, L.D., Suspended sediment transport on the N. Oregon continental shelf. (Geol. Soc. Am. Bull., v. 84, 1973, pp. 3815-3826)

60. Lambe, T.S. and Whitman, R.V., Soil Mechanics. (John Wiley and Sons, publishers, New York, 1969.)

61. Loring, D.H., Marine geology of the Gulf of St. Lawrence. (Earth Sci. Symp. on Offshore Eastern Canada, Geol. Surv. Can., Paper 71-23, 1973, pp. 305-324.)

62. MacIssac, R.R., Identification of ocean bottom sediments through measurements of coherence of acoustic echoes. (Unpubl. M.Eng. thesis, Memorial University, 1977, 99 p.)

63. MacIssac, R.R. and Dunsiger, A.D., Ocean sediment properties using acoustic sensing. (Proceedings of the Fourth International Conference on Port and Ocean Engineering under Arctic Conditions, St. John's, Newfoundland, 1977, pp. 1-13.)

64. MacLean, B. and King, L.H., Surficial geology of the Banquereau and Misaine Bank map area. (Marine Science Paper 3, Geol. Surv. Can., Paper 71-52, 1971.)

65. Matekar, E.J., A treatise on some aspects of modern exploration seismology. (Pan. Am. Petroleum Corp., 1965, 112 p.)

66. McKeown, D.L., Evaluation of the Huntec ('70) Ltd. Hydrosonde Deep Tow Seismic System. (Bedford Institute of Oceanography, Report Series/BI-R-75-4, 1975.)

67. Mitchell, J.K., Shearing resistance of soils as a rate process. (Jour. Soil. Mech. Found. Div. ASCE, v. 90, (SM 1), 1964.)

68. Munsell Soil Colour Charts. (Munsell Soil Colour Co., Inc., Baltimore, 1954.)

69. Nafe, J.E. and Drake, C.L., Physical properties of marine sediments. (The Sea, v. 3, edited by M.N. Hill, Interscience Publishers, N.Y., 1963, pp. 794-815.)

70. Nelson, A.R., Quaternary glacial and Marine stratigraphy of the Qivitu Peninsula, Northern Cumberland Peninsula, Baffin Island, Canada. (Unpublished Ph.D. thesis, University of Colorado, 1978, 213 p.)

71. Nie, H.N., Hull, C.H., Jenkins, J.G., Steinbrenner, K. and Brent, D.H., Statistical Package for the Social Sciences. (McGraw-Hill publishers, 2nd Edition, N.Y., 1975, 675 p.)

72. Nielsen, E., The composition and origin of Wisconsinan till in mainland Nova Scotia. (Unpublished Ph.D. thesis, Dalhousie University, 1976, 256 p.)

73. Overshine, A.T., Observations of iceberg rafting in Glacier Bay, Alaska, and the identification of ancient ice-rafted deposits. (Geol. Soc. Amer. Bull., v. 81, 1970, pp. 891-894.)

74. Paquette, R.G. and Bourke, R.H., Temperature fine structure near the sea-ice margin of the Chukchi Sea. (J. Geophys. Res., v. 84, 1979, pp. 1155-1164.)

75. Parrott, D.R., An interactive program for analyzing high resolution seismic data on PDP-11/20 minicomputer. (Huntec ('70) Ltd., Internal company report no. H7803-01/SB/DRP, 1978.)

76. Peterson, R.A., Fillippone, W.R. and Coker, F.B., The synthesis of seismograms from well log data. (Geophys. v. 20, 1955, pp. 516-538.)

77. Piper, D.J.W., Manual of Sedimentological Techniques. (Depts. of Geology and Oceanography, Dalhousie University, 1974, 106 p.)

78. Piper, D.J.W., Late Quaternary deep water sedimentation off Nova Scotia and Western Grand Banks. (C.S.P.G., Mem. 4, 1975, pp. 195-204.)

79. Piper, D.J.W. and Slatt, R.M., Late Quaternary clay-mineral distribution on the eastern continental margin of Canada. (Geol. Soc. Am. Bull., Vol. 88, 1977, pp. 267-272.)

80. Piper, D.J.W., Mudie, P.J., Aksu, A.E. and Hill, P.R., Late Quaternary sedimentation, 50°N, Northeast Newfoundland Shelf. (Géogr. phys. Quat., Vol. 32, 1978, pp. 321-332.)

81. Prest, V.K., Speculative Isochrones on the Retreat of Wisconsin and Recent Ice in North America. (Geol. Sur. Can., Map 1257A, Ottawa, 1969.)

82. Prest, V.K., Quaternary Geology of Canada: Geology and Economic Minerals of Canada. (Geol. Sur. Can., Econ. Geol. Report 1, Ottawa, 1970, pp. 675-764.)

83. Readings, H.G. and Walker, R.G., Sedimentation of Eocambrian tillites and associated sediments in Finnmark, northern Norway. (Palaeogeogr., Palaeoclimatol., Palaeoecol., v. 2, 1966, pp. 177-212.)

84. Robinson, E.A. and Treitel, S., The fine structure of the normal incidence synthetic seismogram. (Geophys. J.R. astr. Soc., v. 53, 1978, pp. 289-309.)

85. Roksandić, M.M., Seismic facies analysis concepts. (Geophysical Prospecting, v. 26, 1978, pp. 383-398.)

86. Schreiber, B.C., Sound velocity in deep-sea sediments. (J. Geophys. Res., v. 73, 1968a, pp. 1259-1268.)

87. Schreiber, B.C., Marine Geophysical Program 65-67 - Central North Pacific, Area V. (U.S. Naval Oceanogr. Office Contract N62306-1688, Alpine Geophysical Associates, Norwood, N.J., v. 8, Cores, 1968b.)

88. Sengbush, R.L., Lawrence, P.L. and McDonal, F.J., Interpretation of synthetic seismograms. (Geophysics, v. 26, 1961, pp. 138-157.)

89. Sherwood, J.W.C. and Trorey, A.W., Minimum phase and related properties of the response of a horizontally stratified absorptive earth to plane acoustic waves. (Geophysics, v. 30, 1965, pp. 191-197.)

90. Simpkin, P.G., Acoustic and other tests of the Huntec D.T.S. system used during CSS Hudson cruises 1976. (Huntec ('70) Ltd., Internal company report, Feb. 1, 1977.)

91. Simpkin, P.G., Parrott, D.R., Hutchins, R.W. and Ross, D.I., Seabed '75 - Objectives and Achievements. (Bedford Institute of Oceanography, Report Series /BI-R-76-15, 1976.)

92. Slatt, R. M. , Continental Shelf sediments off Eastern Newfoundland: a preliminary investigation. (Can. J. Earth Sci., v. 11, 1974, pp. 362-368.)

93. Stanley, D.J., Swift, D.J.P., Silverberg, N., James, N.P. and Sutton, R.G., Late Quaternary progradation and sand spillover on the outer continental margin off Nova Scotia, Canada. (Smithsonian Contribution to Earth Sci., 1972, v. 8, 88 p.)

94. Stow, D.A.V., Late Quaternary stratigraphy and sedimentation on the Nova Scotia continental margin. (Unpubl. Ph.D. thesis, Dalhousie University, 1977, 360 p.)

95. Treitel, S. and Robinson, E.A., Seismic wave propagation in layered media in terms of communication theory. (Geophysics, v. 31, 1966, pp. 17-32.)

96. Trorey, A.W., Theoretical seismograms with frequency and depth dependent absorption. (Geophysics, v. 27, 1962, pp. 766-785.)

97. Tucholke, B.E. and Shirley, D.J., Comparison of laboratory and in-situ compressional - wave velocity measurements on sediment cores from the western North Atlantic. (J. Geophys. Res., v. 84, 1979, pp. 687-695.)

98. Tucker, C.M., Quaternary studies in Newfoundland: a short review. (Maritime Sediments, v. 12, 1976, p. 61.)

99. Tucker, D.G. and Gazey, B.K., Applied Underwater Acoustics. (Pergamon Press, N.Y., 1966, 244 p.)

100. Tucker, M.E. and Reid, P.C., The sedimentology and context of Late Ordovician glacial marine sediments from Sierra Leone, West Africa. (Palaeogeogr., Palaeoclimatol., Palaeoecol., v. 13, 1973, pp. 289-307.)

101. Tyce, R.C., Towards a quantitative near-bottom seismic profiler. (Ocean Engng., v. 4, 1977, pp. 113-140.)

102. van der Linden, W.J., Fillon, R.H. and Monahan, D., Hamilton Bank, Labrador margin: origin and evolution of a glaciated shelf. (Marine Science Paper 14, Geol. Surv. Can., Paper 75-40, 1976.

103. van Overeem, A.J.A., Shallow-penetration, high resolution sub-bottom profiling. (Marine Geotechnology, v. 3, 1978, pp. 61-84.)

104. Whitman, R.V. and Richart, F.E., Jr., Design procedures for dynamically loaded foundations. (J. Soil Mech. Found. Div. Amer. Soc. Civil Eng., v. 93 (SM6), 1967.)

105. Winokur, R.S. and Chanesman, S., A pulse method for sound speed measurements in cored ocean bottom sediments. (Informal manuscript, I.M. No. 66-5, Accoustical Oceanography Branch, U.S. Navy Oceanographic Office, 1966.)

106. Wuenschel, P.C., Seismogram synthesis including multiples and transmission coefficients. (Geophysics, v. 25, 1960, pp. 106-129.)

107. Zoeppritz, K., Uber Erdebenwellen VIb. (Gottinger Nachricten, 1919, pp. 66-84.)

APPENDIX 1

CORE SITE LOCATIONS

Core # 2; HN78023-13
Lat. 51° 05.38' N; Long. 54" 12.51' W
Water Depth: 230 m

Core # 5; HN78023-19
Lat. 50° 16.645' N; Long. 55° 26.89' W
Water Depth: 296 m

Core # 6; HN78023-20
Lat. 50° 22.32' N; Long. 55° 00.73' W
Water Depth: 280 m

Core # 7; HN78023-21
Lat. 50° 22.4' N; Long. 55° 00.8' W
Water Depth: 280 m

Core # 11; HN78023-31
Lat. 50° 54.25' N; Long. 53° 18.6' W
Water Depth: 440 m

Core # 12; HN78023-32
Lat. 51° 02.35' N; Long. 52° 57.26' W
Water Depth: 485 m

APPENDIX 2

CALCULATION OF SOUND VELOCITY IN THE CORED SEDIMENTS

The velocity is calculated from the measured delay time for a pulse to be transmitted through the 2-phase medium of the plastic core liner and its sediment fill (Fig. A.1). The timing is measured from the trigger point (the start of the pulse generator output) to the first kick of the received signal from zero on trace number 2, Figure 3.3, and is accurate to 0.1 μs using the combination of the delayed trigger facility of an oscilloscope and a timer/counter.

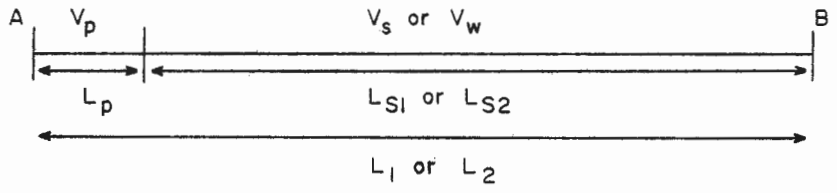

FIGURE A.1

Vp = sound speed in plastic

Vs = sound speed in sediment

Vw = sound speed in water

Lp = length of plastic (= 2x core liner wall thickness)

Ls = length of sediment (inside diameter of core liner)

L_1 = Lp + Ls_1 (= outside diameter of core, L_2 is same)

L_2 = Lp + Ls_2 (this accounts for possible changes in core liner diameter)

The time required for a pulse to propagate from A to B through a calibration liner filled with distilled water = T_1.

$$T_1 = \frac{Lp}{Vp} + L_1 - \frac{Lp}{Vw} + T_t \qquad (1)$$

where T_t = fixed delays in the system. Similarly, when any core liner is sediment filled, the time = T_2.

$$T_2 = \frac{Lp}{Vp} + L_2 - \frac{Lp}{Vs} + T_t \qquad (2)$$

Subtracting (1) from (2), and rearranging, we have:

$$Vs = \frac{(L_2 - Lp)\ Vw}{(T_2 - T_1)\ Vw + L_1 - Lp}$$

If we assume a constant core liner thickness, Lp, and fixed system delays, T_t, then by measuring T_1, L_1, Lp and Vw, we can calibrate the system so that measurements of variations in L_2 and T_2 in the sediment filled cores will give the changes in Vs, the sediment velocity. We assume that the parameters measured initially in the calibration remain unchanged for any scanning period (in this respect it is important to set the system up and leave it unchanged).

On ship, a programmable calculator was used to calculate velocities in ms^{-1} as the measurements were being made. These values were then digitized with distance down core for later computer manipulation.

Appendix 4 gives a listing of the raw velocity and density data for the cores analyzed in this study.

APPENDIX 3

LISTINGS OF DATA FILES GIVING THE CALCULATED GEOTECHNICAL PARAMETERS VERSUS DEPTH IN THE CORES

These data are given for cores 2, 5, 6, 7, 11 and 12, as indicated. The symbols used at the top of each column have the following meanings:

SN = laboratory sample number

DIST = distance of sampling location down core

DENS = bulk density of the sediment sample (g cm^{-3})

POR = porosity of the sample (%)

CONT = water content of sample = $\frac{\text{weight of water}}{\text{dry weight of solid particles}}$

SDEN = solid density (g cm^{-3})

UNDISH = undisturbed shear strength (KN m^{-2})

REMSH = remoulded shear strength (KN m^{-2})

SENS = sensitivity = UNDISH/REMSH

OLD,RES2
/LNH
CORE 2 , SECTIONS 1-3,HN78023-13 GEOTECHNICAL DATA

SN	DIST	DENS	POR	CONT	SDEN	UNDISH	REMSH	SENS
138	30	1.751	55.13	.452	2.688	6.77	1.05	6.44
139	70	1.759	54.93	.446	2.699	7.23	1.52	4.77
140	140	1.619	63.28	.629	2.707	5.37	.70	7.67
141	170	1.589	65.31	.684	2.719	9.45	1.63	5.79
142	215	1.591	65.49	.686	2.734	6.53	1.05	6.22
143	245	1.661	61.26	.574	2.724	9.57	1.40	6.83
144	315	1.614	64.05	.645	2.728	8.75	.93	9.38
145	375	1.649	61.04	.577	2.683	12.13	1.75	6.93
146	410	1.610	63.44	.637	2.690	10.73	1.75	6.13
147	475	1.610	63.16	.633	2.675	13.30	1.40	9.50
148	515	1.721	56.37	.478	2.669	14.00	1.87	7.50
149	555	1.617	62.08	.611	2.645	11.78	1.52	7.77
150	575	1.907	46.22	.315	2.697	9.22	.82	11.29
151	596	1.671	59.84	.548	2.688	6.77	.93	7.25
152	613	1.657	59.33	.548	2.633	9.33	1.98	4.71
153	665	1.980	42.37	.268	2.708	7.00	1.40	5.00
154	695	2.023	39.72	.241	2.705	6.77	1.63	4.14
155	745	2.007	40.24	.247	2.693	10.15	.82	12.43
156	785	1.982	39.57	.246	2.633	16.22	1.52	10.69

/

OLD,RES5
/LNH
CORE 5 , SECTIONS 1+2, HN78023-19 GEOTECHNICAL DATA

SN	DIST	DENS	POR	CONT	SDEN	UNDISH	REMSH	SENS
43	2	1.600	64.07	.654	2.692	2.92	.93	3.13
44	10	1.677	60.36	.552	2.725	2.33	1.17	2.00
45	30	1.453	73.09	.988	2.717	2.57	.58	4.40
46	50	1.545	68.17	.773	2.738	6.53	1.28	5.09
47	70	1.530	69.32	.810	2.756	5.48	1.05	5.22
48	90	1.547	68.00	.768	2.735	5.72	.70	8.17
49	130	1.514	71.55	.876	2.837	5.48	.70	7.83
50	154	1.472	72.09	.938	2.721	6.42	.82	7.86
51	184	1.505	70.54	.863	2.741	9.22	.93	9.88
52	194	1.638	62.09	.599	2.703	7.47	.93	8.00
53	219	1.633	63.01	.616	2.731	5.60	.70	8.00
54	239	0.000	00.00	0.000	0.000	0.00	0.00	0.00
55	110	1.568	66.85	.728	2.736	6.53	.93	7.00
56	132	1.298	81.86	1.654	2.696	0.00	0.00	0.00
57	289	1.525	69.09	.810	2.726	7.70	.58	13.20
58	309	1.485	71.63	.911	2.738	5.02	.58	8.60
59	314	1.226	85.51	2.216	2.632	0.00	0.00	0.00
60	329	1.612	64.38	.652	2.740	3.73	.82	4.57
61	354	1.946	45.05	.297	2.731	3.62	1.17	3.10
62	384	1.806	53.70	.416	2.755	3.62	1.17	3.10
63	404	2.085	36.94	.212	2.728	5.25	1.87	2.81
64	434	2.175	33.14	.177	2.763	7.47	2.10	3.56

/

OLD,RES6
/LNH
CORE 6 , SECTIONS 1_4, HN78023-20 GEOTECHNICAL DATA

SN	DIST	DENS	POR	CONT	SDEN	UNDISH	REMSH	SENS
1	10	1.603	65.63	.680	2.776	3.67	1.05	3.50
2	30	1.630	63.81	.631	2.760	5.25	.93	5.63
3	50	1.622	64.07	.641	2.751	7.35	2.10	3.50
4	70	1.635	62.93	.614	2.732	6.30	1.05	6.00
5	110	1.631	63.69	.628	2.759	9.22	1.40	6.58
6	135	1.645	63.61	.619	2.793	7.58	1.17	6.50
7	155	1.643	62.99	.610	2.757	4.67	1.17	4.00
8	192	1.638	63.51	.621	2.769	10.73	1.87	5.75
9	222	1.637	63.31	.619	2.756	9.68	2.22	4.37
10	242	1.657	61.79	.584	2.738	8.05	2.10	3.83
11	262	1.644	62.63	.604	2.743	4.90	.23	21.00
12	282	1.624	63.82	.635	2.745	7.35	2.22	3.32
13	302	1.628	63.24	.623	2.729	5.95	.93	6.38
14	317	1.676	60.50	.554	2.730	7.35	1.17	6.30
15	338	1.587	65.57	.690	2.728	9.57	.47	20.50
16	353	1.564	67.05	.735	2.736	7.12	1.17	6.10
17	368	1.701	59.27	.525	2.738	12.02	1.40	8.58
18	383	1.711	58.21	.506	2.717	9.33	1.63	5.71
19	408	1.531	68.75	.798	2.725	12.02	.93	12.88
20	436	1.635	62.81	.612	2.726	12.72	1.05	12.11
21	458	1.632	63.26	.621	2.739	11.67	1.17	10.00
22	499	1.597	65.47	.681	2.752	11.78	3.38	3.48
23	539	1.582	66.24	.705	2.749	14.12	1.87	7.56
24	589	1.616	64.67	.654	2.765	16.57	3.15	5.26
25	609	1.581	66.24	.707	2.744	18.55	2.10	8.83
26	655	1.597	65.42	.680	2.749	14.58	1.17	12.50
26	705	1.679	60.73	.556	2.748	7.82	.82	9.57
27	730	1.657	61.91	.586	2.744	12.72	1.75	7.27
28	805	1.574	75.45	.900	3.374	17.38	2.45	7.10
29	835	1.578	75.78	.903	3.424	15.17	3.27	4.64
30	855	1.575	74.47	.877	3.287	18.43	3.73	4.94
31	875	1.585	74.44	.865	3.325	18.20	1.17	15.60
32	895	1.614	74.99	.848	3.492	14.58	1.28	11.36
33	905	1.647	72.70	.774	3.401	14.58	1.63	8.93
34	915	1.817	62.49	.515	3.197	9.22	1.28	7.18
35	932	1.593	76.99	.914	3.618	6.30	.93	6.75
36	946	1.911	59.23	.441	3.251	6.77	1.63	4.14
37	961	1.910	58.73	.436	3.222	9.45	1.98	4.76
38	973	1.896	59.45	.449	3.227	5.37	1.28	4.18
39	989	2.022	53.56	.354	3.214	7.93	2.33	3.40
40	998	2.095	47.03	.285	3.077	6.65	1.17	5.70
41	1009	2.167	42.91	.243	3.053	10.03	1.75	5.73
42	1031	2.126	41.83	.241	2.943	12.13	2.33	5.20

/

```
 OLD,RES7
/LNH
CORE 7 , SECTIONS 1-3,HN78023-21 GEOTECHNICAL DATA
```

SN	DIST	DENS	POR	CONT	SDEN	UNDISH	REMSH	SENS
83	30	1.631	63.28	.622	2.739	7.23	1.98	3.65
84	60	1.668	60.88	.564	2.727	7.47	2.10	3.56
85	105	1.635	62.85	.613	2.728	7.93	1.52	5.23
86	155	1.617	63.66	.637	2.718	9.45	1.28	7.36
87	210	1.561	66.57	.728	2.702	9.92	1.17	8.50
88	240	1.702	58.95	.520	2.728	6.65	1.17	5.70
89	250	1.700	58.61	.517	2.708	7.93	1.17	6.80
90	260	1.604	64.11	.653	2.703	0.00	0.00	0.00
91	285	1.548	67.36	.754	2.703	9.33	1.05	8.89
92	300	1.696	59.30	.528	2.727	10.15	1.40	7.25
93	325	1.625	63.44	.628	2.729	9.57	.93	10.25
94	355	1.596	64.82	.670	2.717	12.48	1.75	7.13
95	395	1.636	62.94	.613	2.736	12.72	1.98	6.41
96	455	1.592	65.59	.687	2.743	14.35	1.63	8.79
97	505	1.623	63.63	.632	2.734	12.72	1.40	9.08
98	555	1.606	64.11	.651	2.711	13.30	.82	16.29
99	595	1.584	65.49	.691	2.714	12.13	1.87	6.50
100	640	1.576	66.06	.707	2.721	15.63	2.10	7.44
101	665	1.617	63.75	.638	2.723	13.65	1.17	11.70
102	680	1.659	61.63	.580	2.737	12.37	1.40	8.83
103	690	1.902	47.63	.329	2.733	10.27	1.40	7.33
104	705	1.587	66.77	.711	2.790	5.72	1.52	3.77
105	730	1.943	45.41	.300	2.737	0.00	0.00	0.00
106	755	1.894	48.28	.337	2.740	5.83	1.40	4.17
107	770	2.093	36.13	.206	2.718	10.15	1.98	5.12
108	800	2.114	34.75	.194	2.714	19.48	1.87	10.44

```
/
```

CORE 11, SECTIONS 1-4,HN78023-31 GEOTECHNICAL DATA

SN	DIST	DENS	POR	CONT	SDEN	UNDISH	REMSH	SENS
109	20	1.398	76.31	1.171	2.718	2.10	.70	3.00
110	50	1.453	72.93	.983	2.707	3.03	.58	5.20
111	90	1.434	73.83	1.035	2.693	5.25	.70	7.50
112	137	1.600	64.26	.658	2.701	6.88	1.05	6.56
113	167	1.417	74.64	1.085	2.679	8.75	1.05	8.33
114	310	1.447	73.08	.996	2.694	8.17	.82	10.00
115	330	1.495	70.90	.881	2.731	7.82	1.17	6.70
116	360	1.561	67.51	.746	2.752	8.17	1.17	7.00
117	390	1.514	69.68	.834	2.724	8.05	.93	8.63
118	460	1.502	70.46	.864	2.728	8.40	1.52	5.54
119	485	1.572	66.02	.709	2.707	11.08	1.28	8.64
120	510	1.499	70.43	.867	2.716	12.13	1.63	7.43
121	576	1.545	67.57	.761	2.706	13.65	2.33	5.85
122	590	1.580	65.55	.695	2.706	12.13	1.52	8.00
123	605	1.536	67.97	.777	2.698	14.47	1.87	7.75
124	615	1.571	66.44	.718	2.725	16.10	1.52	10.62
125	650	1.509	69.35	.832	2.689	14.00	1.28	10.91
126	700	1.506	69.12	.830	2.666	15.40	1.40	11.00
127	750	1.545	68.13	.772	2.736	13.88	1.40	9.92
128	790	1.545	67.41	.758	2.698	15.52	2.33	6.65
129	820	1.833	51.36	.383	2.725	11.90	1.98	6.00
130	840	1.701	59.00	.521	2.727	8.63	1.17	7.40
131	870	1.754	56.51	.467	2.748	10.97	1.63	6.71
132	895	1.939	45.28	.300	2.727	0.00	0.00	0.00
133	910	1.897	47.80	.331	2.730	14.93	1.87	8.00
134	950	1.894	47.98	.334	2.730	13.53	1.63	8.29
135	985	1.908	47.35	.325	2.734	16.57	1.05	15.78
136	1010	1.969	43.73	.281	2.731	14.47	1.87	7.75
137	1025	2.000	41.18	.255	2.709	26.13	2.68	9.74

/

CORE 12, SECTIONS 1+2,HN78023-32 GEOTECHNICAL DATA

SN	DIST	DENS	POR	CONT	SDEN	UNDISH	REMSH	SENS
65	20	1.564	67.13	.737	2.740	3.03	.47	6.50
66	45	1.584	66.02	.700	2.741	4.08	.93	4.38
67	70	1.578	66.17	.707	2.733	3.27	.58	5.60
68	120	1.501	70.51	.867	2.726	7.47	.82	9.14
69	170	1.514	69.71	.835	2.725	5.25	.93	5.63
70	220	1.440	73.83	1.028	2.713	5.60	.70	8.00
71	281	1.483	70.82	.893	2.685	7.12	.70	10.17
72	316	1.558	67.60	.751	2.747	7.35	1.28	5.73
73	336	1.830	51.20	.382	2.714	4.20	.82	5.14
74	346	1.825	51.50	.387	2.713	3.38	1.28	2.64
75	361	1.685	60.04	.543	2.732	6.77	1.63	4.14
76	371	1.895	46.82	.323	2.693	9.80	3.27	3.00
77	396	1.811	51.55	.391	2.687	7.58	2.57	2.95
78	430	1.872	49.13	.350	2.725	7.23	1.75	4.13
79	450	1.883	48.38	.340	2.721	5.83	1.17	5.00
80	470	1.938	45.44	.302	2.728	5.60	1.75	3.20
81	510	1.975	42.75	.272	2.711	8.87	1.63	5.43
82	540	1.926	46.88	.317	2.754	9.22	3.50	2.63

/

APPENDIX 4

LISTINGS OF DATA FILES OF PRESSURE-WAVE VELOCITIES AND BULK DENSITIES VERSUS DEPTH FOR CORES 2, 5, 6, 7, 11 AND 12

These parameters are given in the order of depth (cm), velocity (ms^{-1}) and density ($g\ cm^{-3}$).

Note that all the velocity values are measured, whereas the density values were interpolated from the measured data given in Appendix 2.

OLD,APPED2
/LNH

Data File, Distance down core, Velocity, Density$ HN78023-13, CORE2

6.00	1555.00	1.75	10.00	1558.00	1.75	15.00	1540.00	1.75
20.00	1523.00	1.75	25.00	1523.00	1.75	30.00	1530.00	1.75
32.00	1512.00	1.75	35.00	1519.00	1.75	40.00	1526.00	1.75
45.00	1519.00	1.75	50.00	1530.00	1.76	55.00	1535.00	1.76
60.00	1537.00	1.76	65.00	1534.00	1.76	70.00	1554.00	1.76
75.00	1534.00	1.75	80.00	1531.00	1.74	86.00	1503.00	1.73
90.00	1491.00	1.72	95.00	1487.00	1.71	100.00	1489.00	1.70
105.00	1482.00	1.69	109.00	1478.00	1.68	115.00	1482.00	1.67
120.00	1482.00	1.66	123.00	1478.00	1.65	130.00	1478.00	1.64
135.00	1475.00	1.63	140.00	1475.00	1.62	145.00	1475.00	1.61
150.00	1468.00	1.61	155.00	1468.00	1.60	160.00	1468.00	1.60
165.00	1471.00	1.59	170.00	1471.00	1.59	175.00	1471.00	1.59
179.00	1463.00	1.59	185.00	1462.00	1.59	190.00	1465.00	1.59
195.00	1464.00	1.59	200.00	1467.00	1.59	205.00	1466.00	1.59
210.00	1478.00	1.59	215.00	1488.00	1.60	220.00	1486.00	1.61
225.00	1473.00	1.63	230.00	1472.00	1.64	235.00	1472.00	1.65
240.00	1475.00	1.66	245.00	1478.00	1.66	250.00	1475.00	1.66
255.00	1475.00	1.65	260.00	1476.00	1.65	265.00	1466.00	1.65
270.00	1466.00	1.64	275.00	1466.00	1.64	280.00	1476.00	1.64
285.00	1473.00	1.63	290.00	1480.00	1.63	295.00	1480.00	1.63
300.00	1474.00	1.62	305.00	1477.00	1.62	310.00	1469.00	1.61
313.00	1498.00	1.62	315.00	1478.00	1.62	320.00	1478.00	1.62
325.00	1505.00	1.62	330.00	1478.00	1.63	333.00	1530.00	1.63
335.00	1490.00	1.63	340.00	1519.00	1.63	345.00	1478.00	1.64
350.00	1478.00	1.64	355.00	1481.00	1.64	360.00	1478.00	1.64
365.00	1480.00	1.65	370.00	1483.00	1.65	375.00	1612.00	1.64
380.00	1478.00	1.64	385.00	1482.00	1.62	390.00	1482.00	1.62
395.00	1480.00	1.62	400.00	1470.00	1.61	405.00	1474.00	1.61
410.00	1474.00	1.61	415.00	1474.00	1.61	420.00	1473.00	1.61
425.00	1478.00	1.61	430.00	1488.00	1.61	435.00	1482.00	1.61
440.00	1480.00	1.61	445.00	1480.00	1.61	450.00	1480.00	1.61
455.00	1480.00	1.61	460.00	1480.00	1.61	465.00	1470.00	1.61
470.00	1470.00	1.61	475.00	1473.00	1.63	480.00	1473.00	1.65
490.00	1471.00	1.67	495.00	1481.00	1.69	500.00	1491.00	1.71
505.00	1514.00	1.72	508.00	1728.00	1.71	510.00	1554.00	1.71
515.00	1579.00	1.70	520.00	1625.00	1.68	525.00	1520.00	1.70
530.00	1506.00	1.66	535.00	1473.00	1.64	540.00	1491.00	1.63
545.00	1485.00	1.62	550.00	1516.00	1.76	555.00	1588.00	1.81
560.00	1577.00	1.85	565.00	1651.00	1.91	570.00	1964.00	1.85
575.00	1642.00	1.79	580.00	1609.00	1.73	585.00	1524.00	1.67
590.00	1541.00	1.67	595.00	1497.00	1.67	600.00	1838.00	1.66
605.00	1546.00	1.66	610.00	1543.00	1.66	615.00	1583.00	1.66
620.00	1578.00	1.70	625.00	1520.00	1.74	630.00	1590.00	1.78
635.00	1614.00	1.82	640.00	1567.00	1.86	645.00	1901.00	1.90
650.00	1710.00	1.94	653.00	1843.00	1.97	655.00	1697.00	1.98
658.00	2431.00	1.99	660.00	1766.00	1.99	663.00	1748.00	1.99
665.00	1680.00	1.99	670.00	1803.00	2.00	675.00	1678.00	2.01
677.00	2012.00	2.01	680.00	1695.00	2.02	685.00	2018.00	2.02
690.00	1859.00	2.02	695.00	1671.00	2.02	699.00	1909.00	2.02
700.00	1748.00	2.02	704.00	1659.00	2.02	705.00	1865.00	2.02
710.00	1651.00	2.02	715.00	1799.00	2.02	716.00	1953.00	2.02
720.00	1671.00	2.02	725.00	1680.00	2.02	730.00	1667.00	2.01
735.00	1634.00	2.01	740.00	1659.00	2.00	745.00	2011.00	2.00
750.00	1704.00	2.00	755.00	2414.00	2.00	760.00	1758.00	1.99
761.00	1878.00	1.99	765.00	1815.00	1.99	770.00	1801.00	1.99
775.00	1675.00	1.98						

/

```
OLD,APPED5      Data File, Distance down core, Velocity, Density  HN79023-19, CORE5
/ENH
```

5.00	1614.00	1.63	10.00	1554.00	1.68	15.00	1526.00	1.61
17.00	1591.00	1.90	20.00	1646.00	1.57	25.00	1584.00	1.51
30.00	1547.00	1.45	35.00	1512.00	1.48	38.00	1580.00	1.49
40.00	1508.00	1.50	42.00	1634.00	1.51	45.00	1502.00	1.52
47.00	1565.00	1.53	50.00	1565.00	1.55	55.00	1529.00	1.54
60.00	1565.00	1.54	65.00	1488.00	1.53	70.00	1492.00	1.53
75.00	1498.00	1.53	78.00	1572.00	1.54	80.00	1495.00	1.54
85.00	1495.00	1.54	90.00	1536.00	1.55	95.00	1502.00	1.54
99.00	1515.00	1.54	100.00	1508.00	1.54	105.00	1498.00	1.53
110.00	1498.00	1.53	115.00	1614.00	1.53	120.00	1529.00	1.52
125.00	1498.00	1.52	130.00	1546.00	1.51	134.00	1508.00	1.51
136.00	1533.00	1.50	145.00	1496.00	1.48	150.00	1489.00	1.47
154.00	1592.00	1.48	155.00	1592.00	1.48	160.00	1509.00	1.48
165.00	1516.00	1.49	170.00	1496.00	1.49	175.00	1495.00	1.50
180.00	1489.00	1.51	185.00	1492.00	1.56	186.00	1516.00	1.57
190.00	1513.00	1.64	192.00	1603.00	1.64	195.00	1630.00	1.64
197.00	1900.00	1.64	200.00	1540.00	1.64	202.00	1693.00	1.64
205.00	1509.00	1.64	210.00	1569.00	1.63	215.00	1526.00	1.63
220.00	1573.00	1.62	225.00	1502.00	1.62	229.00	1596.00	1.61
230.00	1536.00	1.61	235.00	1530.00	1.60	240.00	1505.00	1.59
242.00	1596.00	1.58	245.00	1489.00	1.58	249.00	1655.00	1.57
250.00	1689.00	1.57	255.00	1547.00	1.50	259.00	1655.00	1.45
260.00	1655.00	1.43	265.00	1492.00	1.37	267.00	1676.00	1.34
269.00	1592.00	1.31	270.00	1537.00	1.30	275.00	1492.00	1.38
280.00	1492.00	1.45	285.00	1499.00	1.53	290.00	1499.00	1.52
293.00	1603.00	1.51	295.00	1492.00	1.51	297.00	1511.00	1.50
300.00	1502.00	1.50	305.00	1506.00	1.49	310.00	1506.00	1.23
315.00	1530.00	1.35	319.00	1555.00	1.43	320.00	1533.00	1.48
324.00	1555.00	1.59	325.00	1548.00	1.61	327.00	1607.00	1.64
330.00	1548.00	1.68	333.00	1415.00	1.72	335.00	1631.00	1.75
336.00	1832.00	1.76	340.00	1701.00	1.81	342.00	1732.00	1.84
345.00	1659.00	1.88	346.00	1741.00	1.90	348.00	1774.00	1.92
350.00	1732.00	1.95	352.00	1765.00	1.94	355.00	1793.00	1.92
357.00	1827.00	1.91	360.00	1663.00	1.89	362.00	1769.00	1.88
365.00	1540.00	1.86	367.00	1580.00	1.85	370.00	1584.00	1.84
379.00	1710.00	1.81	380.00	1710.00	1.81	383.00	1680.00	1.84
385.00	1812.00	1.88	387.00	1900.00	1.90	390.00	1884.00	1.95
394.00	1812.00	2.00	395.00	1755.00	2.02	398.00	1827.00	2.06
400.00	1663.00	2.09	403.00	2090.00	2.09	405.00	1832.00	2.10
410.00	1715.00	2.12	415.00	1967.00	2.13	420.00	1793.00	2.15
421.00	1895.00	2.15	425.00	1774.00	2.16	430.00	1724.00	2.18
434.00	1928.00	2.18	435.00	2300.00	2.18	436.00	2253.00	2.18

/

OLD,APPED7
/LNH

Data File, Distance down core, Velocity, Density; HN78023-21, CORE7

7.00	1488.00	1.55	10.00	1488.00	1.55	15.00	1498.00	1.55
19.00	1547.00	1.60	20.00	1536.00	1.61	25.00	1498.00	1.62
30.00	1502.00	1.63	35.00	1502.00	1.64	40.00	1505.00	1.64
45.00	1505.00	1.65	46.00	1562.00	1.65	50.00	1505.00	1.66
55.00	1502.00	1.66	60.00	1509.00	1.67	65.00	1509.00	1.67
70.00	1502.00	1.66	75.00	1498.00	1.66	80.00	1498.00	1.65
85.00	1492.00	1.65	90.00	1498.00	1.65	95.00	1498.00	1.64
100.00	1495.00	1.64	105.00	1498.00	1.64	108.00	1544.00	1.63
110.00	1596.00	1.63	115.00	1502.00	1.63	120.00	1512.00	1.63
125.00	1512.00	1.63	130.00	1512.00	1.63	135.00	1512.00	1.62
137.00	1558.00	1.62	140.00	1515.00	1.62	145.00	1515.00	1.62
150.00	1600.00	1.62	155.00	1515.00	1.62	160.00	1526.00	1.61
165.00	1652.00	1.61	170.00	1604.00	1.60	175.00	1529.00	1.60
178.00	1588.00	1.59	180.00	1495.00	1.59	185.00	1512.00	1.59
190.00	1551.00	1.58	192.00	1766.00	1.58	195.00	1522.00	1.58
200.00	1780.00	1.57	205.00	1498.00	1.57	210.00	1508.00	1.56
215.00	1498.00	1.59	231.00	1521.00	1.66	235.00	1528.00	1.68
240.00	1560.00	1.70	245.00	1518.00	1.70	247.00	1549.00	1.70
250.00	1535.00	1.70	255.00	1613.00	1.61	259.00	1819.00	1.61
260.00	1775.00	1.60	265.00	1497.00	1.60	267.00	1564.00	1.59
270.00	1501.00	1.58	275.00	1507.00	1.57	280.00	1501.00	1.56
285.00	1504.00	1.55	290.00	1504.00	1.60	295.00	1553.00	1.65
300.00	1521.00	1.70	305.00	1518.00	1.68	310.00	1497.00	1.67
315.00	1511.00	1.65	320.00	1542.00	1.64	325.00	1501.00	1.63
330.00	1538.00	1.62	333.00	1556.00	1.62	335.00	1574.00	1.62
340.00	1521.00	1.61	343.00	1556.00	1.61	345.00	1497.00	1.61
350.00	1504.00	1.60	355.00	1497.00	1.60	360.00	1497.00	1.60
365.00	1605.00	1.61	370.00	1507.00	1.61	375.00	1504.00	1.62
380.00	1504.00	1.62	385.00	1504.00	1.63	390.00	1504.00	1.63
395.00	1504.00	1.64	400.00	1528.00	1.63	405.00	1507.00	1.63
410.00	1494.00	1.62	415.00	1501.00	1.62	420.00	1507.00	1.62
425.00	1571.00	1.61	430.00	1542.00	1.61	435.00	1497.00	1.61
437.00	1549.00	1.60	440.00	1490.00	1.60	445.00	1490.00	1.60
450.00	1487.00	1.60	455.00	1490.00	1.59	460.00	1511.00	1.60
465.00	1511.00	1.60	470.00	1524.00	1.60	471.00	1567.00	1.60
475.00	1521.00	1.60	480.00	1523.00	1.61	482.00	1703.00	1.61
485.00	1586.00	1.61	490.00	1497.00	1.61	495.00	1497.00	1.62
500.00	1497.00	1.62	505.00	1549.00	1.62	510.00	1524.00	1.62
515.00	1571.00	1.62	517.00	1556.00	1.62	530.00	1570.00	1.62
535.00	1510.00	1.62	539.00	1589.00	1.61	540.00	1517.00	1.61
545.00	1664.00	1.61	546.00	1761.00	1.61	550.00	1496.00	1.61
555.00	1500.00	1.61	560.00	1503.00	1.60	565.00	1510.00	1.60
570.00	1493.00	1.60	575.00	1493.00	1.60	580.00	1493.00	1.60
585.00	1500.00	1.60	590.00	1854.00	1.59	594.00	1668.00	1.59
595.00	1531.00	1.58	600.00	1503.00	1.58	605.00	1510.00	1.58
610.00	1490.00	1.58	615.00	1493.00	1.58	617.00	1548.00	1.58
620.00	1496.00	1.58	625.00	1496.00	1.58	630.00	1496.00	1.58
635.00	1500.00	1.58	640.00	1500.00	1.58	645.00	1513.00	1.58
650.00	1513.00	1.59	652.00	1559.00	1.59	655.00	1520.00	1.60
660.00	1517.00	1.61	662.00	1552.00	1.61	665.00	1809.00	1.62
669.00	1548.00	1.63	670.00	1548.00	1.63	672.00	1660.00	1.64
675.00	1563.00	1.65	680.00	1597.00	1.66	685.00	1952.00	1.78
690.00	1711.00	1.90	695.00	2196.00	1.78	700.00	1567.00	1.65
705.00	1597.00	1.59	708.00	1644.00	1.63	710.00	1616.00	1.66
712.00	1818.00	1.69	715.00	1593.00	1.73	717.00	1632.00	1.75
720.00	1541.00	1.80	723.00	1780.00	1.84	725.00	1677.00	1.87
730.00	1885.00	1.94	731.00	1918.00	1.94	735.00	1656.00	1.93
740.00	1789.00	1.92	745.00	1725.00	1.91	750.00	1620.00	1.90
755.00	1559.00	1.89	757.00	1632.00	1.92	761.00	1890.00	1.98
765.00	1935.00	2.03	766.00	1963.00	2.04	771.00	1864.00	2.09
775.00	1720.00	2.10	778.00	1969.00	2.11	780.00	1814.00	2.11
781.00	1885.00	2.11	785.00	1854.00	2.12	787.00	2240.00	2.12
790.00	1854.00	2.13	795.00	1891.00	2.14	800.00	1819.00	2.14
802.00	2419.00	2.14	805.00	2073.00	2.14	807.00	2427.00	2.14
810.00	2099.00	2.14	815.00	2759.00	2.14	820.00	2004.00	2.14
825.00	2047.00	2.14						

/

```
OLD,APPED11
/LNH            Data File, Distance down core, Velocity, Density; HN78023-31, CORE11

    8.00  1464.00  1.40    10.00  1461.00  1.40    15.00  1464.00  1.40
   20.00  1464.00  1.40    25.00  1521.00  1.41    26.00  1594.00  1.41
   30.00  1461.00  1.42    35.00  1461.00  1.43    40.00  1461.00  1.43
   45.00  1467.00  1.44    50.00  1467.00  1.45    55.00  1464.00  1.45
   60.00  1467.00  1.45    65.00  1504.00  1.45    70.00  1467.00  1.44
   75.00  1467.00  1.44    80.00  1467.00  1.44    85.00  1467.00  1.44
   90.00  1467.00  1.43    95.00  1451.00  1.45   100.00  1461.00  1.47
  105.00  1458.00  1.49   110.00  1451.00  1.51   127.00  1459.00  1.57
  160.00  1469.00  1.45   165.00  1479.00  1.43   168.00  1479.00  1.42
  171.00  1459.00  1.42   175.00  1476.00  1.42   180.00  1472.00  1.42
  185.00  1463.00  1.42   190.00  1479.00  1.42   195.00  1479.00  1.42
  200.00  1479.00  1.42   205.00  1479.00  1.43   210.00  1472.00  1.43
  215.00  1469.00  1.43   220.00  1479.00  1.43   225.00  1472.00  1.43
  230.00  1492.00  1.43   235.00  1496.00  1.43   240.00  1476.00  1.43
  245.00  1485.00  1.43   250.00  1476.00  1.43   255.00  1472.00  1.44
  260.00  1472.00  1.44   265.00  1472.00  1.44   270.00  1472.00  1.44
  275.00  1485.00  1.44   280.00  1469.00  1.44   285.00  1466.00  1.44
  290.00  1472.00  1.44   295.00  1463.00  1.44   300.00  1466.00  1.45
  305.00  1466.00  1.45   310.00  1463.00  1.45   315.00  1466.00  1.46
  320.00  1466.00  1.47   325.00  1466.00  1.48   330.00  1463.00  1.50
  335.00  1472.00  1.50   337.00  1548.00  1.51   340.00  1469.00  1.52
  345.00  1472.00  1.53   350.00  1469.00  1.54   355.00  1466.00  1.55
  360.00  1463.00  1.56   365.00  1469.00  1.55   370.00  1469.00  1.55
  375.00  1472.00  1.54   380.00  1472.00  1.53   385.00  1472.00  1.52
  390.00  1472.00  1.51   395.00  1472.00  1.51   400.00  1466.00  1.51
  415.00  1464.00  1.51   420.00  1464.00  1.51   425.00  1467.00  1.51
  430.00  1464.00  1.51   435.00  1471.00  1.51   440.00  1471.00  1.51
  445.00  1454.00  1.51   450.00  1411.00  1.50   455.00  1405.00  1.50
  460.00  1362.00  1.50   465.00  1326.00  1.52   469.00  1433.00  1.53
  475.00  1451.00  1.54   480.00  1373.00  1.56   485.00  1353.00  1.57
  490.00  1310.00  1.56   493.00  1396.00  1.55   495.00  1402.00  1.54
  500.00  1393.00  1.53   505.00  1411.00  1.51   510.00  1458.00  1.50
  515.00  1448.00  1.50   520.00  1471.00  1.51   525.00  1471.00  1.51
  530.00  1407.00  1.51   535.00  1458.00  1.51   540.00  1433.00  1.52
  545.00  1471.00  1.52   550.00  1467.00  1.52   555.00  1474.00  1.53
  560.00  1481.00  1.53   565.00  1474.00  1.53   570.00  1442.00  1.54
  575.00  1385.00  1.55   577.00  1471.00  1.55   580.00  1471.00  1.56
  585.00  1471.00  1.57   590.00  1484.00  1.58   595.00  1474.00  1.57
  600.00  1474.00  1.55   605.00  1497.00  1.54   610.00  1471.00  1.55
  615.00  1474.00  1.57   620.00  1471.00  1.56   625.00  1471.00  1.55
  630.00  1471.00  1.55   635.00  1471.00  1.54   640.00  1471.00  1.53
  645.00  1471.00  1.52   649.00  1504.00  1.51   650.00  1451.00  1.51
  653.00  1433.00  1.51   658.00  1323.00  1.51   677.00  1464.00  1.51
  680.00  1471.00  1.51   685.00  1474.00  1.51   690.00  1461.00  1.51
  698.00  1455.00  1.51   700.00  1467.00  1.51   720.00  1425.00  1.52
  725.00  1356.00  1.53   730.00  1451.00  1.53   735.00  1471.00  1.53
  740.00  1500.00  1.54   745.00  1329.00  1.54   750.00  1473.00  1.55
  753.00  1520.00  1.55   755.00  1473.00  1.55   760.00  1473.00  1.55
  765.00  1467.00  1.55   770.00  1653.00  1.55   775.00  1471.00  1.55
  780.00  1524.00  1.55   783.00  1552.00  1.55   785.00  1503.00  1.55
  789.00  1954.00  1.55   795.00  1669.00  1.59   800.00  1582.00  1.64
  805.00  1721.00  1.69   808.00  1781.00  1.72   810.00  1632.00  1.74
  815.00  1582.00  1.79   820.00  1786.00  1.83   825.00  1624.00  1.80
  827.00  1682.00  1.88   830.00  1605.00  1.77   835.00  1640.00  1.73
  836.00  1669.00  1.73   841.00  1835.00  1.70   843.00  1791.00  1.71
  844.00  1943.00  1.71   850.00  1582.00  1.72   855.00  1538.00  1.73
  860.00  1513.00  1.74   862.00  1586.00  1.74   865.00  1531.00  1.75
  867.00  1563.00  1.75   871.00  1563.00  1.75   875.00  1665.00  1.79
  877.00  1721.00  1.81   880.00  1586.00  1.83   881.00  1489.00  1.84
  883.00  1704.00  1.85   885.00  1597.00  1.87   890.00  1620.00  1.90
  895.00  1673.00  1.54   900.00  1605.00  1.93   904.00  1653.00  1.91
  907.00  1616.00  1.91   910.00  1704.00  1.90   913.00  2434.00  1.90
  915.00  1791.00  1.90   916.00  1872.00  1.90   921.00  2063.00  1.90
  925.00  1604.00  1.90   929.00  1657.00  1.90   935.00  1632.00  1.90
  939.00  1686.00  1.90   945.00  1628.00  1.89   949.00  2137.00  1.89
  952.00  1748.00  1.90   954.00  1882.00  1.90   960.00  1589.00  1.90
  962.00  1778.00  1.90   965.00  1628.00  1.90   969.00  1877.00  1.90
  975.00  1669.00  1.90   980.00  1605.00  1.91   986.00  1708.00  1.91
  990.00  1640.00  1.91   993.00  1762.00  1.91   995.00  1699.00  1.91
 1001.00  1909.00  1.92  1003.00  1628.00  1.92
/
```

OLD,APPED12
/LNH

Data File, Distance down core, Velocity, Density; HN78023-32, CORE12

8.00	1444.00	1.55	10.00	1447.00	1.56	15.00	1457.00	1.56
20.00	1467.00	1.56	25.00	1451.00	1.57	27.00	1460.00	1.57
30.00	1454.00	1.57	35.00	1451.00	1.58	40.00	1451.00	1.58
45.00	1454.00	1.58	50.00	1457.00	1.58	55.00	1457.00	1.58
60.00	1541.00	1.58	65.00	1616.00	1.58	70.00	1480.00	1.58
75.00	1454.00	1.57	80.00	1457.00	1.56	85.00	1463.00	1.55
90.00	1570.00	1.55	92.00	1570.00	1.54	95.00	1482.00	1.54
100.00	1482.00	1.53	105.00	1454.00	1.52	110.00	1447.00	1.52
115.00	1447.00	1.51	120.00	1447.00	1.50	125.00	1447.00	1.50
130.00	1447.00	1.50	135.00	1447.00	1.50	140.00	1447.00	1.51
145.00	1447.00	1.51	150.00	1447.00	1.51	155.00	1454.00	1.51
160.00	1460.00	1.51	165.00	1454.00	1.51	170.00	1460.00	1.51
175.00	1444.00	1.51	180.00	1441.00	1.50	185.00	1447.00	1.49
190.00	1447.00	1.48	195.00	1444.00	1.48	200.00	1447.00	1.47
205.00	1447.00	1.46	210.00	1447.00	1.46	215.00	1467.00	1.55
220.00	1476.00	1.44	225.00	1454.00	1.44	230.00	1447.00	1.45
235.00	1447.00	1.45	240.00	1447.00	1.45	245.00	1441.00	1.46
256.00	1474.00	1.47	260.00	1473.00	1.47	265.00	1473.00	1.47
270.00	1477.00	1.48	275.00	1477.00	1.48	280.00	1480.00	1.48
285.00	1483.00	1.49	290.00	1480.00	1.50	295.00	1490.00	1.51
300.00	1527.00	1.53	305.00	1535.00	1.54	310.00	1496.00	1.55
315.00	1473.00	1.56	320.00	1493.00	1.63	323.00	1514.00	1.67
325.00	3253.00	1.70	327.00	4093.00	1.73	330.00	1625.00	1.77
335.00	1556.00	1.83	340.00	1535.00	1.83	342.00	1586.00	1.83
345.00	1571.00	1.83	350.00	1535.00	1.78	355.00	1510.00	1.73
360.00	1527.00	1.69	365.00	1493.00	1.79	370.00	1625.00	1.90
375.00	1686.00	1.88	380.00	1601.00	1.86	385.00	1682.00	1.84
390.00	1578.00	1.83	395.00	1586.00	1.81	400.00	1609.00	1.82
405.00	1861.00	1.83	410.00	1617.00	1.84	415.00	1653.00	1.85
418.00	1776.00	1.85	420.00	1553.00	1.85	425.00	1583.00	1.86
430.00	1846.00	1.87	435.00	1468.00	1.87	440.00	1579.00	1.88
445.00	1578.00	1.88	450.00	1617.00	1.88	455.00	1625.00	1.90
460.00	1602.00	1.91	466.00	1346.00	1.92	470.00	1629.00	1.94
475.00	1717.00	1.94	478.00	1695.00	1.95	480.00	1625.00	1.95
485.00	1722.00	1.95	487.00	1629.00	1.95	490.00	1695.00	1.96
495.00	1777.00	1.96	497.00	1893.00	1.96	500.00	1590.00	1.97
505.00	1662.00	1.97	507.00	1739.00	1.97	510.00	1649.00	1.98
512.00	1687.00	1.97	515.00	1649.00	1.97	517.00	1954.00	1.96
520.00	1645.00	1.96	525.00	1717.00	1.95	527.00	1791.00	1.94
530.00	1613.00	1.94	535.00	1645.00	1.93	540.00	1629.00	1.93

/

APPENDICES 5 AND 6

COUNTS OF THE MICROFOSSIL ASSEMBLAGES IN SAMPLES TAKEN FROM CORES 6 (APPENDIX 5) AND 11 (APPENDIX 6)

Note that the total assemblage has been counted for the samples from core 6, whereas only the total numbers of Benthonic species, Planktonic species and numbers of Cribroelphidium excavatum clavatum were counted in samples from core 11. (This is explained in the text of Chapter 4.)

Appendix 5: Table of total foraminifera counts. (cont.)

Distance Down Core #6 (cm)	499	539	589	609	655	730	805	835	855	875	895	905	915	932	946	961	973	989	999	1009	1031
GLOBIGERINA PACHYDERMA	-	-	-	4	20	6	25	3	8	6	10	-	10	4	3	1	2	3	2	-	-
GLOCIGERINA BULLOIDES	-	-	-	-	-	-	-	-	-	-	-	-	-	-	-	-	-	-	-	-	-
TOTAL PLANKTONICS	-	-	-	4	20	6	25	3	8	6	10	-	10	4	3	1	2	3	2	-	-
CRIBROELPHIDIUM EX. CLAVATUM	8	172	57	41	38	224	59	22	17	31	266	304	52	88	18	4	11	41	79	38	11
ISLANDIELLA ISLANDICA	2	10	20	13	98	190	19	3	10	28	114	96	108	3	4	3	3	9	20	13	1
ISLANDIELLA TERETIS	-	4	6	3	14	102	3	3	7	7	58	40	30	-	-	-	-	4	-	-	-
NONIONELLA LABRADORICA	1	2	-	8	38	6	2	-	2	-	86	64	-	-	-	-	1	1	7	3	1
ASTRONONION GALLOWAYI	-	-	-	1	4	2	-	-	-	-	4	-	-	-	-	-	-	1	3	-	1
NONION BARLEEANUM	-	-	-	-	6	-	-	-	-	-	-	-	-	-	-	-	-	-	-	-	-
PROTELPHIDIUM ORBICULARE	-	-	-	-	-	2	1	-	-	1	4	-	-	-	-	-	-	-	2	1	-
VIRGULINA FUSIFORMIS	-	-	-	-	-	-	-	-	-	-	-	-	-	-	-	-	-	-	-	-	-
VIRGULINA LOELDICHI	-	-	-	40	-	-	-	2	-	5	2	-	-	-	-	-	-	-	1	1	-
ELPHIDIELLA ARCTICA	-	-	1	-	60	-	1	-	1	2	36	4	2	-	-	-	-	-	-	-	-
OTHER BENTHONICS	-	6	15	8	60	68	6	7	15	8	18	40	8	2	2	7	3	8	5	5	1
TOTAL BENTHONICS	11	196	99	120	318	594	91	43	52	89	588	548	200	93	24	14	18	60	121	61	15
	*																**	**	**	**	**

* Orange-Brown organic remains (abundant)
** Coal

Distance Down Core #6 (cm)	10	30	50	70	110	135	155	192	222	242	262	282	302	317	338	353	368	383	408	436	458
GLOBIGERINA PACHYDERMA	3	2	2	16	4	-	4	4	12	2	-	4	16	8	8	16	2	11	4	-	5
GLOBIGERINA BULLOIDES	-	-	-	-	-	-	-	-	-	-	-	-	-	-	-	-	-	2	-	-	-
TOTAL PLANKTONICS	3	2	2	16	4	-	4	4	12	2	-	4	16	8	8	16	2	13	4	-	5
CRIBROELPHIDIUM EX. CLAVATUM	62	292	160	71	42	146	80	58	152	136	140	392	338	1328	188	87	156	330	324	28	27
ISLANDIELLA ISLANDICA	101	96	45	75	184	150	209	180	220	180	308	288	106	680	68	40	44	18	136	50	38
ISLANDIELLA TERETIS	85	38	29	94	204	76	163	48	104	38	104	24	50	152	18	12	30	2	26	19	20
NONIONELLA LABRADORICA	9	26	6	10	2	28	24	8	-	24	32	20	2	24	2	-	-	-	2	-	1
ASTRONONION GALLOWAYI	15	2	4	11	8	-	4	-	-	-	-	-	2	8	-	-	-	-	-	1	1
NONION BARLEEANUM	13	14	8	15	62	14	-	6	-	-	-	-	-	16	2	-	-	2	4	-	-
PROTELPHIDIUM ORBICULARE	-	-	-	-	2	-	16	-	-	-	-	-	2	20	-	-	-	2	-	-	-
VIRGULINA FUSIFORMIS	-	2	-	3	4	-	4	8	-	6	-	-	2	-	-	-	-	-	-	-	-
VIRGULINA LOELDICHI	8	18	14	2	10	24	8	2	8	-	-	-	-	4	-	2	2	8	-	1	8
ELPHIDIELLA ARCTICA	-	-	-	-	-	-	-	4	4	-	-	-	-	8	4	-	-	2	-	3	4
OTHER BENTHONICS	31	78	42	79	220	70	92	54	116	80	92	28	50	88	44	13	38	17	60	12	12
TOTAL BENTHONICS	262	566	308	360	738	508	600	368	604	464	686	752	552	2248	326	154	270	381	552	114	111

Appendix 5: Table of total foraminifera counts for core #6

Distance Nos. down core (cm)	Nos. Tot. Benthonic species	Nos. C. Ex. Clavatum	Nos. Planktonic species
20	376	56	36
50	388	92	26
90	864	464	60
137	612	376	52
167	304	208	40
330	30	4	3
360	33	5	2
390	116	9	1
460	25	1	10
485	17	11	5
510	50	13	1
540	184	20	20
576	366	48	54
590	508	64	32
605	272	72	24
615	222	81	63
650	162	93	10
700	44	11	14
750	82	32	19
790	99	16	9
820	920	400	32
840	59	41	0
870	29	9	3
895	19	9	2
910	344	50	24
950	242	56	14
985	416	156	24
1010	234	54	28
1025	314	82	32

Appendix 6: Table of foraminifera counts for core No. 11.

APPENDIX 7

REPLAYED D.T.S. DATA INCLUDING INSTANTANEOUS AND SMOOTHED INSTANTANEOUS ENERGIES FROM CORE SITES 2, 6 AND 7

The general format and the respective amplitude and time scales applicable to the data are given in Figure A.2 below. Each shot has a header (e.g. 1978/209/1817 300); these numbers correspond to year, Julian day, Greenwich time and digitized shot number, respectively.

Shots 301 to 310 are from the vicinity of core site 6.

Shots 350 to 362 are from the vicinity of core site 7. (Also included for these data are shot by shot displays of traces and smoothed instantaneous energies alone. This is to facilitate comparison of coherent events between shots for both data formats.)

Shots 572 to 588 are from the vicinity of core site 2. (It should be noted that these data have a different amplitude scaling, as indicated at the beginning of that data section.)

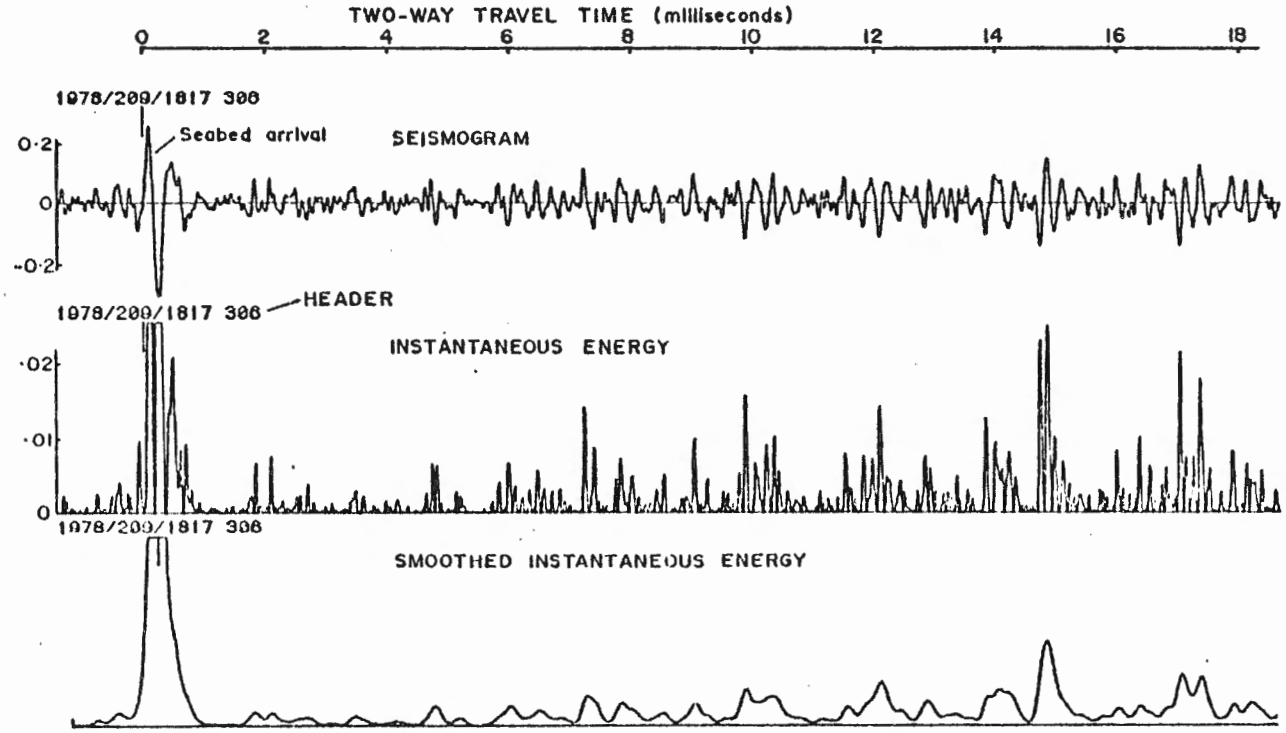

Fig.A.2 : An example of D.T.S. data replay including instantaneous and smoothed instantaneous energy. The seabed reflection is indicated as is the tape header which records the year, Julian day, Greenwich time and digitized shot number.

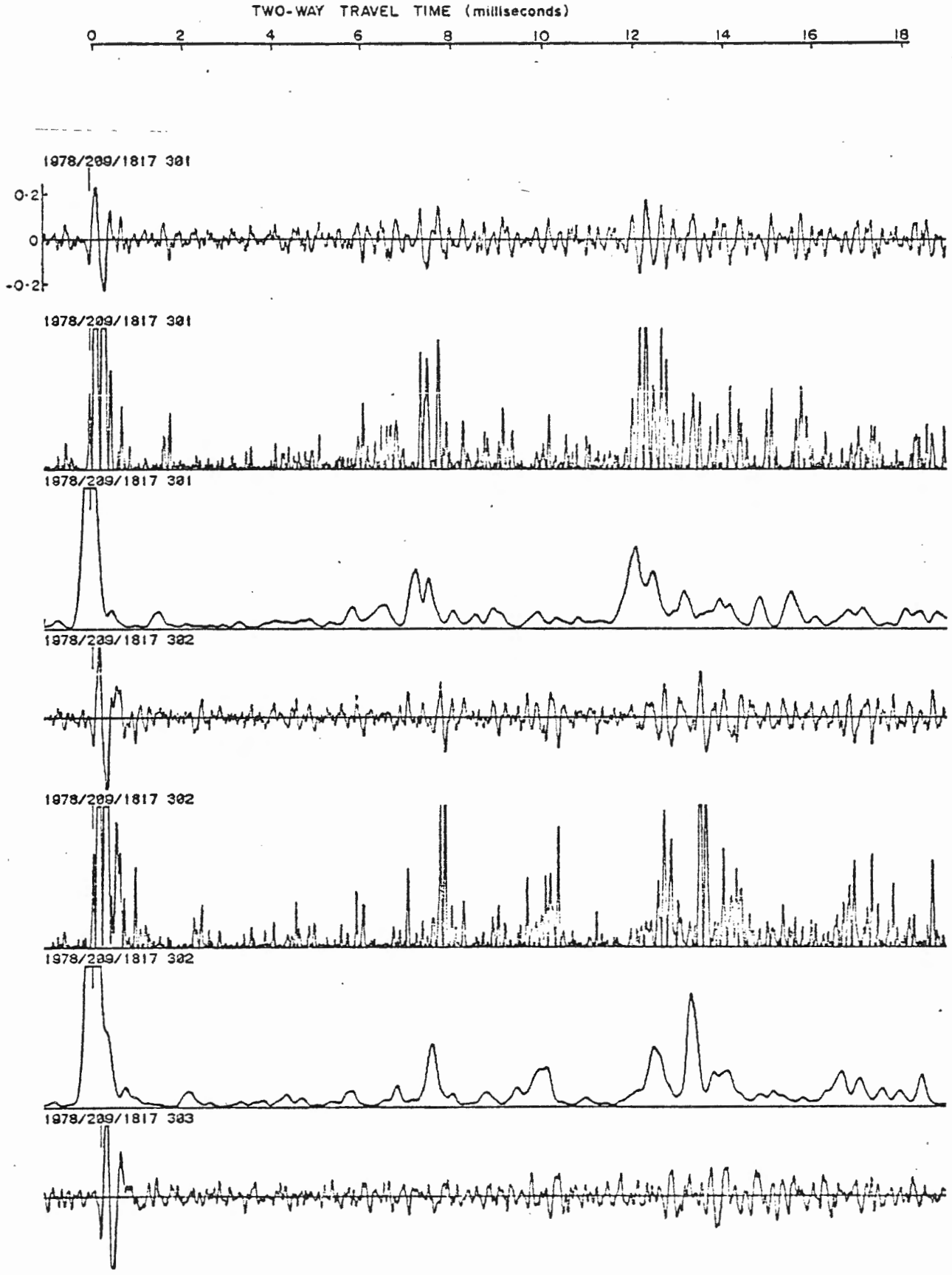
TWO-WAY TRAVEL TIME (milliseconds)
0
2
4
6
8
10
12
14
16
18
1978/209/1817 301
0·2
0
-0·2
1978/209/1817 301
1978/209/1817 301
1978/209/1817 302
1978/209/1817 302
1978/209/1817 302
1978/209/1817 303

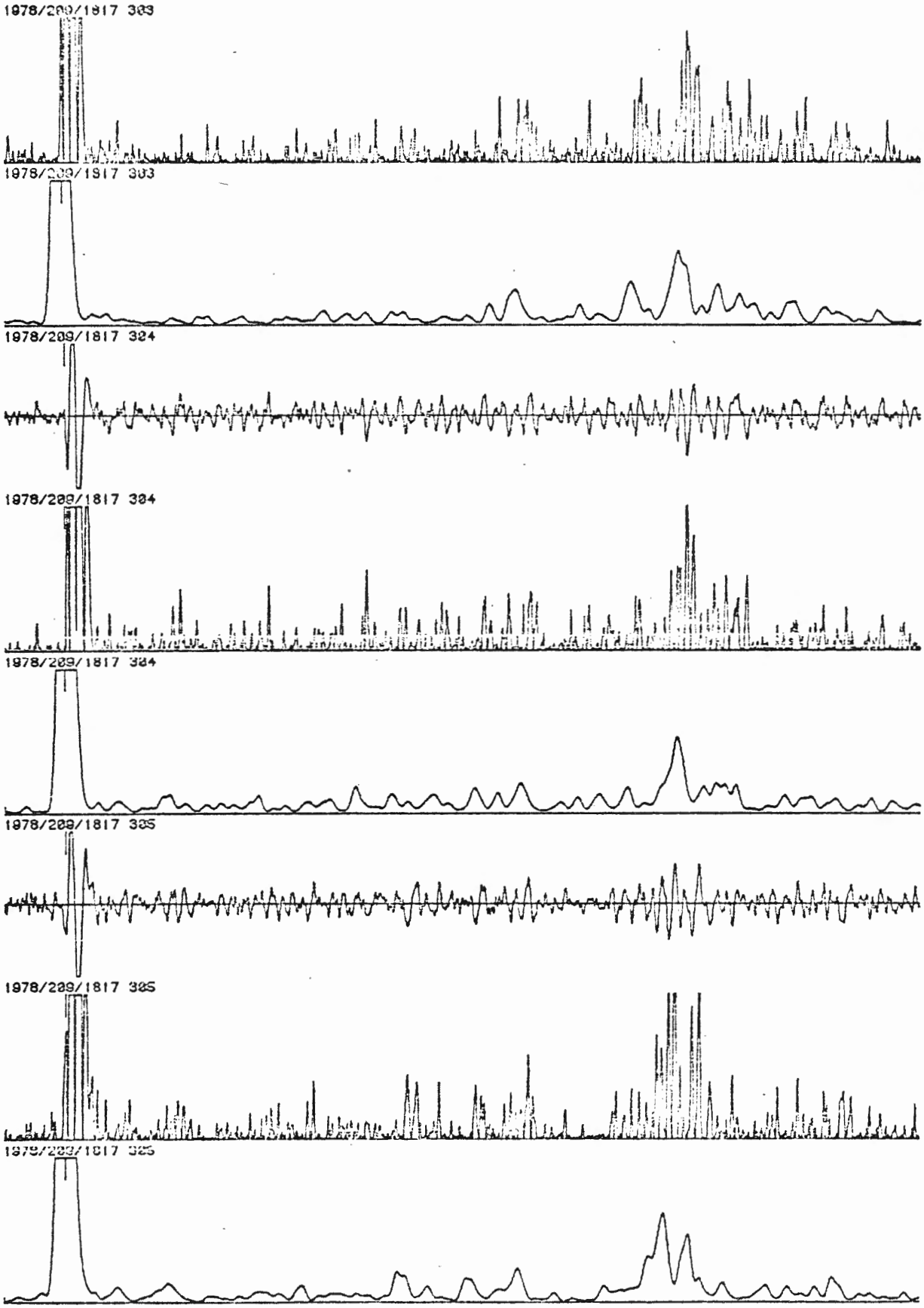
1978/209/1817 303
1978/209/1817 303
1978/209/1817 304
1978/209/1817 304
1978/209/1817 304
1978/209/1817 305
1978/209/1817 305
1978/209/1817 305

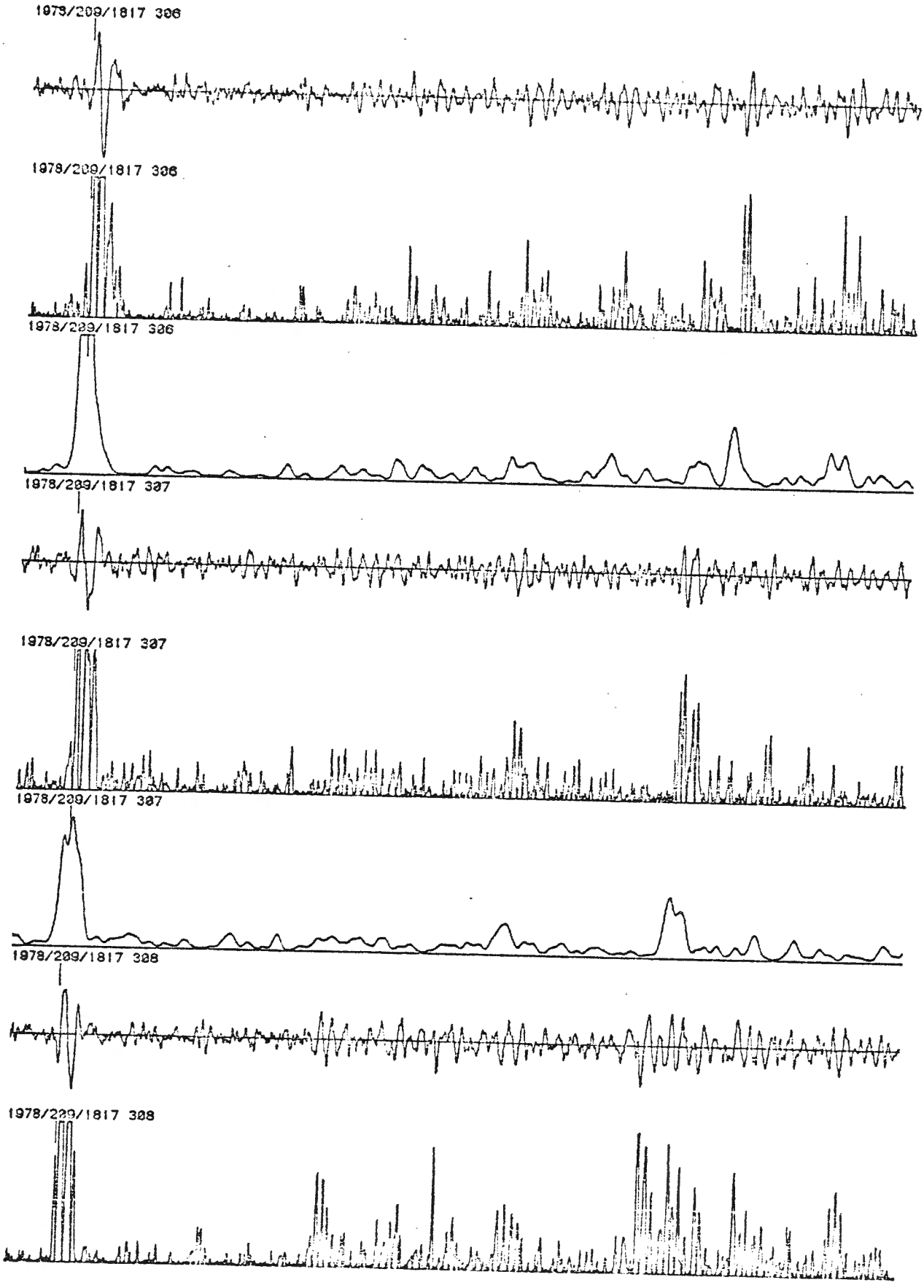
1978/209/1817 306
1978/209/1817 306
1978/209/1817 306
1978/209/1817 307
1978/209/1817 307
1978/209/1817 307
1978/209/1817 308
1978/209/1817 308

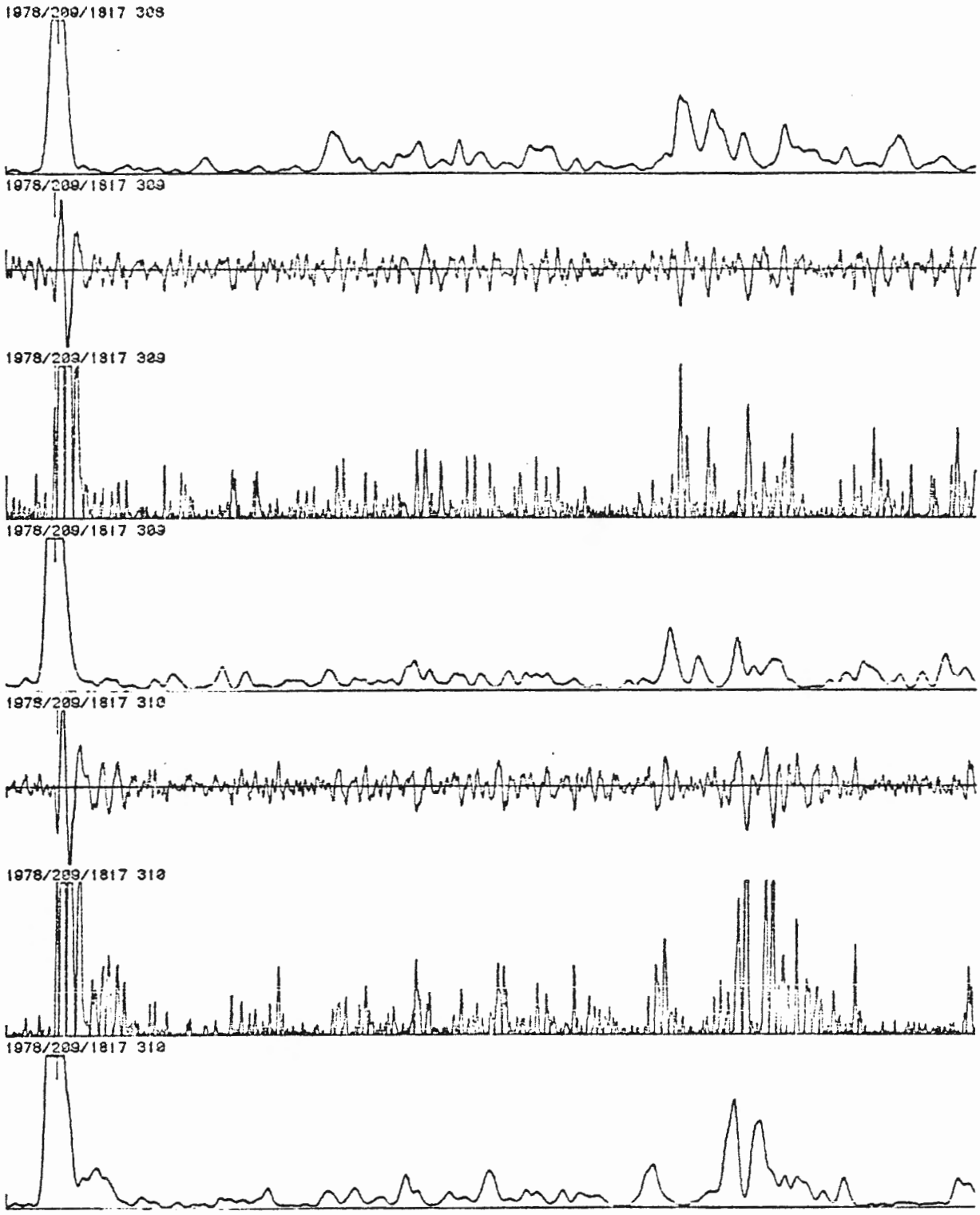
1978/289/1817 308
1978/289/1817 309
1978/289/1817 329
1978/289/1817 309
1978/289/1817 310
1978/289/1817 310
1978/289/1817 310

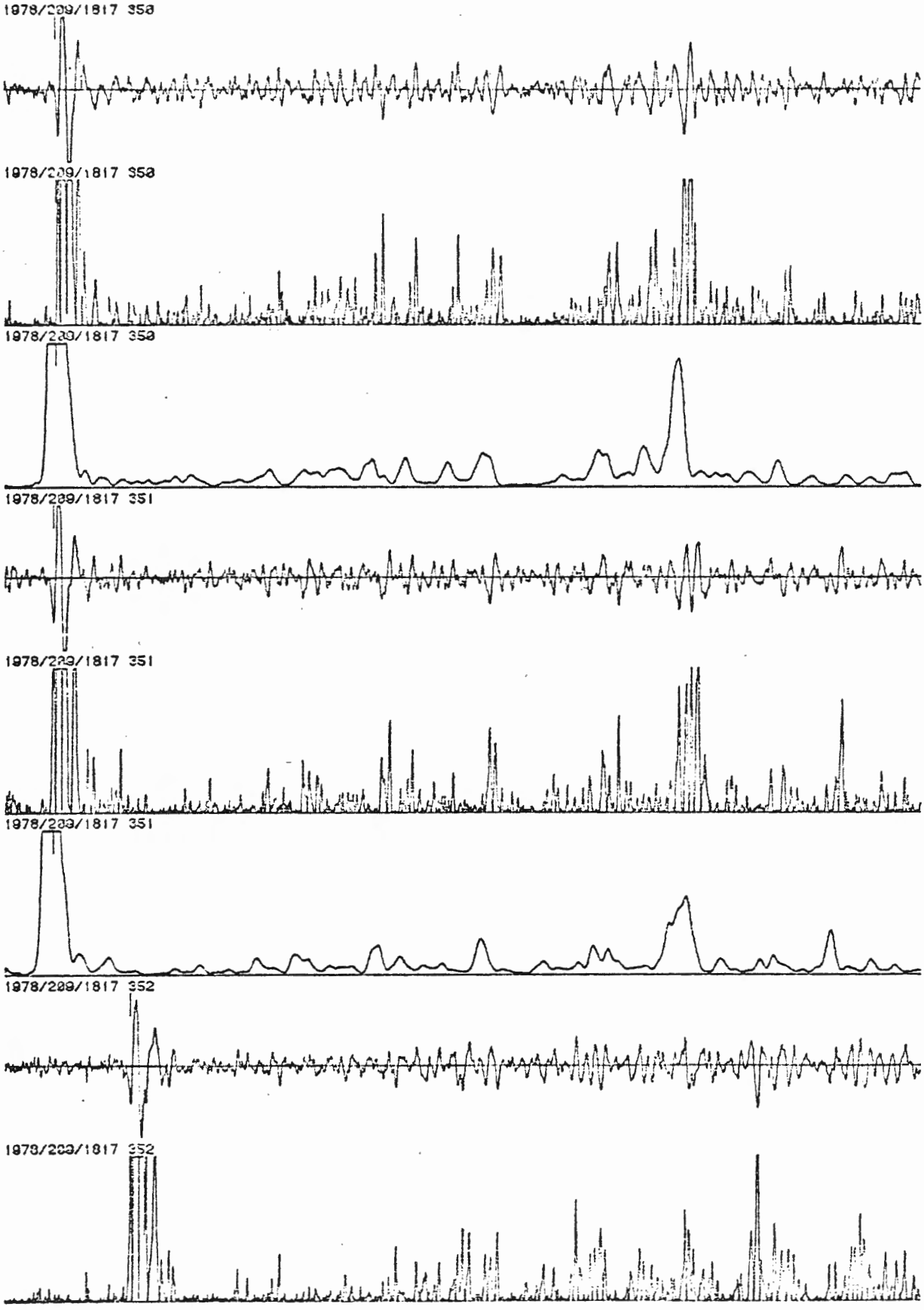
1978/289/1817 350
1978/289/1817 350
1978/289/1817 350
1978/289/1817 351
1978/289/1817 351
1978/289/1817 351
1978/289/1817 352
1978/289/1817 352

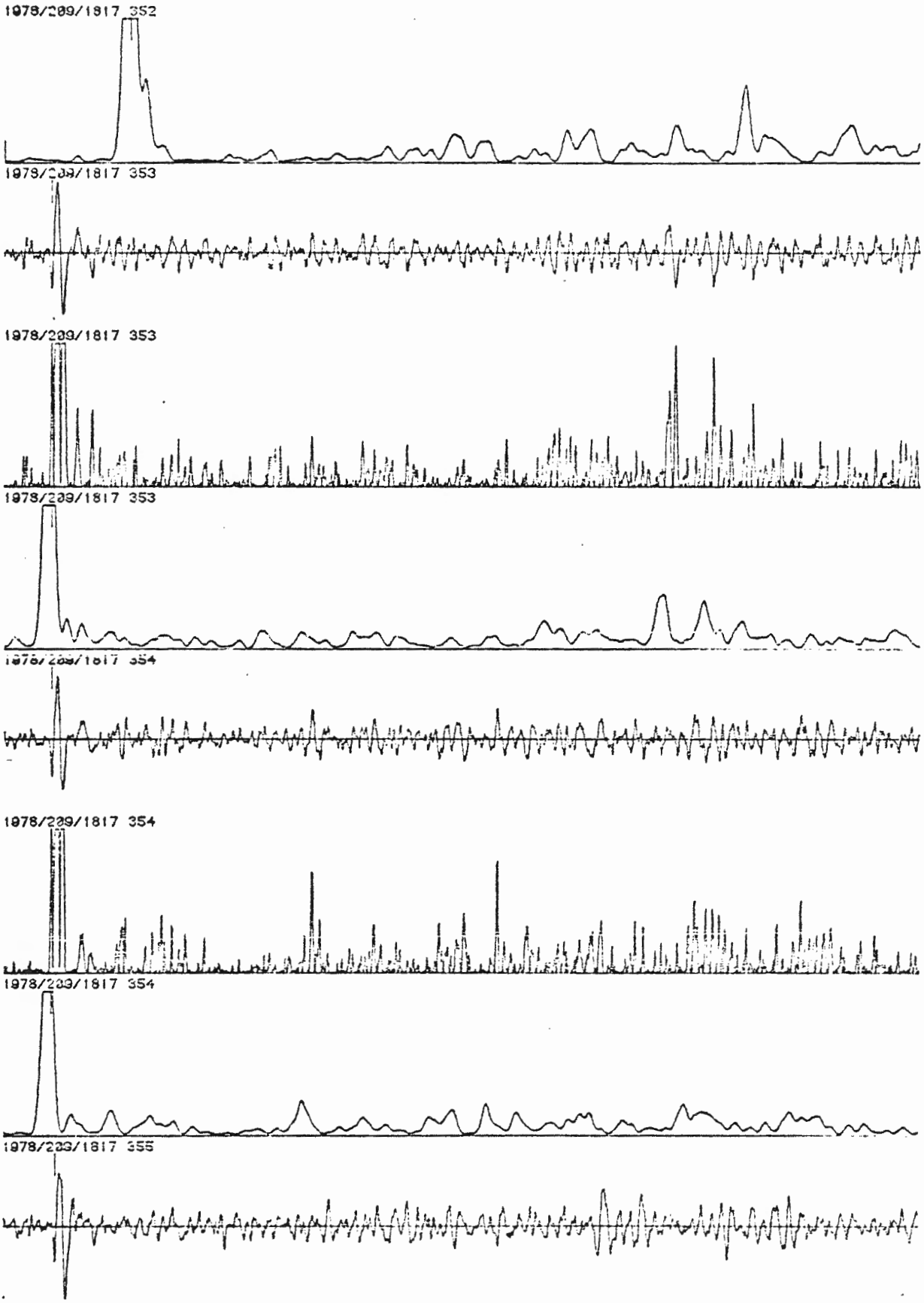
1978/209/1817 352
1978/209/1817 353
1978/209/1817 353
1978/209/1817 353
1978/209/1817 354
1978/209/1817 354
1978/209/1817 354
1978/209/1817 355

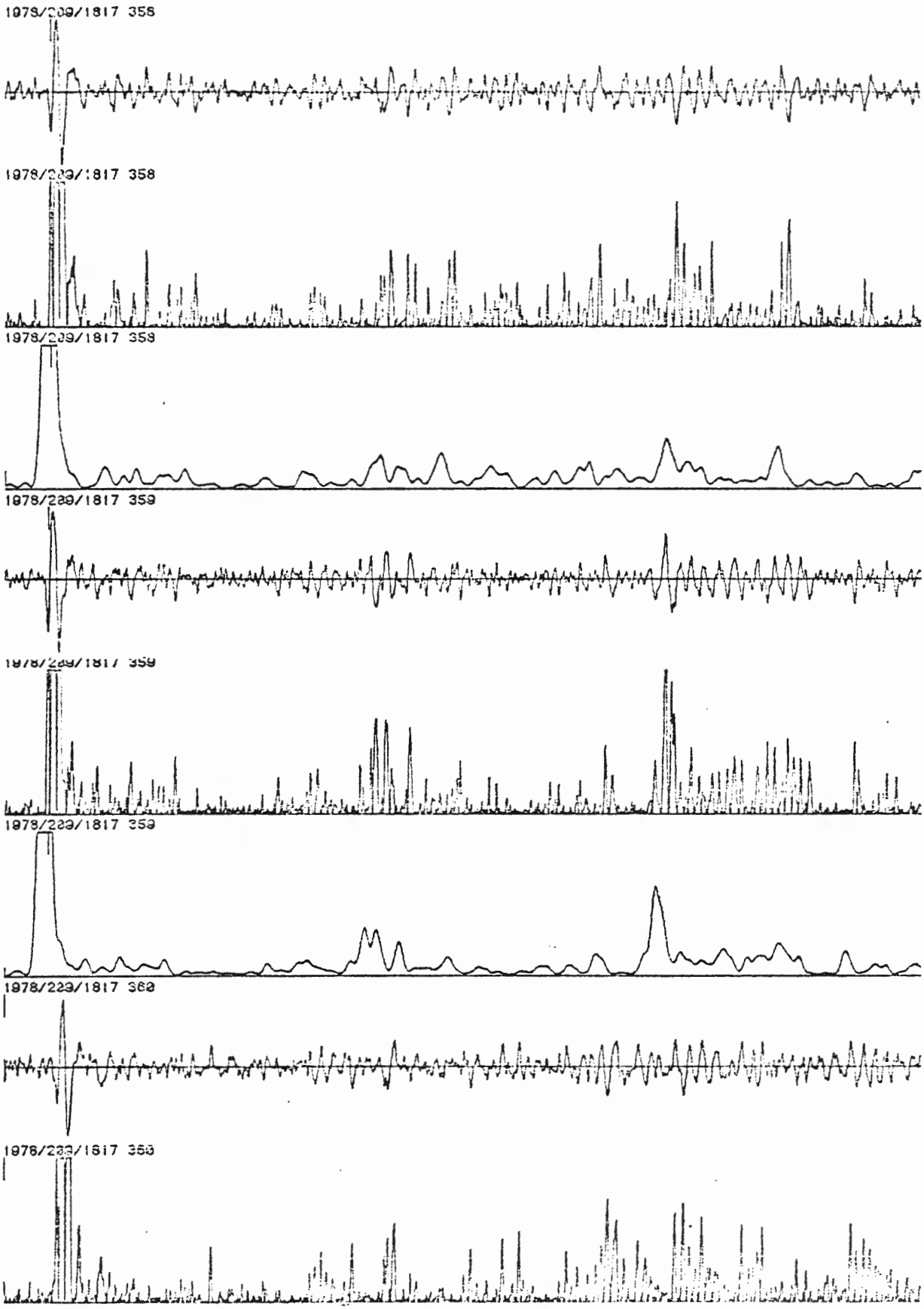
1978/229/1817 358
1978/229/1817 358
1978/229/1817 358
1978/229/1817 359
1978/229/1817 359
1978/229/1817 359
1978/229/1817 360
1978/229/1817 360

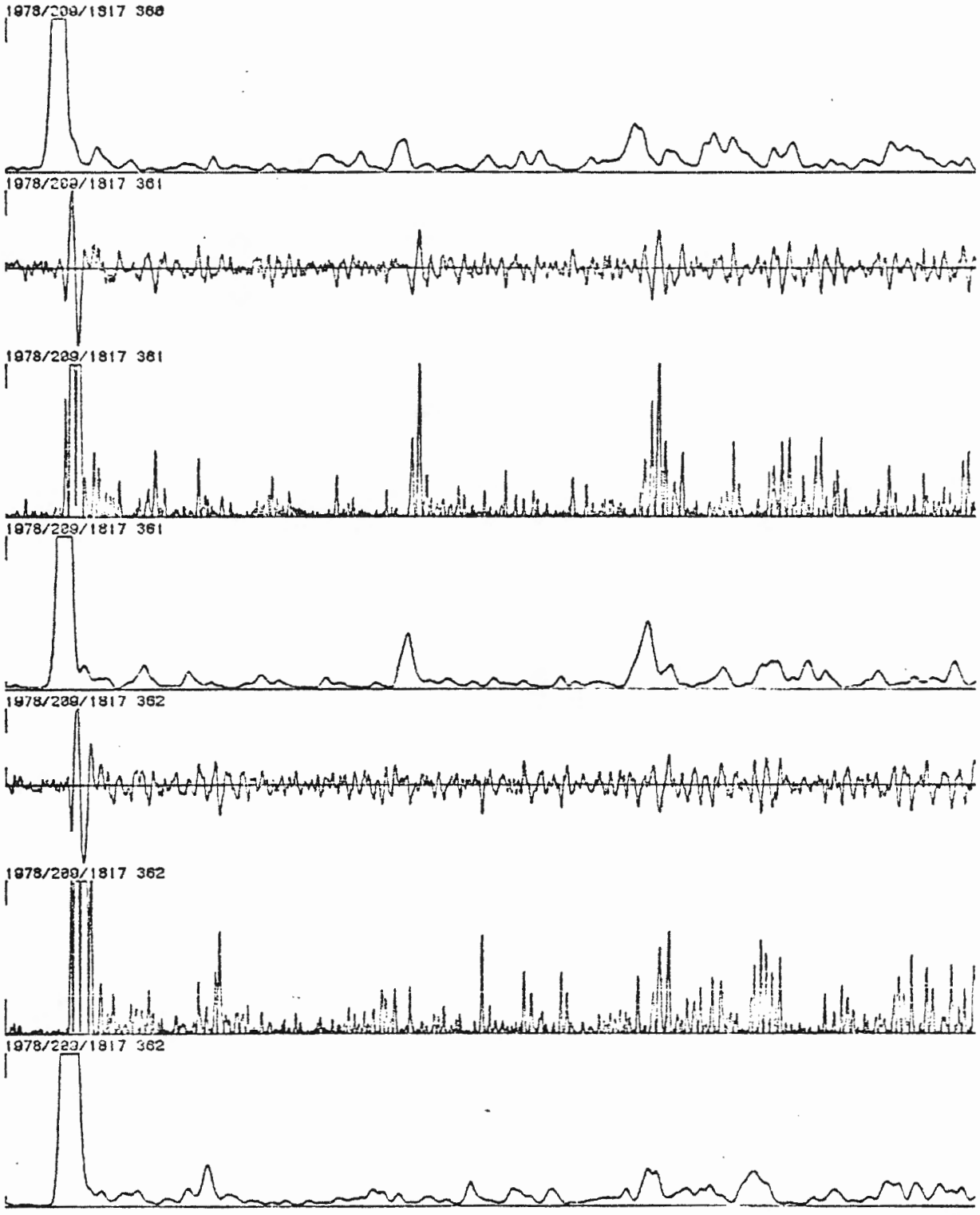
1978/209/1817 360
1978/209/1817 361
1978/209/1817 361
1978/209/1817 361
1978/209/1817 362
1978/209/1817 362
1978/209/1817 362

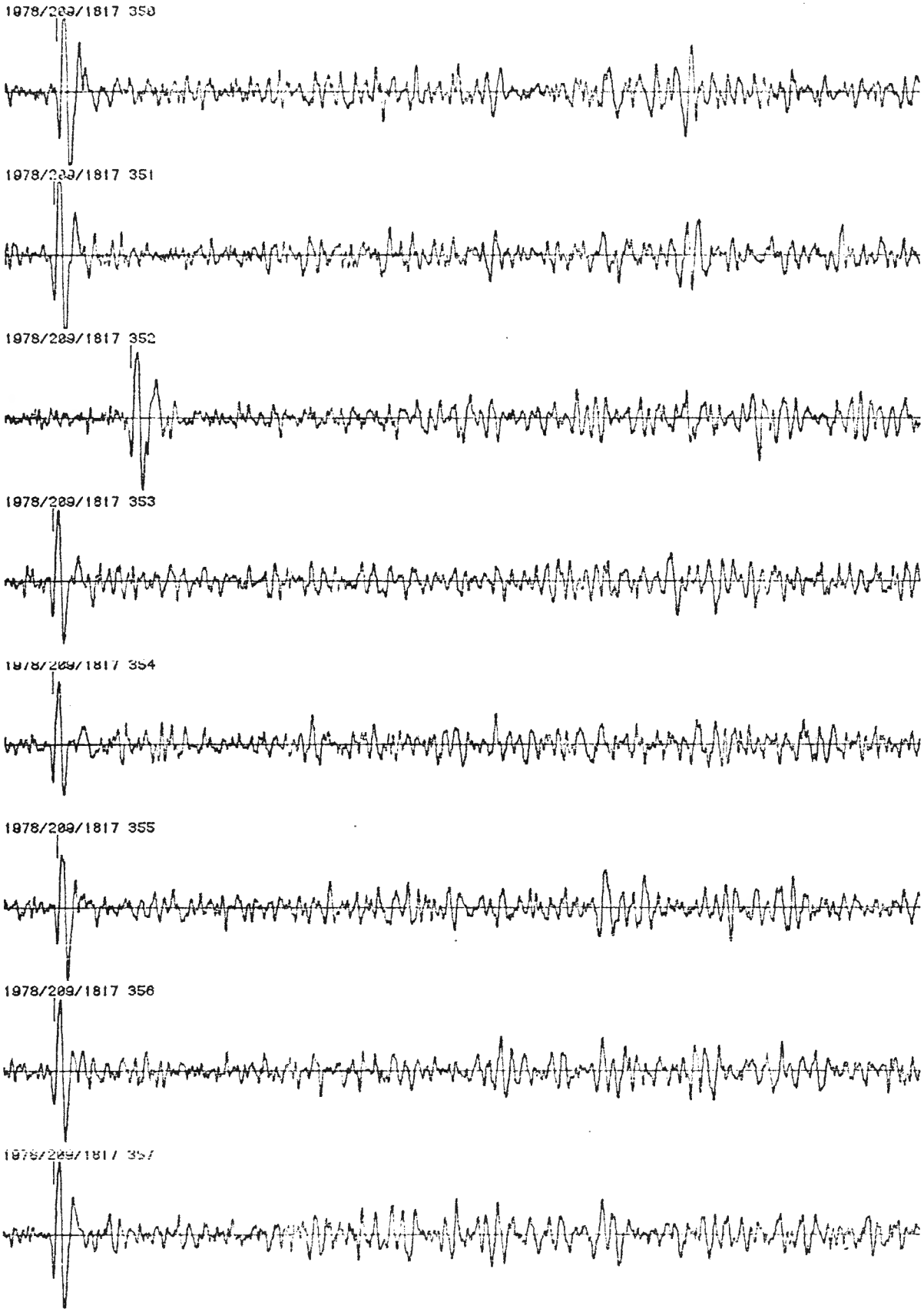
1978/289/1817 350
1978/289/1817 351
1978/289/1817 352
1978/289/1817 353
1978/289/1817 354
1978/289/1817 355
1978/289/1817 356
1978/289/1817 357

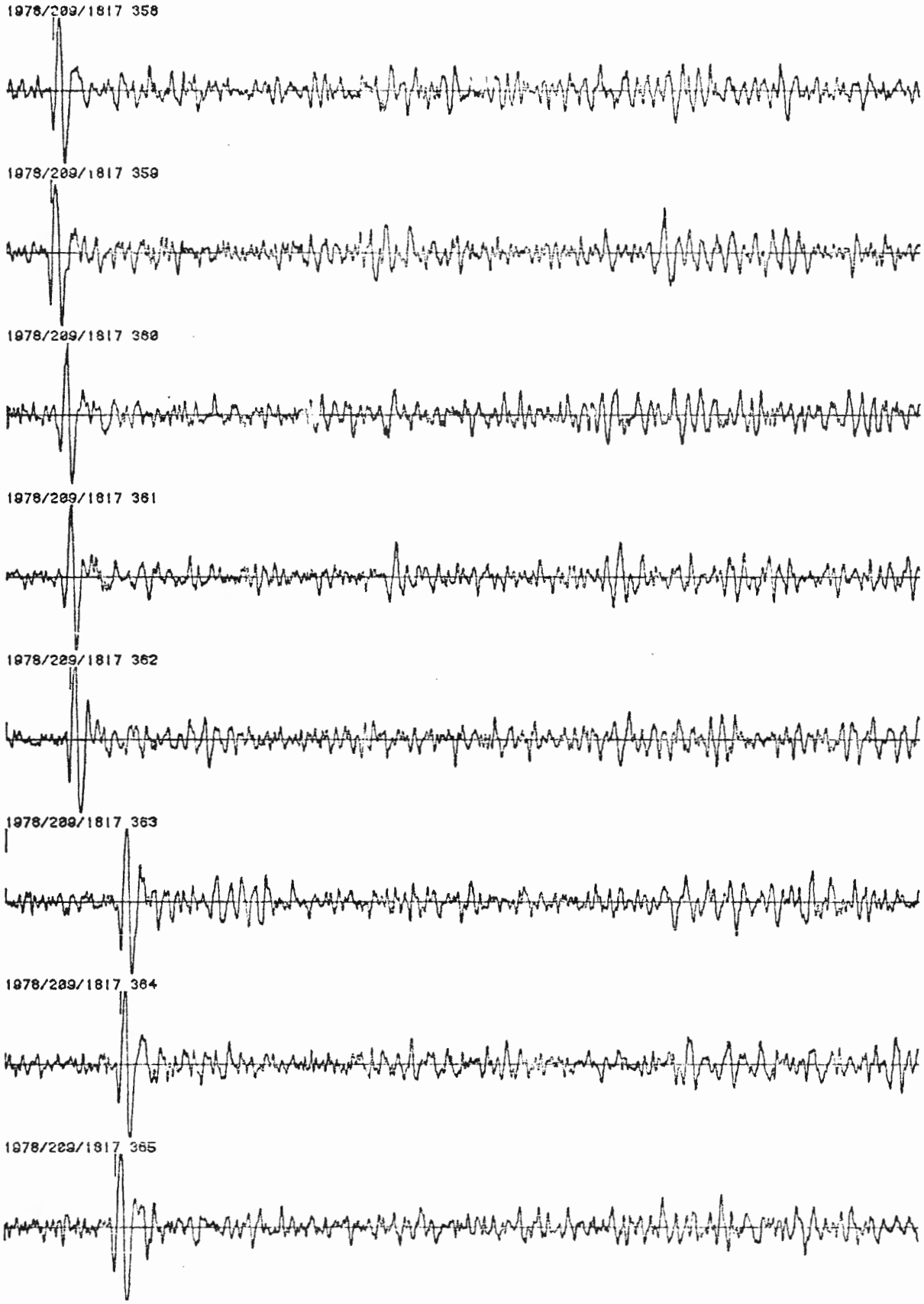
1978/289/1817 358
1978/289/1817 359
1978/289/1817 360
1978/289/1817 361
1978/289/1817 362
1978/289/1817 363
1978/289/1817 364
1978/289/1817 365

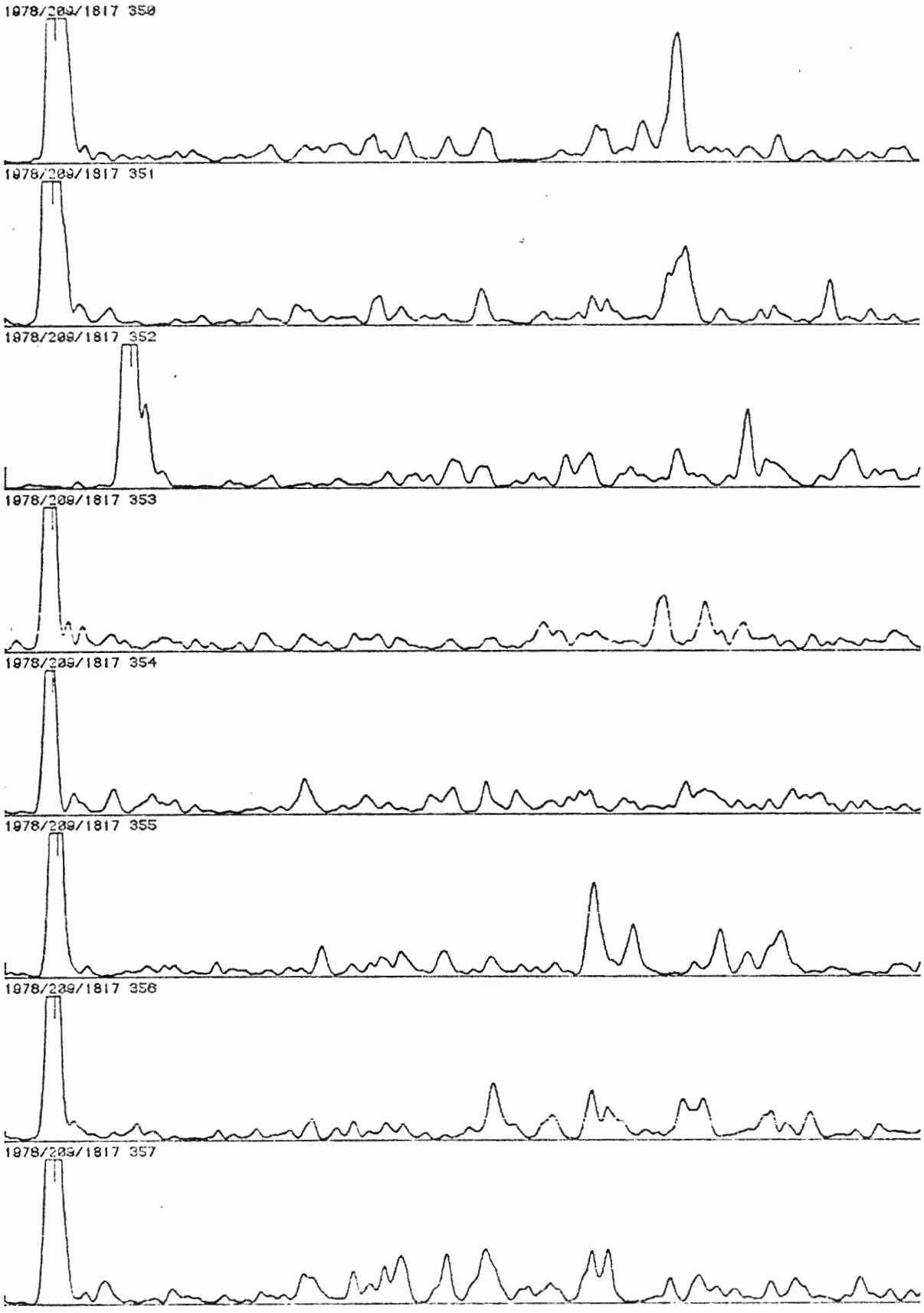
1978/209/1817 350
1978/209/1817 351
1978/209/1817 352
1978/209/1817 353
1978/209/1817 354
1978/209/1817 355
1978/209/1817 356
1978/209/1817 357

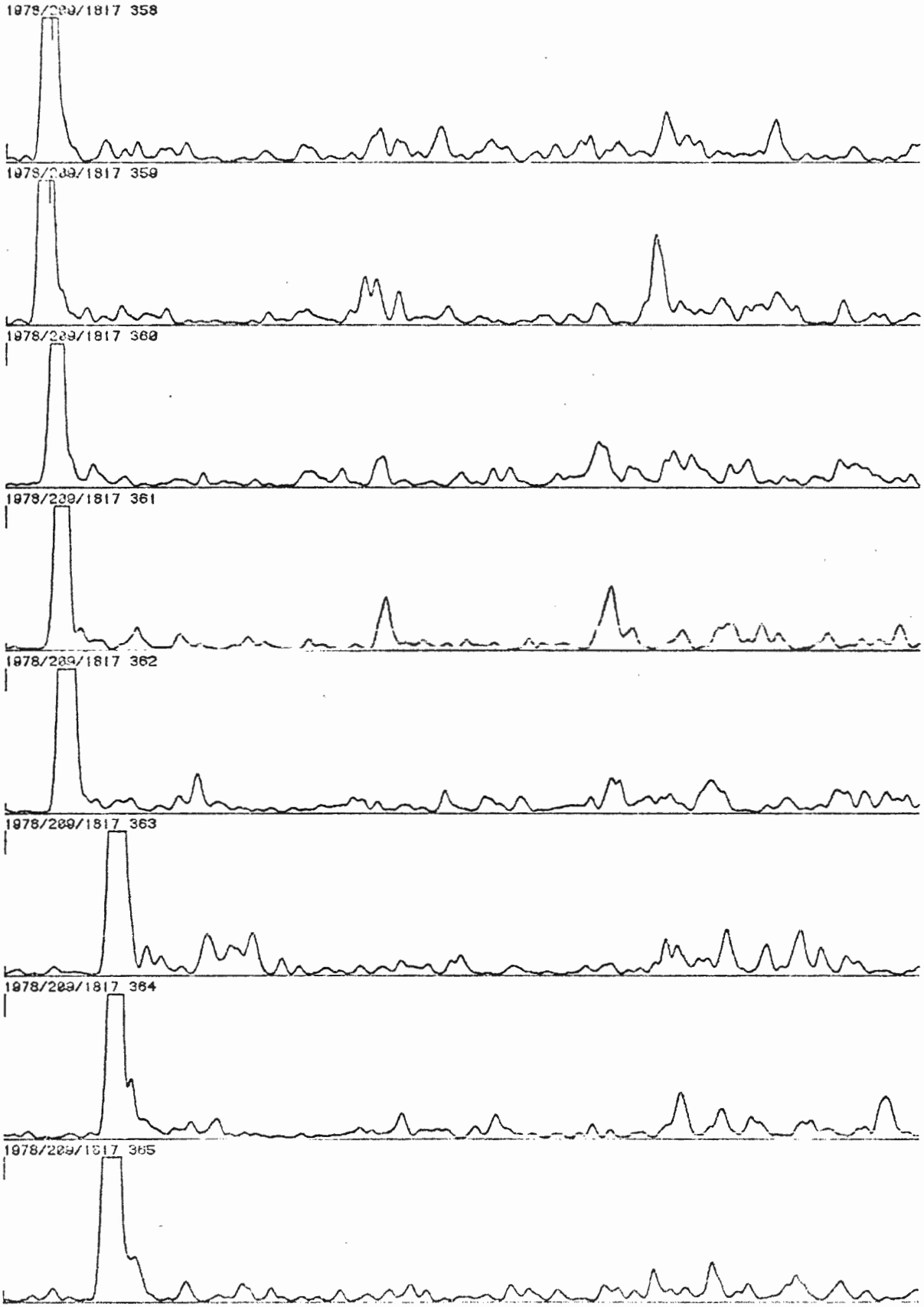
1978/209/1817 358
1978/209/1817 359
1978/209/1817 360
1978/209/1817 361
1978/209/1817 362
1978/209/1817 363
1978/209/1817 364
1978/209/1817 365

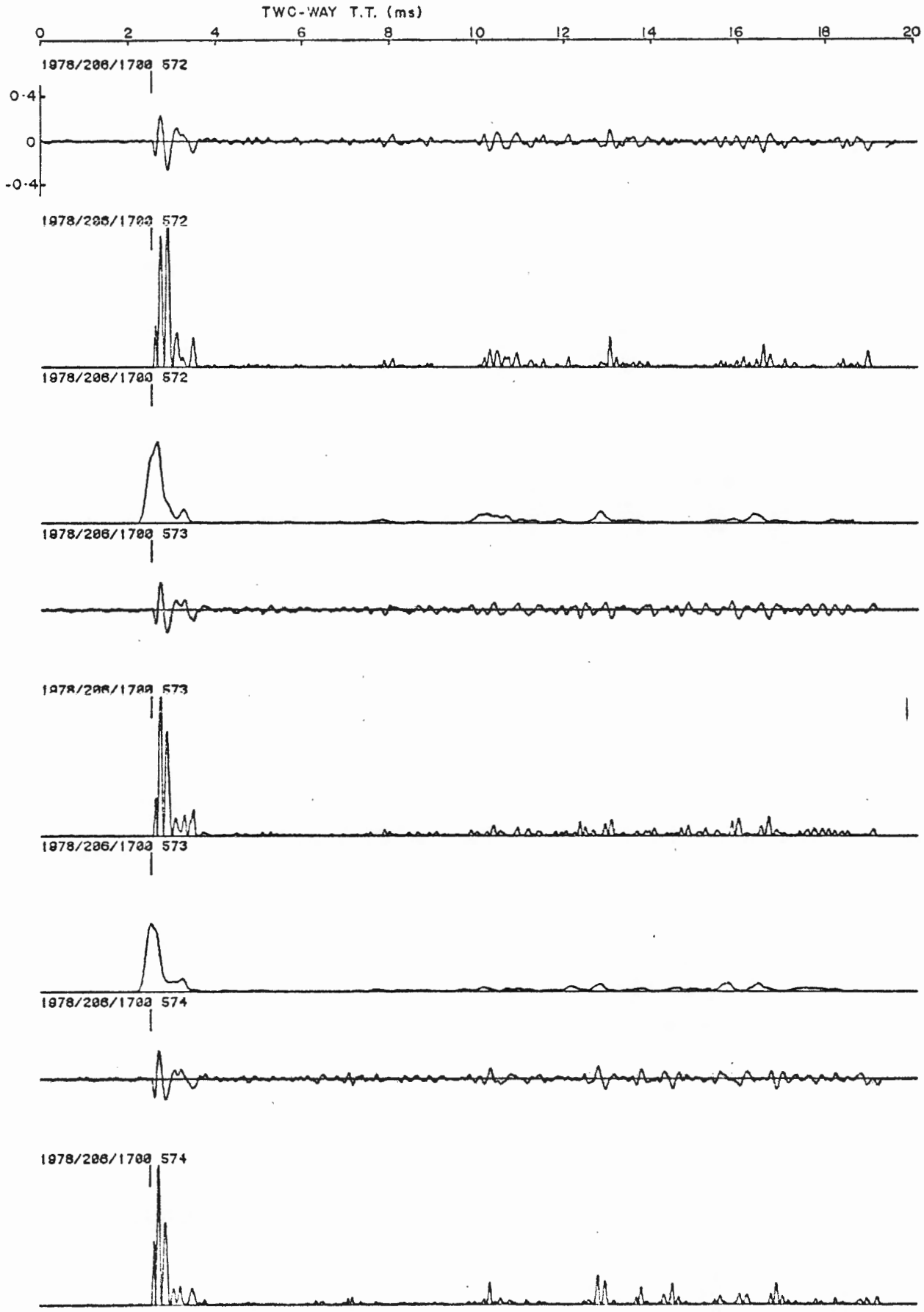
TWO-WAY T.T. (ms)
0
2
4
6
8
10
12
14
16
18
20
1978/206/1700 572
0·4
0
-0·4
1978/206/1700 572
1978/206/1700 572
1978/206/1700 573
1978/206/1700 573
1978/206/1700 573
1978/206/1700 574
1978/206/1700 574

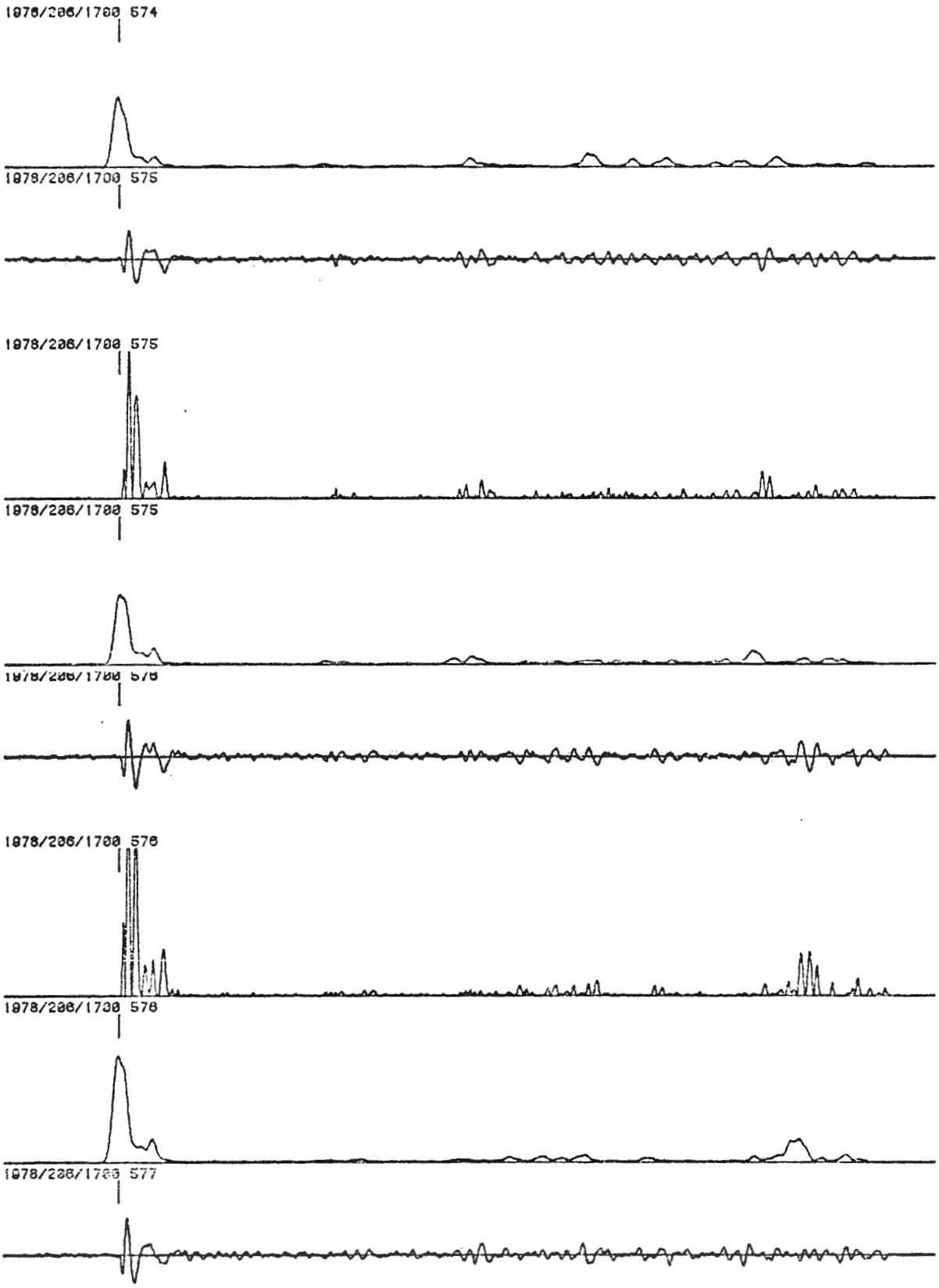
1978/206/1700 574
1978/206/1700 575
1978/206/1700 575
1978/206/1700 575
1978/206/1700 576
1978/206/1700 576
1978/206/1700 577

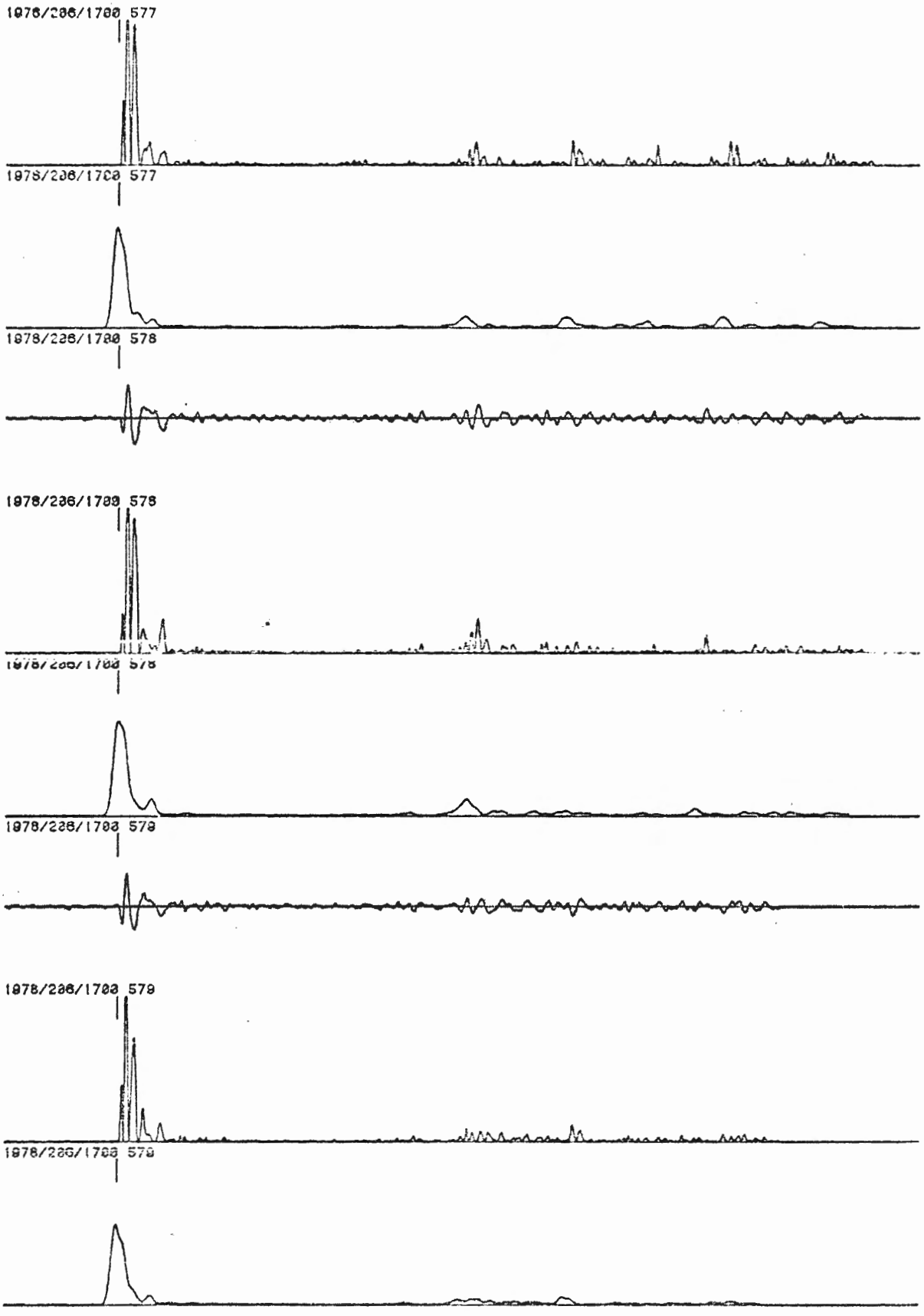
1978/236/1700 577
1978/236/1700 577
1978/236/1700 578
1978/236/1700 578
1978/236/1700 579
1978/236/1700 579
1978/236/1700 579
1978/236/1700 579

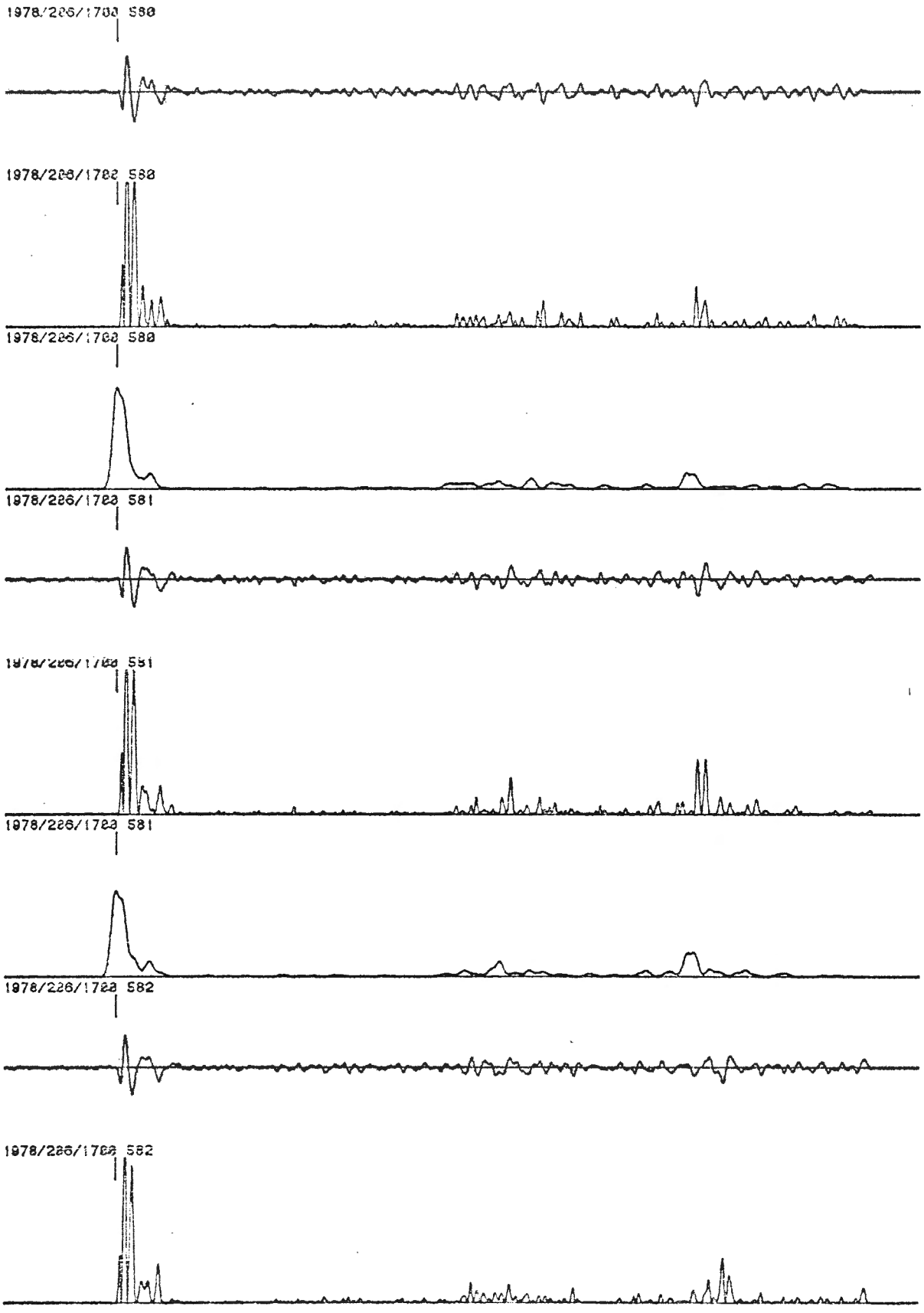
1978/226/1700 580
1978/226/1702 580
1978/226/1702 580
1978/226/1703 581
1978/226/1700 581
1978/226/1703 581
1978/226/1703 582
1978/226/1703 582

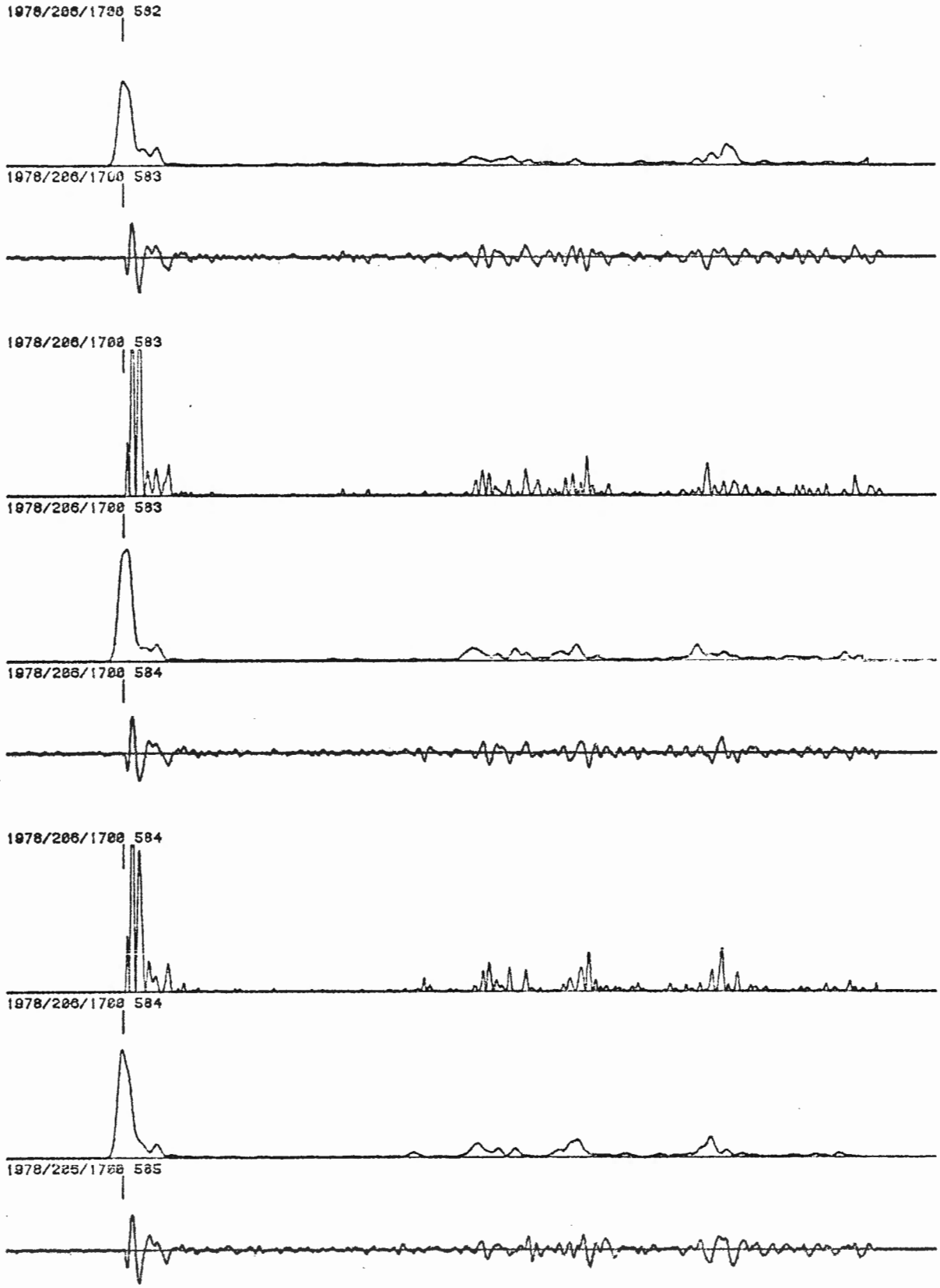
1978/206/1700 582
1978/206/1700 583
1978/206/1700 583
1978/206/1700 583
1978/206/1700 584
1978/206/1700 584
1978/206/1700 584
1978/225/1700 585

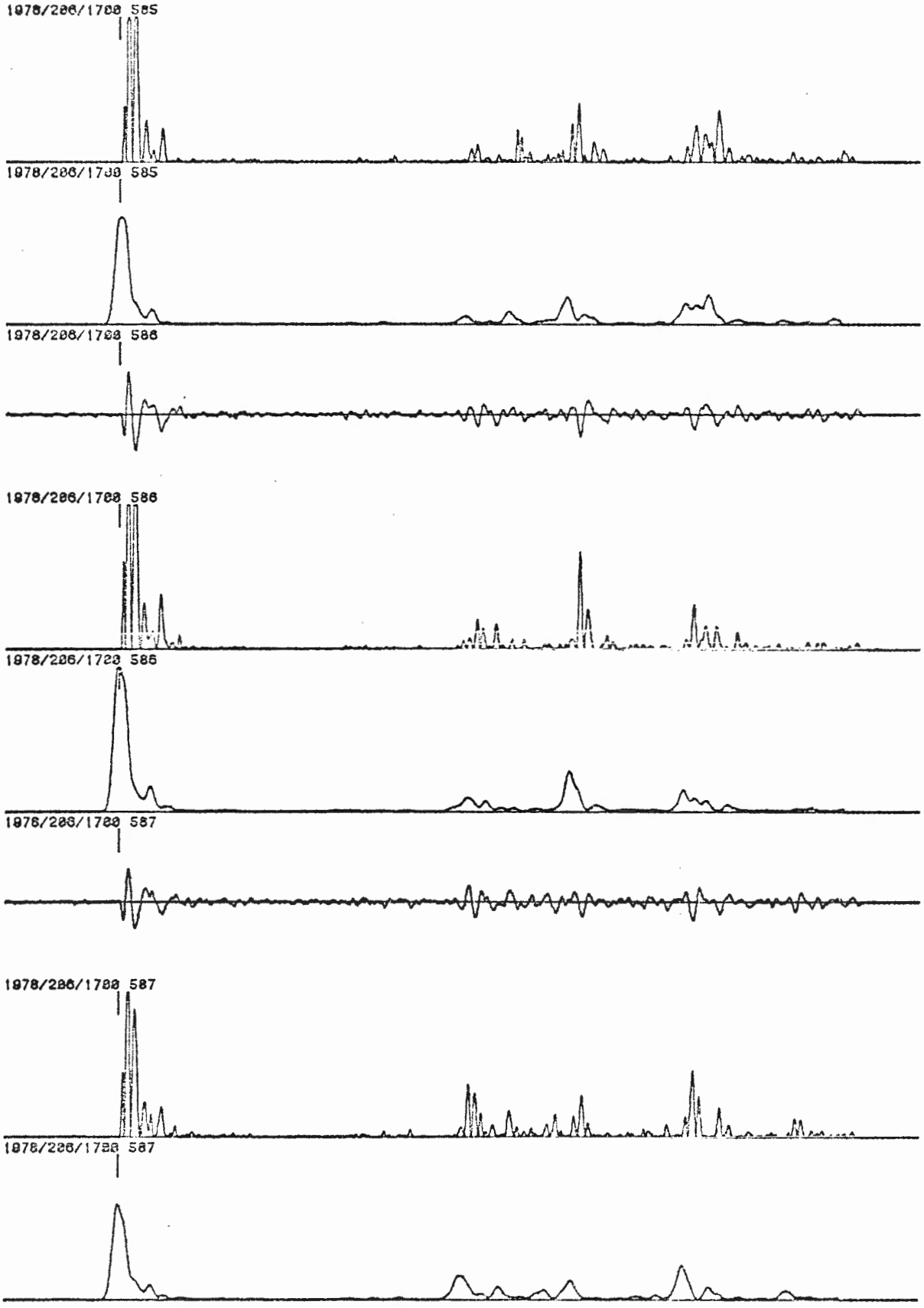
1978/286/1700 585
1978/286/1700 585
1978/286/1700 586
1978/286/1700 586
1978/286/1700 586
1978/286/1700 587
1978/286/1700 587
1978/286/1700 587

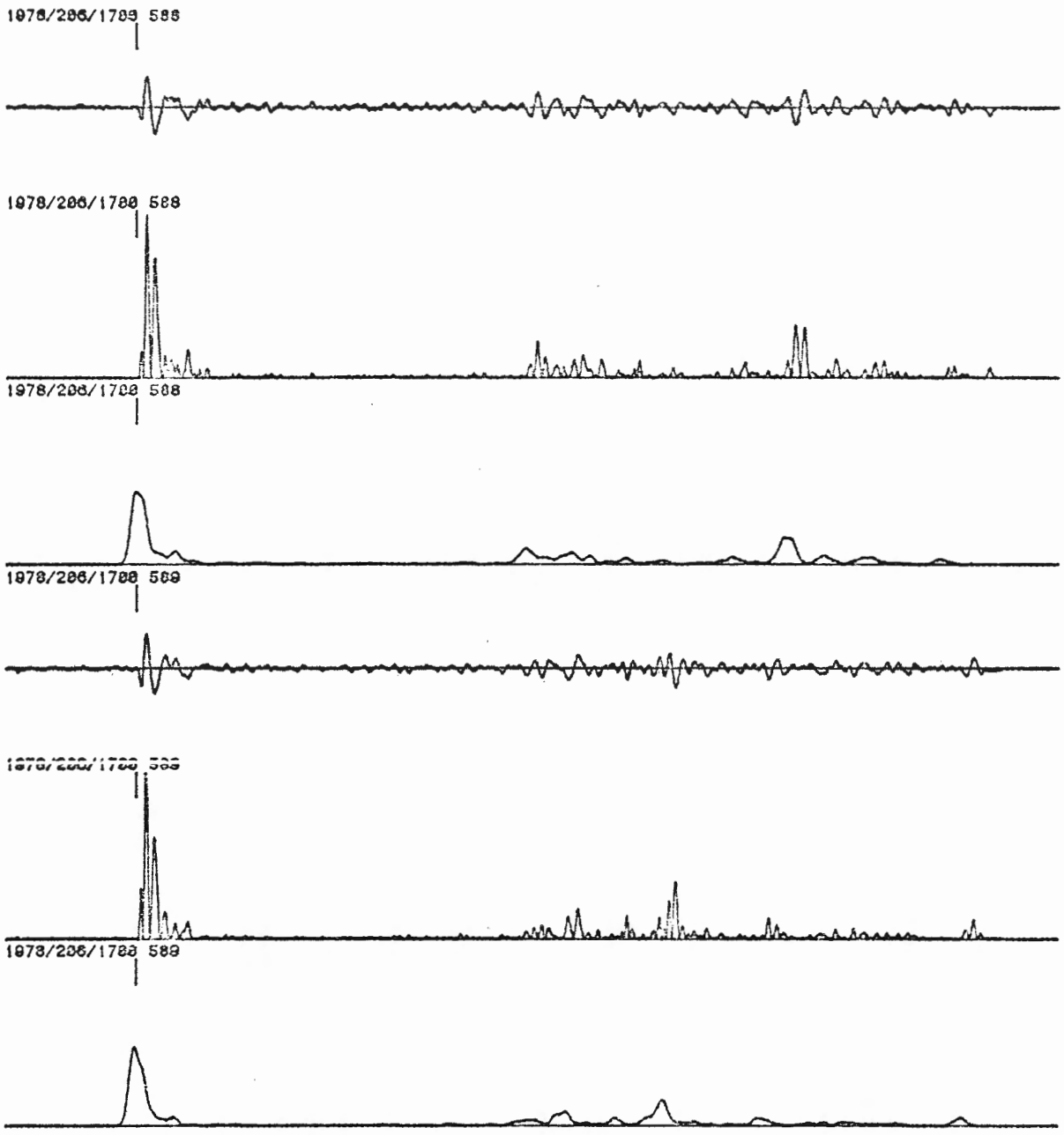
1978/206/1708 587
1978/206/1708 588
1978/206/1708 589

APPENDIX 8

A LISTING OF THE COMPUTER PROGRAM WALLOP, USED TO COMPUTE NORMAL INCIDENCE REFLECTION SYNTHETIC SEISMOGRAMS

```
      PROGRAM WALLOP(OUTPUT,TAPE6=OUTPUT,TAPE1,TAPE2,TAPE3)
C
C  THIS PROGRAM IS DESIGNED TO COMPUTE A REFLECTIVITY MODEL
C  FROM MEASUREMENTS OF VELOCITY AND DENSITY MADE ON SEDIMENTS
C  COLLECTED WITH PISTON CORE DEVICES. THE MODEL CONSISTS OF
C  UP TO 1000 LAYERS OF 10 MICROSECOND THICKNESS (ONE-WAY T.T.)
C  THE REFLECTIVITY MODEL IS THE IMPULSE RESPONSE FOR THE SEDIMENTS
C  DISREGARDING THE EFFECTS OF TRANSMISSION LOSSES OR INTERNAL
C  RAY-PATH MULTIPLES. WHEN CONVOLVED  WITH AN APPROPRIATE
C  PULSE SHAPE IT WILL PRODUCE A SYNTHETIC SEISMOGRAM.
C
      DIMENSION X(400),V(400),T(400),M(400),RHO(400),
     1XX(400),VV(400),TT(400),RRHO(400),R(400),PED(400)
      COMMON SYN(1000),REF(1000),VEL(1000),DANC(1000),PULS(23),
     1ICOUNT
C
C  INITIALISE ALL ARRAYS EQUAL TO ZERO
C
      DO 10 I=1,400
      X(I)=0.0
      V(I)=0.0
      M(I)=0.0
      RHO(I)=0.0
      PED(I)=0.0
      T(I)=0.0
   10 CONTINUE
      DO 11 I=1,1000
      VEL(I)=0.0
      DANC(I)=0.0
      REF(I)=0.0
      SYN(I)=0.0
   11 CONTINUE
C
C  DANC(I) IS THE IMPEDANCE PROFILE
C  REF(I) IS THE REFLECTIVITY
C  SYN(I) IS THE SYNTHETIC SEISMOGRAM
C
C
C  READ IN DATA FROM VELOCITY AND DENSITY
C  FILES, SET COUNT EQUAL TO ZERO
C
      N=0
      READ(1,100)S1,R1,D1
      IF(EOF(1))12,13
   13 N=N+1
      T1=S1/(R1*100.)
      X(N)=S1
      V(N)=R1
      RHO(N)=D1
      T(N)=T1*100000.
C
C  THIS STORES THE FIRST VALUES OF DISTANCE AND VELOCITY
C  AND TIME IN ARRAYS
C
```

```
   12 CONTINUE
      READ(1,100)S2,R2,D2
      IF(EOF(1))14,15
C
C  SET UPPER AND LOWER LIMITS ON VELOCITY
C
   15 IF(R2.GT.2000.) R2=2000.
      IF(R2.LT.1300.) R2=1300.
      N=N+1
C
C  CALCULATE THE DISTANCE IN METRES BETWEEN ADJACENT POINTS
C
      DIFFS=(S2-S1)/100.
C
C  CALCULATE THE WEIGHTED AVERAGE VELOCITY BETWEEN POINTS
C
      AVV=2*R1*R2/(R1+R2)
C
C  NEXT THE ONE-WAY TRAVEL TIME
C
      DIFT=DIFFS*100000./AVV
      T(N)=T(N-1)+DIFT
      V(N)=R2
      X(N)=S2
      RHO(N)=D2
      S1=S2
      R1=R2
      D1=D2
      GO TO 12
C
C  INITIALISE THE ARRAYS FOR VELOCITY AND DENSITY ETC.
C  THROUGH THE WATER COLUMN; VALUES ARE TAKEN FROM FILE INITAL
C  NOTE THERE ARE 10 LINES IN INITAL, THE 10TH LINE CORRESPONDS
C  TO THE SEDIMENT-WATER INTERFACE AND IS CHANGED FOR EACH DIFF
C  ERENT CORE.
C
   14 CONTINUE
      READ(2,230)(TT(I),VV(I),XX(I),RRHO(I),I=1,10)
      DO 23 J=1,N
      K=J+10
      TT(K)=T(J)+50
      VV(K)=V(J)
      XX(K)=X(J)
      RRHO(K)=RHO(J)
   23 CONTINUE
      DO 24 J=1,K
      T(J)=TT(J)
      V(J)=VV(J)
      RHO(J)=RRHO(J)
      X(J)=XX(J)
C
C  CALCULATE IMPEDANCE PROFILE FROM V(J) AND RHO(J)
C
      PED(J)=V(J)*RHO(J)*1000.
```

```
C      WRITE(6,300)X(J),T(J),V(J),RHO(J),PED(J)
   24 CONTINUE
C
C
C  CALCULATE REFLECTION COEFFICEINTS
C
       JJ=K-1
       R(1)=0.0
       DO 30 I=1,JJ
       R(I+1)=(PED(I+1)-PED(I))/(PED(I+1)+PED(I))
   30 CONTINUE
C
C  READ IN THE PULSE SHAPE FROM PULS
C
       READ(3,301)(PULS(I),I=1,23)
C
C  PLACE VELOCITIES, IMPEDANCES(PED) AND REFLECTION
C  COEFFS IN APPROPRIATELY ADDRESSED POSITIONS XWITHIN
C  1000 PT ARRAYS, USE INTEGER MULTIPLES OF 10 MICROSECS
C
       DO 40 L=1,K
C
C  FIND INTEGER MULTIPLE OF 10 MICROSECS DOWN CORE
C
       M(L)=T(L)+0.5
       N=T(K)+0.5
       DO 40 KK=1,N
C
C  TO PREVENT THE POSSIBILITY OF ADJACENT VALUES OF
C  VELOCITY, IMPEDANCE OR REFLECTIVITY BEING PUT
C  IN THE SAME ADDRESS IN THE 1000 PT ARRAY
C
       IF(M(KK+1).EQ.M(KK))M(KK+1)=M(KK+1)+1
       IF(M(L).NE.KK)GO TO 40
       VEL(KK)=V(L)
       DANC(KK)=PED(L)
       REF(KK)=R(L)
C      WRITE(6,400)KK,VEL(KK),DANC(KK),REF(KK)
   40 CONTINUE
C      WRITE(6,302)(PULS(I),I=1,23)
       ICOUNT=N
       CALL CONV
       CONTINUE
       DO 41 K=1,N
       WRITE(6,400)K,VEL(K),DANC(K),REF(K),SYN(K)
   41 CONTINUE
C  FORMATS
  230 FORMAT(F4.1,F8.2,F4.1,F7.4)
  100 FORMAT(3(F12.2))
  300 FORMAT(5(F12.2))
  301 FORMAT(F6.3)
  302 FORMAT(F6.3)
  400 FORMAT(I6,F12.2,E14.7,F12.8,F10.5)
       STOP
       END
```

```
      SUBROUTINE CONV
      COMMON SYN(1000),REF(1000),VEL(1000),DANC(1000),PULS(23),
     2ICOUNT
      LPULS=23
      LR=ICOUNT
      LS=LPULS+LR
      DO 70 I=1,LPULS
      DO 70 J=1,LR
      K=I+J-1
   70 SYN(K)=SYN(K)+PULS(I)*REF(J)
      DO 71 N=1,ICOUNT
C     WRITE(6,303)N,SYN(N)
   71 CONTINUE
  303 FORMAT(I4,F7.4)
      RETURN
      END
/EOR
```

APPENDIX 9

AN EXAMPLE OF AN OUTPUT FROM A TYPICAL RUN OF THE COMPUTER PROGRAM WALLOP

LAYER NUMBER	VELOCITY OF LAYER 0·0 => NO MEASURE-MENT ms^{-1}	ACOUSTIC IMPEDANCE Kg $m^{-2}s^{-1}$	REFLECTIVITY	SYNTHETIC SEISMOGRAM
40	1466.50	.1505362E+07	0.00000000	0.00000
41	0.00	0.	0.00000000	0.00000
42	0.00	0.	0.00000000	0.00000
43	0.00	0.	0.00000000	0.00000
44	0.00	0.	0.00000000	0.00000
45	1466.50	.1505362E+07	0.00000000	0.00000
46	0.00	0.	0.00000000	0.00000
47	0.00	0.	0.00000000	0.00000
48	0.00	0.	0.00000000	0.00000
49	0.00	0.	0.00000000	0.00000
50	1488.00	.2306400E+07	.21014893	0.00000
51	0.00	0.	0.00000000	.01051
52	0.00	0.	0.00000000	.07986
53	0.00	0.	0.00000000	.17863
54	0.00	0.	0.00000000	.21015
55	1488.00	.2306400E+07	0.00000000	.17653
56	0.00	0.	0.00000000	.09457
57	1488.00	.2306400E+07	0.00000000	0.00000
58	0.00	0.	0.00000000	-.04623
59	0.00	0.	0.00000000	-.04623
60	1498.00	.2321900E+07	.00334896	-.03467
61	0.00	0.	0.00000000	-.02925
62	0.00	0.	0.00000000	-.03235
63	1547.00	.2475200E+07	.03195681	-.03288
64	1536.00	.2472960E+07	-.00045269	-.02868
65	0.00	0.	0.00000000	-.01449
66	0.00	0.	0.00000000	.00328
67	1498.00	.2426760E+07	-.00942911	.01056

52°N

51°30'N

MEAN SEA LEVEL

51°N

50°30'N

55°W

54°30'W

54°W

53°30'W

VERTICAL SCALE

TWO-WAY TRAVEL TIME (sec)

0
0·2 — 200 DEPTH AT 1500 m/s
0·4 — 400
0·6
0·8 — 600
1·0

ALL FENCE CROSS-SECTIONS ARE DRAWN RELATIVE TO 0·7 secs T.T.

KEY

- AREAS OF MUD ACCUMULATION
- GLACIAL DRIFT
- MESOZOIC - CENOZOIC SEDIMENTARY ROCKS
- MISSISSIPPIAN AND PENNSYLVANIAN SEDIMENTARY STRATA

FENCE DIAGRAM OF AIRGUN SEISMIC DATA NORTHEAST NEWFOUNDLAND CONTINENTAL SHELF

C. Dale, 1979